SOME STUDIES IN FAST NEUTRON SPECTROMETRY

by

J. SHIELDS

DEPARTMENT OF NATURAL PHILOSOPHY,

UNIVERSITY OF GLASGOW

- - - - - - - - - - - - - - - - - - -

PRESENTED AS A THESIS FOR THE DEGREE

OF PH.D. IN THE UNIVERSITY OF GLASGOW

SEPTEMBER 1955

- -

SOME STUDIES IN FAST NEUTRON SPECTROMETRY

--- CONTENTS ---

PREFACE

This thesis describes work which was performed by the author, during the period from October 1951 to September 1954, upon the development of techniques suitable for the quantitative measurements of the intensity and energy of neutrons in the range of energies from 1 MeV to 20 MeV.

The thesis is divided into four main parts, the contents of which will now be described.

PART I is an introductory review on the importance in nuclear physics of measurements on fast neutrons and the techniques which have been available in such measurements. In the light of this review the properties of an ideal fast neutron spectrometer are enumerated. The possibility of realisation of such properties using scintillation counters is then discussed. The material for this review has been obtained from the current literature on nuclear physics and mention is made in the text of the relevant references.

The experimental investigations carried out by the author on the development of liquid scintillation counters for measurements on nuclear radiations are described in Part II. In this part the work on light collection from volumes of scintillator, investigation of photo-multiplier noise, and response of liquid scintillators to different radiations was carried out solely by the author. The remainder of the work was performed in collaboration with Mr. R. Giles and Mr. D.J. Silverleaf.

PART III deals with the application of the liquid scintillators, of Part II in several forms of fast neutron spectrometer. The work on the Collimating Tube Spectrometer and the Borate Spectrometer was performed by the author. The remainder of the work in Part III was carried out in collaboration with Mr. D.J.Silverleaf. The time-of-flight spectrometer was suggested by Mr. D.J.Silverleaf, but the design of the scintillators used and the experiments were undertaken jointly.

Cont'd ...

PART IV gives a general discussion of the importance of the work described in the thesis in relation to that of other workers in the field of fast neutron scintillation spectrometry. The field of application in relation to Part I is briefly mentioned.

The appendices describe work, the nature of which, although an integral part of the research programme, could be considered more adequately therein.

I must thank Professor P.I. Dee for his interest in this project and also Mr. R. Giles for his advice during the course of the research programme.
I take this opportunity of thanking the Department of Scientific and Industrial Research for financial assistance during the three years in which this research was undertaken.

J.S.

September, 1955.

PART I GENERAL INTRODUCTION

Measurements on X-ray spectra and the α-particles from radioactive nuclei lead to the hypothesis of the existence of discrete nuclear energy levels. It is hoped that, by careful investigation of the properties of these levels, the problem of the nature of nuclear forces will be elucidated. The main method of investigation available to the nuclear physicist is the detection and measurement of the various radiations resulting from nuclear reactions. In this connection a vast amount of work has proceeded in the field of ionising particles and X-rays but so far no comparable advance has taken place in the study of fast neutrons.

In this part of the thesis we shall discuss:-

(i) the types of measurement on fast neutrons in the range of energy 1 MeV to 20 MeV, of importance in nuclear theory;

(ii) the techniques available by which these measurements have been performed;

(iii) the extent to which these techniques have been successful;

and (iv) the properties of the instrument which would be ideal for these measurements.

I.(i) IMPORTANCE IN NUCLEAR THEORIES OF MEASUREMENTS ON FAST NEUTRONS IN RANGE 1 MeV to 20 MeV.

Fast neutrons are involved as emitted particles in nuclear interactions either as product particles from interactions of nuclei with other radiations or scattered particles from interaction of nuclei with neutrons. As product particles they appear in investigations on light nuclei, photo-disintegration and deuteron stripping reactions, and as scattered particles in elastic, inelastic and polarisation scattering of neutrons.

(a) ENERGY LEVELS OF LIGHT NUCLEI.

The main purpose of investigations into the properties of light nuclei is to provide the theorist with information on the position, width, and quantum numbers of spin and parity for as many states as possible in any nucleus. The dependence of nuclear forces on charge must also be investigated by consideration of variations of position of the energy levels in related nuclei such as C^{12}(6 neutrons, 6 protons) B^{12}(7 neutrons, 5 protrons) and N^{12}(5 neutrons, 7 protons). Determination of neutron energies and intensities of groups yields precise information of the positions and widths of the energy levels through which the transitions are taking place. Angular distribution and correlation measurements enable the assignment of quantum numbers of spin and parity to be made to the involved nuclear levels.

Typical of the theoretical approach to the problem of "light" nuclear energy levels is that of Flowers (1) in his treatment of odd A nuclei such as O^{17}, in which, by consideration of movement of odd neutron outside the central core formed by the other nucleons, he predicts the properties and positions of nuclear levels and compares them with those experimentally obtained.

(b) PHOTO-DISINTEGRATION

In photo-disintegration where a high energy X-ray is incident on a nucleus it seems at first glance that an explanation of cross-section and angular distribution etc. of the emitted particles could be found by applying a statistical theory of emission of particles from a highly excited nucleus. The large cross-sections and non-uniform angular distributions however could not be explained using a simple Weisskopf theory. Various alternative suggestions have been put forward but no evidence completely in favour of one particular theory has been found. Goldhaber and Teller (2) suggest a dipole transition in which the protons as a group are displaced relative to the neutrons. This theory

predicts the "giant resonance" in the cross-section for (γ,n) but fails in the prediction of observed particle energies. Other theories such as those of Wilkinson (3) and Courant (4) use, instead of these statistical models, single particle models which, although predicting resonance cross-sections and the presence of high energy particles have still to be verified in respect of the angular distribution of emitted radiations.

It is thus obvious from this short discussion that much more precise information on energy, intensity, and angular distribution of the neutrons emitted in (γ,n) reactions is required by the theorists before they can set up a more definite model for photo-disintegration.

(c) DEUTERON STRIPPING

Investigations on the angular distribution of neutrons emitted during the bombardment of nuclei with 15 MeV deuterons by Roberts (5) showed an anomalous behaviour which could only be explained by the stripping of the protons from the deuteron by the bombarded nucleus. At these high energies the theory given by Serber (6) has proved quite successful in explaining the observed effects. At low deuteron energies of the order of 1 MeV, it should be expected that the stripping process would be unimportant and formation of compound nucleus would predominate. It has, however, been shown by various observers, e.g. Swartz (7) and Holt (8), that the angular distribution measurements disagree with either deuteron stripping or compound nucleus. Explanation of the angular distributions have been profferred by workers such as Butler (9) and Huby (10) using a mixture of compound nucleus and deuteron stripping. Further experiments, particularly on angular distributions and correlations of the emitted neutrons and associated γ-rays are still required so that more precise theoretical determinations can be made about the nature of the forces binding the deuteron.

(d) ELASTIC SCATTERING OF NEUTRONS

For neutrons of energy greater than 6 MeV the elastic scattering from nuclei is mainly coherent, i.e. one obtains a diffraction pattern similar to optical Fraunhoffer diffraction which depends for its shape on the neutron energy and the nuclear radius. The radius of the nucleus can be obtained by considering a particular nuclear model; for example, transparent, cloudy, or opaque nuclear model. These theories predict different types of variation of radius with change of atomic weight of the form $R = KA^{1/3}$, the value of the constant K varying from one model to the other.

Amaldi et alia (11) have observed the angular distribution of elastically scattered 14 MeV neutrons from lead. They have determined from the diffraction pattern the type of theory which best fits their results. It is necessary, however, that much more complete data is obtained on the angular distributions of the neutrons in this type of experiment for as many nuclei as possible so that a more comprehensive picture, of variation of radius with atomic weight, can be drawn.

(e) INELASTIC SCATTERING OF NEUTRONS

Under the heading of inelastic scattering of neutrons fall the reactions (n,n^1), $(n,2n)$, and $(n,3n)$. The predominance of each type depends on the incident neutron energy. In the "medium-to-heavy" nuclei with $A \sim 50$, at 2 to 3 MeV. (n,n^1) predominates, 10 to 14 MeV, $(n,2n)$ and 14 - 20 MeV, $(n,3n)$.

Using the (n,n^1) reaction in $A \sim 50$, information can be obtained on the low lying energy levels of these nuclei. These low lying levels have been investigated previously in only certain elements which displayed β-decay phenomena. Observations, of the type performed by Preston (12), on the energy, angular distribution, and angular correlation of the scattered neutrons allow assignment of position and quantum numbers to these low lying states. The extension, thus obtained, to the β-decay measurements which have been explained successfully using a nuclear

shell model, will enable more extensive tests to be made, particularly to the assumptions on the coupling existing between the orbital and spin momenta of the extra particle in odd A nuclei, embodied in the shell model.

At higher energies of the incident neutron, the nuclei considered are in highly excited states, so that instead of discrete levels we must consider the emission of neutrons from a continuum of levels. In (n,2n) reactions at the order of 10 to 14 MeV incident neutron energy, the cross-section has been measured for a number of elements from A = 30 to A = 141 by Cohen (13) and close agreement using a Weisskopf statistical model has been obtained. Measurements are lacking, however, in the determinations of energies and angular distributions of the emitted neutrons. It is important theoretically to find the precise manner in which two neutrons are emitted from an excited nucleus as measurements of this type will indicate the manner of binding of pairs of neutrons inside the nucleus.

No extensive experimental data exists for the theoretically possible (n,3n) reactions, because of the predicted low cross-sections and difficulties in measurement. In the same manner as in the (n,2n) case, this type of reaction is extremely important for determination of pair binding energy inside a nucleus. Measurements of a similar nature to the (n,2n) case are required here.

(f) NUCLEAR POLARISATION OF FAST NEUTRONS

The nuclear shell model predicts a certain splitting in the levels of odd mass nuclei due to interaction between the spin and orbital momentum of the nucleon outside the core formed by the other nucleons. Investigation of the magnitude of this splitting particularly in low A nuclei will serve to test the assumptions of its size used by theorists in predicting the positions of odd A nuclear energy levels, e.g. Flowers (1). One method by which the problem can be attacked is by observing the polarisation of a beam of polarised neutrons of low energy a few MeV in scattering from even A nuclei.

This polarisation can be investigated by observing the asymmetry of the angular distribution, as has been pointed out by Schwinger (14). Experiments of this type have been carried out by a number of investigators with rather inconclusive results. (Adair (15); Hall et alia (16), Staub (17)).

This determination of spin-orbital coupling is also of importance in determinations on the interaction of nucleons at high energies.

(Note: By polarisation is meant the preferential separation of spin-up or spin down in the outgoing neutron beam).

This general discussion of neutron measurements should serve to illustrate their importance in present-day nuclear physics. From the above it is obvious that the types of measurement which are required are : (1) intensity of emitted neutrons; (2) energy of emitted neutrons; (3) angular distribution of the neutrons; (4) angular correlations between neutrons and other radiations.

I. (ii) REVIEW OF PREVIOUS TECHNIQUES USED IN FAST NEUTRON MEASUREMENTS

In this section a brief review of the methods available for the various investigations listed above will be given. No attempt will be made to show to what extent these have proved successful. This will be discussed in Part I(iii).

The main obstacle in neutron detection is the inability of many detectors to discriminate against γ-rays which almost always accompany neutrons. Another difficulty is the problem of obtaining high efficiency in fast neutron detection due mainly to small scattering and absorption cross-sections.

The methods employed in fast neutron measurements can be considered in two main groups: (a) those suitable for detection alone; and (b) those suitable for both detection and energy measurement. In group (a) we included Boron Tri-fluoride and Boron lined chambers, Uranium or Thorium fission chambers, radio-active threshold techniques; in group (b) photographic emulsions, cloud chambers, and proportional chambers.

(a) DETECTION TECHNIQUES

(i) BF_3 and B-lined Chambers.

In this method the difficulties in fast neutron detection mentioned above are overcome by slowing down the fast neutrons in a paraffin or graphite moderator and then detecting the subsequent slow neutrons in a BF_3 or B lined proportional chamber. These counters are fully described in Rossi and Staub (18). They generally consist of a proportional chamber 50 cm long and filled with B^{10} enriched, Boron Tri-fluoride gas, or well coated with B^{10} (enriched). The high slow neutron cross-section for the B^{10} $(n,\alpha)Li^7$ reaction enables high efficiency, of the order of 80%, to be obtained. These counters are however not completely insensitive to X-rays as pile-up of pulses due to recoil electrons becomes important in cases of intense X-ray backgrounds.

(ii) Fission Chambers

In cases where X-ray background is intense, fission chambers employing coatings of U^{235} or pure Thorium become useful, since in this case the pulses produced are very much larger than those for recoil electrons. The efficiency in this case is smaller than in (i), but the other characteristics which will now be considered are similar.

Characteristics of the Techniques

The advantages of these types of counters lie in their comparative insensitivity to X-rays, high efficiency and usefulness in continuous monitoring of a fast neutron beam. Their disadvantages appear in their inability to discriminate between neutrons of varying energy, slow response time, bulk, and finally an efficiency which is energy dependent.

(iii) Radioactive Threshold Technique

A simple and accurate method of fast neutron detection is to expose in the fast neutron beam a foil of some material, which has a high cross-section for neutron induced radio-activity. Measurement of the radioactivity is made to

determine the neutron flux using conventional β-particle counting techniques. Estimates of the energies of the incident neutrons can be obtained from the threshold for the particular foil used; for example, foils of P^{31} and S^{32} are suitable only for neutrons of energy greater than 2 MeV since the (n,p) reaction has its threshold at the order of 2 MeV; at higher energies foils exhibiting (n,2n) reactions, with thresholds at the order of 9 MeV, are chosen. Extremely fine papers on this technique are found in Hanson (19) and Cohen (13).

Characteristics of the Technique

The main advantage of this technique is its complete insensitivity to γ-ray background. The disadvantages are rather numerous viz:- the time required to obtain results is long; the subsidiary counting apparatus is bulky; it is not continuously sensitive; its response time is infinitely long.

(b) TECHNIQUES FOR DETECTION AND ENERGY MEASUREMENTS

The energies of fast neutrons are generally measured by observations on the recoil protons produced in their interactions with hydrogenous materials. The techniques considered below are of this type.

(i) Photographic Emulsions

The method employed is to expose a plate with emulsion, ~100 μ thick, in a beam of collimated neutrons. After development, the measurement of ranges and angles of recoil of elastically scattered protons, under a microscope, determines the energies of the incident neutrons. Corrections for variation of (n,p) scattering cross-section with energy are necessary if intensity measurements are required.

Several variations of this direct method are also used. Loading emulsions with Li^6 and determination of the energy of the neutrons, from the ranges of the particles from the $Li^6(n,\alpha)\ H^3$ reaction, enables uncollimated neutron beams to be investigated, a considerable advantage, see:- Keepin (20). Another method is to

employ an external hydrogenous radiator with the emulsion placed behind it in a vacuum. Simple measurement of the proton recoils in the emulsion enable the energies of the collimated neutrons incident on the radiator to be determined since the angle of recoil is defined by the position of the emulsion relative to the radiator (Allred et alia (21)).

Characteristics of these methods

These methods are tedious and time consuming; their efficiency is small, the order of 1 neutron in 10^5 incident per sq.cm. being useful; time discrimination between recorded events is impossible. Their main advantages lie in their insensitivity to X-rays and their exceptional energy resolution the order of 0.05 MeV, provided sufficient statistics are obtained. A good article on resolution in photographic emulsions, is to be found in Nereson (22).

(ii) Cloud Chambers

Very similar to the photographic emulsion technique in its advantages and limitations is the use of the hydrogen-filled cloud chamber for measuring the energies of collimated neutron beams. This method is not used to any great extent. Hughes (23) has used cloud chambers on neutrons of the order of 2 MeV.

(iii) Proportional Chambers

Attempts, using electronic techniques have been made to overcome the disadvantages of speed of recording results mentioned in (i) and (ii) above. The simplest method is to measure the energies of the recoil protons in a hydrogen or methane filled proportional counter. Difficulties arise here, however from the uniform distribution of proton energies from zero to the energy of the neutron and from wall effects, positive ion effects, straggling etc. which tend to distort the edge of the ideal distribution. Various modifications to this direct method have been constructed to overcome these difficulties.

Giles (24) has used an anticoincidence screen-walled proportional chamber

which eliminates those proton recoils which do not proceed in the forward direction. By this method he has obtained energy resolutions of the order of 4% at 3 MeV, efficiency of the order of 1 in 10^4 incident neutrons and a resolving time the order of one micro-second. The apparatus is insensitive to γ-rays provided the dimensions of the chamber are small compared to the ranges of moderately energetic electrons.

Other methods, which have been investigated, include proportional counter telescopes (Rossi and Staub) (18) employing a thin hydrogeneous radiator followed by an array of coincidence proportional chambers and absorbers which measure the range of the recoil protons; He^3 filled proportional chambers in which the proton energies from the $He^3(n,p)H^3$ reaction are measured; a time-of-flight method using a thin hydrogeneous radiator followed by a multiple proportional chamber in which the recoil protons are collimated and their ranges estimated using the time taken for the ionisation electrons to traverse the distance from the end-point of the recoil range to a fixed collecting plate. Holt (8).

Of these additional methods the third mentioned is the most recent and shall be considered later in the thesis; the first mentioned, in spite of its low efficiency, the order of 10^{-6}, has been the most successful of the electronic counting techniques for measurement of neutron energies.

Scintillation counter techniques, developed during the course of the author's work, have been purposely omitted from this section of the thesis so that the author may, in more detail, compare his own work to that of other investigators in the field of fast neutron scintillation spectrometry.

I.(iii) [illegible]

Sections (i) and (ii) of this part of the thesis have [illegible] description of the problems existing in fast neutron physics and the characteristics of the techniques which have been available for their solution. This section is considered under the same headings as section (i) and describes briefly the extent to which these techniques have been applied successfully and also the particular measurements on which much more information is required.

(a) Energy Levels of Light Nuclei

Fast neutrons are emitted from light nuclei in their interactions with deuterons, alpha particles, and protons. Measurements, which are of importance on the emitted neutrons are :-

(a) the variation of intensity as the incident particle energy is changed;

(b) the energies of the groups;

(c) The angular distributions;

(d) the angular correlations with other radiations.

None of the techniques of I(ii) is capable of such a wide range of applicability so that the experimentalist has contented himself with using a technique which performed successfully some of the required measurements.

In the case of (a), BF_3 and B lined chambers have been very successful, since no energy discrimination is needed. An example of the power of the technique can be seen from the data on the positions of the energy levels in the compound nucleus N^{15}, in the reaction $C^{14}(p,n)N^{14}$ where nine energy levels have been observed in the range of proton energy from 1.1 to 2.6 MeV (Preston (25)). Some attempts have also been made to apply the radioactive foil technique in this type of measurement but the time required to record the results is too long to make the method a reasonable proposition. From these excitation functions, study is limited to states in the compound nucleus of excitation energy greater than the Q value for

reaction, thus, in (d,n) and (α,n) reactions, since the excitation energy is high, no resonances are observed in the excitation function, to show the presence of discrete energy levels.

For energy measurements photographic emulsions have been most successful. Although the data takes a considerable time to collect the energy resolution is very good. Typical of this type of measurement is the study of the $B^{11}(d,n)C^{12}$ and $B^{10}(d,n)C^{11}$ by Johnson (26) where the resolution is good but the statistics poor. Cloud chamber measurements are not so important although the work of Hughes (23) on 2 MeV neutrons is worthy of note. Using his screen walled proportional Chamber Giles (24) has studied the high energy groups in the $B^{11}(d,n)C^{12}$ reaction but no further measurements have been obtained.

In the past few years in the study of energy levels of light nuclei the emphasis has shifted from the experiments which determine the positions of energy levels to those which determine their properties. In angular distributions of neutron groups photographic emulsions (Swartz(7)) and, to a lesser extent, radioactive threshold technique (Harris (27)) have been very successful. It is in the field of angular correlation measurements, however, that the techniques of I(ii) have proved deficient, mainly due to their poor efficiency and slow speed of response.

(b) Photodisintegration

Of interest in (γ,n) reactions are measurements of threshold, total yield of neutrons with variation of γ-ray energy, and the energy and angular distribution of the emitted neutrons. The main obstacle in the path of accurate determination of these properties is the source of γ-rays which is generally used in photo-disintegration experiments, viz., the betatron. The continuous energy distribution and unknown shape of the γ-ray spectrum from the betatron present formidable difficulties in the interpretation of results.

Threshold measurements have been made by observation of the γ-ray energy at which the target nucleus becomes radioactive (both (28) and (29)). A further measurement of variation of activity with γ-ray energy also enabled Katz to find the total neutron yield. This method has been a very successful and powerful tool in this field. Recently BF_3 counters, encased in a large block of paraffin have been used successfully to measure threshold values and neutron yields (Koch(30)).

Neutron energy measurements are difficult to interpret because of the continuous γ-ray spectrum. Some measurements have, however, been made using cloud chamber techniques (Atkinson (31)), with betatron γ-rays, in the photo disintegration of N^{14}, and using photographic emulsions and cloud chambers on the low threshold elements D and Be disintegrated by natural γ-rays (Wattenberg (32)).

By measurement of the radioactivity induced in Iodine surrounded by Cadmium foil and placed at varying angles to the target Halban et alia (33) have measured the angular distribution of neutrons in the reaction D(γ,n)p where the γ-rays used are natural γ-rays of energy greater than threshold value for the reaction.

It is in energy measurements and angular distributions that much more information is required before a detailed theory of photo-disintegration can be obtained.

(c) Deuteron Stripping

We have already noted in I(i) that the presence of high energy neutrons and the forward peak in the angular distribution in the experiments on high energy deuteron interaction with nuclei can be explained using the theory of deuteron stripping due to Serber. These results have been obtained using photographic plates and at very high energies using proportional counter telescopes.

To elucidate the problem at low deuteron energies ~ 1 MeV, data is required on angular distributions and correlations. A few angular distribution measurements have been made using (a) photographic emulsion e.g. the neutrons from $Be^9(d,n)B^{10}$ have been measured by Swartz (7), and (b) the time-of-flight proportional

chamber due to Holt (8).

No work of importance has been attempted on [illegible] essential to a proper understanding of the problem, because of the lack of efficiency and slow response of the techniques considered under I(ii). The measurements already made on low energy (d,n) reactions in nuclei, although quite satisfactory, are not sufficiently conclusive to test the theoretical predictions of admixtures of compound nucleus and deuteron stripping. It is, therefore, essential that further experimentation should be performed especially in angular correlation measurements.

(d) Elastic Scattering of Neutrons

The main measurements required, in this section, are angular distributions with energy discrimination to distinguish between the elastic and inelastically scattered neutrons. The method used by Amaldi et alia (11) on elastic scattering of 14 MeV neutrons from lead was radioactive foil technique with Cu^{63} as a foil which has a threshold at 10.9 MeV for the (n,2n) reaction, thus allowing energy discrimination.

Some further work has proceeded in this field using photographic emulsions. These methods although capable of making satisfactory measurements are extremely tedious in this particular case.

(e) Inelastic Scattering of Neutrons

Of theoretical importance in this field are experimental results on energy, yield, angular distributions and correlations of the inelastically scattered neutrons. These measurements are extremely difficult since they require a technique which can distinguish between the elastic and inelastically scattered neutrons. The methods which have been employed are photographic emulsions and cloud chambers filled with hydrogen or methane.

Preston (12) has used photographic emulsions very successfully in the study of the inelastic scattering from Fe^{56} of 2 to 3 MeV neutrons from $Li^7(d,n)Be^8$ reaction. No angular distribution measurements are available because of the lack of

efficiency in this technique. Cloud chamber measurements have been carried out by Bonner (34) with the same limitation as mentioned above.

It is worthy of note that the inelastically scattered neutrons have been detected by a stilbene scintillation spectrometer in coincidence with a Na.I spectrometer which records the X-rays associated with the neutrons. An angular correlation between the neutrons and X-rays has been obtained (Shapiro (35))

An indirect method using NaI crystals to detect the associated X-rays has been used very successfully in determination of the states excited in a nucleus by interaction with neutrons (e.g. Grace (36)).

Measurements in (n,2n) reactions have been restricted to thresholds and cross-sections since only applicable technique is the radioactive foil method. Cohen (13) has investigated this reaction in a large number of elements.

In this field a vast amount of data is still required in measurements of all the types mentioned in the first paragraph.

(f) Nuclear Polarization of Neutrons

Of importance in this section are data on the energies and angular distributions of the scattered neutrons.

For reasons of low cross-section and difficulty in observation in many cases, the measurements to detect the polarization have been restricted to the $He^4(n,n^1)He^4$ reaction. In this case the polarization is detected by measurement of the α-particle recoils in a He^4 filled proportional chamber. By this method the energy and angular distribution of the neutrons can be calculated. (Adair (15); Hall & Kootz (16)). None of these experiments, however, gives results which are entirely conclusive.

The lack of efficiency of the methods considered in I(ii) forbids the direct observation of the energy and angular distribution of the scattered neutrons.

From the short discussion in I(iii) it is obvious, that the techniques which have been used in neutron spectroscopy during the past twenty years are not

adequate for all the measurements which are of importance to theoretical predictions, especially in the field of angular correlations. The next sub-section in this part of the thesis shall be devoted to the consideration of the properties of an ideal neutron spectrometer .

I(iv) AN IDEAL FAST NEUTRON SPECTROMETER

In order that measurements on intensity, energy, angular distributions and angular correlations can be performed, the essential features which a satisfactory spectrometer for the study of fast neutrons, must possess are :-

(a) A response which is proportional to the energy of the incident radiation, including resolution between particles of neighbouring energy values;

(b) fast response and recovery when a neutron is incident. This is essential if coincidence techniques, which require short resolving times, are necessary in investigations, e.g. angular correlation experiments.

(c) High efficiency for detection of fast neutrons. This property is essential to enable coincidence experiments and investigations at low source strengths to be performed.

(d) The ability to distinguish between neutrons and other radiations.

It is obvious from the discussion of the characteristics of the techniques described in I(ii) that none of them satisfy many of the requirements noted above. The development of a successful γ-ray scintillation spectrometer suggested that a similar technique could be applied in fast neutron spectrometry. The following parts of this thesis describe the author's work in the successful development of such a fast neutron spectrometer.

REFERENCES TO PART I.

1. FLOWERS, B.H. :- Glasgow Nuc.Phys.Conference (1954)
2. GOLDHABER,M. & TELLER,E. :- Phys.Rev.74 p.1046 (1948)
3. WILKINSON, D.H. :- Glasgow Nuc.Phys. Conference. (1954)
4. COURANT, E.D. :- Phys.Rev.82 p.703 (1951)
5. ROBERTS, J.H. :- Phys.Rev.72 p.76 (1947)
6. SERBER, R. :- Phys.Rev.72 p.1008 (1947)
7. SWARTZ, H.M. :- Phys.Rev.87 p.534 (1952)
8. HOLT, J.R. :- Glasgow Nuc.Phys. Conference (1954)
9. BUTLER, S.T. :- Phys.Rev.80 p.1095 (1950)
10. HUBY, R. :- Proc.Roy.Soc. A215 p.385 (1952)
11. AMALDI, E. :- Nuovo Cimenta 3. pp.15 & 21 (1946)
12. PRESTON, W.M. :- Phys.Rev.86 p.132 (1952)
13. COHEN, B.L. :- Phys.Rev.81 p.184 (1951)
14. SCHWINGER, J. :- Phys.Rev.69 p.681 (1946)
15. ADAIR, R.K. :- Phys.Rev.86 p.155 (1952)
16. HALL , R. :- Phys.Rev.72 p.196 (1947)
17. STAUB, H. :- Phys.Rev.57 p.596 (1940)
18. ROSSI,B. & STAUB, H. :- Ionisation Chambers and Counters (1949)
19. HANSON, A.O. :- Phys.Rev.73. p.106 (1948)
20. KEEPIN, G.R. :- Rev.Sci.Inst.21 p.163 (1950)
21. ALLRED, J.C. et alia :- Rev.Sci.Inst.21 p.225 (1950)
22. NERESON,N. & REINES, F. :- Rev.Sci.Inst.21 p.534 (1950)
23. HUGHES, J.P. :- Phys.Rev.72 p.902 (1947)
24. GILES, R. :- Rev.Sci.Inst.24 p.986 (1953)
25. PRESTON, W.M. :- Phys.Rev.83 p.1133 (1951)

REFERENCES TO PART I (cont'd)

26. JOHNSON, V.R. :- Phys.Rev.86 p.302 (1952)

27. HARRIS, S.P. :- Phys.Rev.82 p.266 (1951)

28. KATZ, L. :- Phys.Rev.80 p.1062 (1950)

29. KATZ. L. :- Phys.Rev.82 p.271 (1951)

30. KOCH, H.W. :- Glasgow Nuc.Phys. Conference (1954)

31. ATKINSON, J.R. :- Glasgow Nuc.Phys. Conference (1954)

32. WATTENBERG, A. :- Prel.Report No.6 Nuc.Sci.Series (—)

33. HALBAN, H. :- Phys.Rev.81 p.219 (1951)

34. BONNER, T.W. :- Phys.Rev.53 p.192 (1938)

35. SHAPIRO, D. :- Phys.Rev.94 p.751 (1954)

36. GRACE, M.A. :- Phys.Rev.82 p.969 (1951)

PART II LIQUID SCINTILLATION COUNTERS

II(i) THE SCINTILLATION COUNTER

In the few years that the scintillation counter has been in general use it has developed into one of the most important and valuable tools in nuclear physics. The fields of future development of this technique in industrial, medical, and nuclear research are vast indeed.

It has been found that certain fluorescent materials have the property of being excited by the passage through them of an ionising particle. The flash of light produced is called a scintillation and the materials scintillators. The flash of light produced is generally proportional to the amount of energy lost by the particle in the scintillator.

A scintillation counter consists essentially of a scintillator, and a photo-multiplier which converts the flash of light into an electrical pulse of proportional amplitude. It is clear from the above, that the scintillation counter can be used for the detection and energy measurement of any ionising radiations. Its most important application, however, has been in the study of X-rays, which produce scintillations by the ejection of electrons from the material of the scintillator. Its great advantage in this connection lies in its high efficiency. The scintillation counter has also the merit of an extremely short resolving time. Scintillators have been found in which the duration of the scintillation is as short as 10^{-9} secs. The multiplier has also very fast response. These two properties, i.e. high efficiency and short resolving time mean that the scintillation counter is very suitable for coincidence experiments.

Fast neutrons can also be detected in organic scintillators by virtue of the proton recoils which they produce. It is clear that such a neutron detector will satisfy many of the requirements mentioned in I(iv). This thesis describes the development of a scintillation spectrometer for fast neutrons capable of

FIG.II.1a. - SCINTILLATION COUNTER ARRANGEMENT

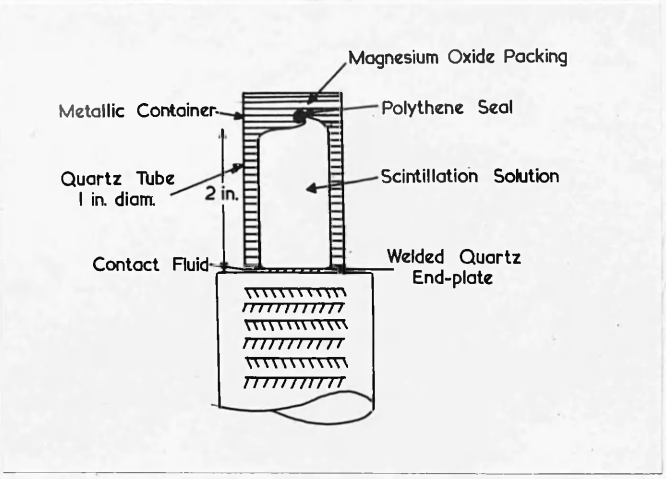

FIG. II.1b LIQUID SCINTILLATOR ASSEMBLY

distinguishing between neutrons of different energies and sensitivity in the presence of X-rays. The difficulties involved in this are described in Part III.

Two main types of organic scintillators are available in the form of solid crystalline materials, e.g. anthracene, and solutions, e.g. saturated terphenyl in xylene. Although solutions have the disadvantage of a relatively low energy conversion efficiency, they have the merit of a very short resolving time. They can be obtained easily and cheaply in clear volumes of any shape and size, whereas crystals can only be prepared at considerable expense to volumes of the order of a few inches cube. For these reasons, liquid scintillators were chosen for the following work on neutron spectrometry.

II(2) DEVELOPMENT OF LIQUID SCINTILLATION COUNTER TECHNIQUE

INTRODUCTION

Some general investigations into the properties of liquid scintillators were carried out before a convenient and satisfactory arrangement (Fig.II.1.(a) &(b)) for work on neutron spectroscopy was found. The final arrangement for a liquid scintillator was to surround all but one face of a quartz container with magnesium oxide, as a reflector, and place the uncovered face on the photo-multiplier. This part of the thesis is devoted to the work required before such an experimental scheme was derived.

II(2) (a) Scintillation Materials

Some preliminary investigations by Mr. R. Giles on the use of solutions of terphenyl in xylene as scintillators showed that the scintillations produced by X-rays were largely quenched in the solution. This quenching of the fluorescence was traced to the presence of sulphur in the xylene. The author performed some experiments on the transmission of light of varying wavelengths through 1 cm. of various samples of xylene and solutions of terphenyl in xylene using a Beckmann Spectra-photometer. The results (Fig.II 2) show the considerable increase in

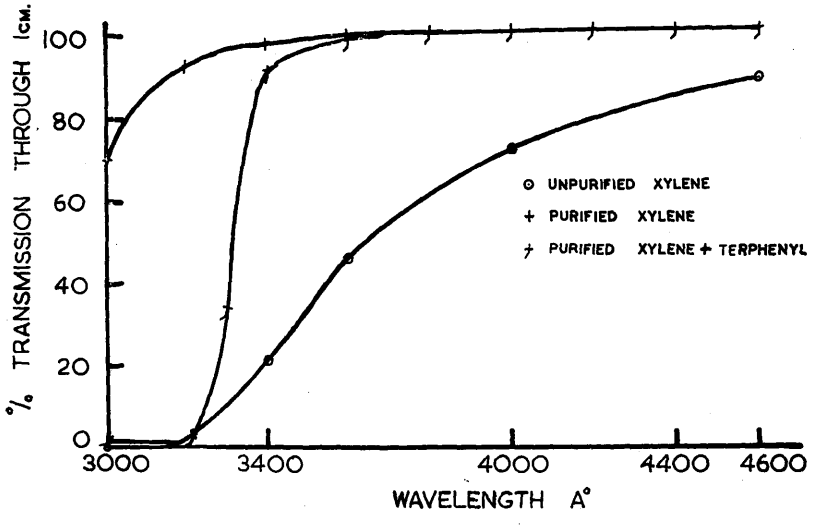

FIG. II.2 TRANSMISSION CURVES FOR LIQUIDS USED IN SCINTILLATION COUNTERS

transparency of the solution after the removal of oxygen and fractional distillation of the xylene. Various samples of xylene have been purified and tested in this way. This transmission test has been used with success, as a method of testing liquids and solutions of the various chemicals used for degree of contamination and thus fluorescent efficiency. It was found, by experiment, that it was essential to have the optical transmission of the solutions under test as good as that of the solution of terphenyl in xylene in Fig.II 2 since a small absorption of light in the solution causes a large attenuation of the output pulse because of the long light paths in the solution due to multiple reflections from the cell walls.

(e.g. a cell 3" x 1" x 1" with collection through 1" x 1" face.

Mean path per reflection ~ 2".

Mean number of reflections ~ 10

Mean path of light collected = 20"

This simple calculation shows that an absorption as small as 1% per cm. will cause a large attenuation of the output pulse)

II(2) (b) Reflection Experiments

Mr. R. Giles and Mr. D. Silverleaf, in the Glasgow Physics Department had previously considered the best type of material for reflection of light from the scintillator to the photo-multiplier cathode. The bad reflection coefficients of metals ruled out the use of metallic containers. They found that the best known and easily available reflectors were various white powders, of which the most efficient was magnesium oxide. Because of the impracticability of making a container with walls of Magnesium oxide, a cell with transparent walls was made and packed round with the powder. The reflection coefficient of the powder is shown in Table II 1.

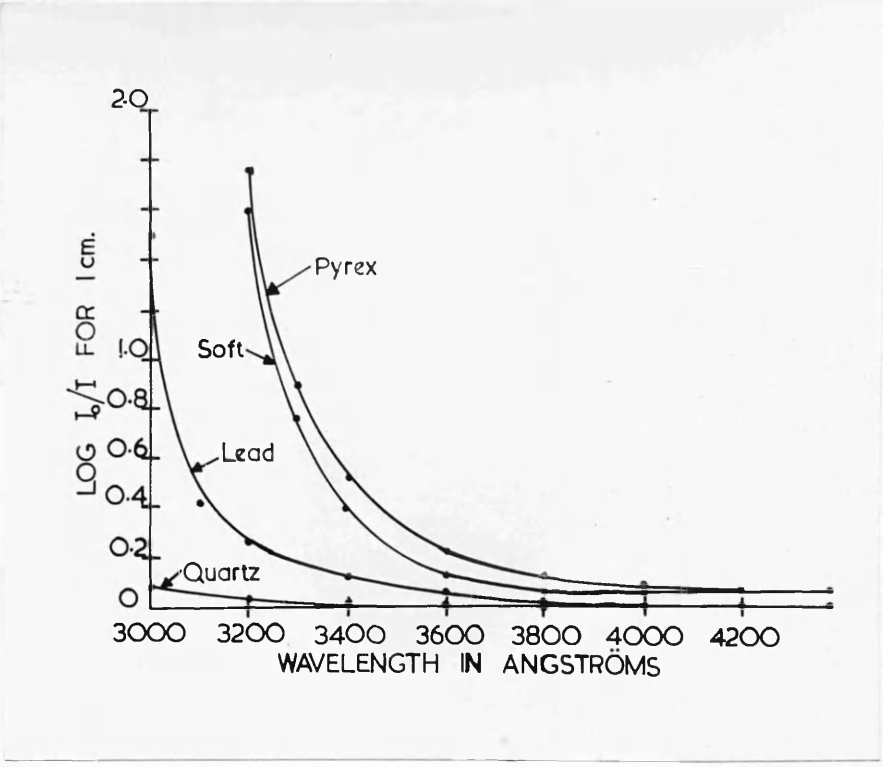

FIG. II.3. TRANSMISSION CURVES FOR GLASSES

FIG. II.4 VARIOUS SCINTILLATION CELLS

Wavelength in A°	3500	4000	4500	5000	5500
Reflection Coefft. %	96	97.2	98	98.6	99.1

TABLE II.1.

During the course of investigation into the properties of the powder the author found that the substance had to be used in a very dry form before the best reflection was obtained. A specially prepared white paint was also tested for reflecting properties but comparison of the pulse heights from an identical scintillator with a magnesium oxide covering showed that the paint produced a large attenuation of the pulses. This effect was due to the bad reflection properties of the oil content of the paint which made contact between the container and the titanium oxide base of the paint.

II(2) (c) Materials of the Containers

The transmission curves of various glasses and quartz were measured and specimen containers constructed. These curves are shown in FIG.II.3. From these curves and experiments on specimen containers, it was evident that the most satisfactory container material was quartz, which absorbs a negligible amount of light at the emission wavelengths of the scintillators. Fig. II.4. is a photograph of the scintillation cells constructed, both in quartz and glass, during the course of the author's work. More details of the shape of the cells will be considered in later sections of the thesis.

II(2) (d) Contact Fluids

Experiments were performed to obtain some information on the most suitable material for use as a contact between the quartz end-plate of a cell and the glass surface of the multiplier to avoid losses due to total reflection at an air gap between these two surfaces. Such an air gap has been found to produce an attenuation of pulse height of 50%.

Measurements of the transmission properties of glycerine, liquid paraffin

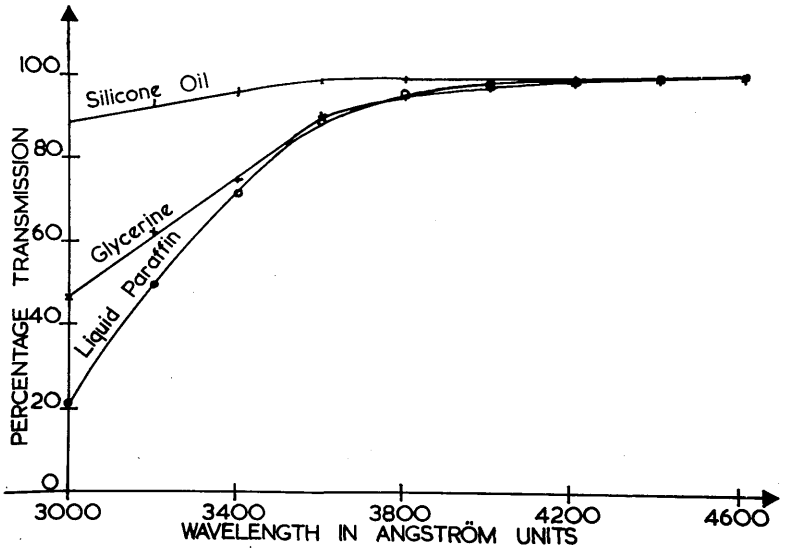

FIG. II.5 TRANSMISSION CURVES FOR CONTACT FLUIDS

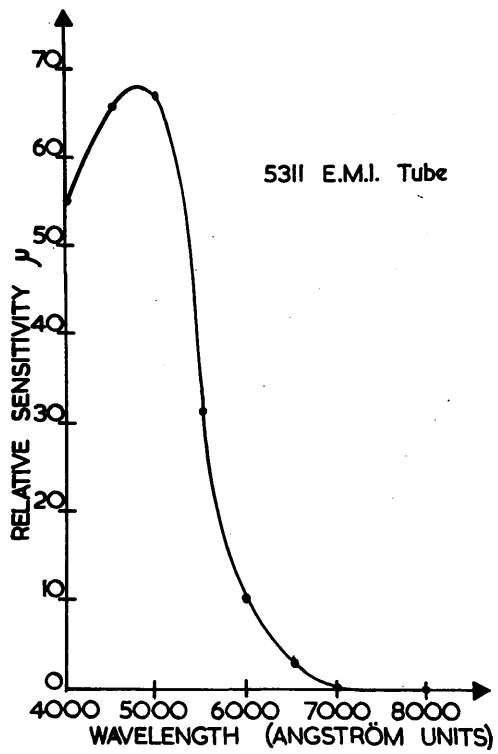

FIG. II.6 SPECTRAL RESPONSE OF EMI 5311 PHOTOTUBE

and silicone oil showed that these materials were transparent to wavelengths greater than 4000 A° (FIG. II.5.). Of these silicone oil was used as the contact fluid because of its advantages in being more viscous and having better light transmission and electrical insulating properties.

II(2) (e) Emission Spectra of Liquid Scintillators

The spectral response of thephotocathode of the E.M.I. 5311 multipliers used in these experiments, is shown in FIG. II.6. From this, it is clear that for maximum light conversion efficiency the wavelength of the emitted radiation should fall in the region 4500 -- 5000 A°, where the photo-cathode has its maximum sensitivity. It is also noteworthy that the problem of light collection is eased considerably by operation at the longer wavelengths, since the greater the wavelength the better is the reflecting power of the magnesium oxide powder (TABLE II.1.). Data on the emission spectrum of terphenyl in xylene (Kallmann(1)) showed that the wavelength of the radiation lay in the region from 3250 — 4000 A°, i.e. outside the region of maximum response of the photo-cathode and in a low efficiency range for the reflecting powder. Work reported by Kallmann, showed that it was possible by the addition of small quantities (~0.1 g/l) of a second solute to increase the wavelength of the emitted radiation. Of the chemicals investigated the two most successful were anthranilic acid and phenyl alpha-naphthalamine. The latter is the one now used by the author. In this case, an increase in pulse height of about 40%, to X-rays of energy of the order of 1 MeV, was obtained when the response of a standard scintillator filled with 5 g/l terphenyl in xylene was compared with the same cell filled with 5 g/l terphenyl in xylene plus 0.1 g/l phenyl alpha-naphthalamine.

II (3) PHOTO-MULTIPLIER TUBES

II.(3)(a) INTRODUCTION

In the application of scintillation counters to the measurement of particle energies it is important to know the lower limit of energy, for a particular type of particle, which can be recorded using a scintillator in conjunction with a particular multiplier. This lower limit is governed by the quantum conversion coefficient of the photo-cathode (i.e. the average number of photo-electrons released per quantum of energy of the particular wavelength). This coefficient is the order of 5% for the E.M.I. 5311 multiplier used with a liquid scintillation counter. A calculation based on this figure shows that the minimum energy of electrons which can be detected is ~ 6000 eV. and of protons ~ 12,000 eV. This means that an electron of energy ~ 6 KeV, incident on a liquid scintillation counter, will on the average release sufficient light to knock one photo-electron from the photo-cathode. (For adequate resolution of a particle energy, however, it is necessary that the number of electrons released from the photo-cathode be sufficient to reduce the possible statistical fluctuations in the number of output electrons from the collector to a few per cent. Thus the 6 KeV electrons considered above set the lower limit of detectable energy, but not the lower limit of resolvable energy.)

II.(3) (b) Variation of tube gain with Multiplier Voltage

The variation of output pulse height P from the E.M.I. 5311 multiplier with equal stage voltages and total applied voltage V, is given by the relation $P = KV^n$ where n is a constant of the order of 7.7. This figure has been obtained by the author using a standard source and scintillator together with a multiplier, cathode follower and amplifier. It is a useful property of the photo-tube that the gain can be easily varied by alteration of the total voltage across it. This sensitivity to voltage, however, necessitates the use of a

well regulated high voltage supply because it is clear that a small change in E.H.T. voltage can cause a large change in the output signal. The high voltage supply for the tubes used by the author was obtained from a standard T.R.E. 2 KV power pack, whose stability proved very satisfactory, provided its mains input was monitored.

II (3) (c) Stability of Response

During an investigation into the properties of these photo-tubes a slight alteration of gain was noted after certain running times. At the beginning of an experiment the gain changed slightly, until a stable condition was reached after about 30 minutes, and again after long periods of continuous running the gain of the tube decreased, returning to the normal running value after a recovery time of the order of 24 hours. These effects were ascribed to fatigue of the photo-cathode causing a change in the conversion efficiency. For consistent results it was necessary to ensure that stable conditions were obtained during an experiment.

II (3) (d) Investigations of Noise

In the use of photo-multiplier tubes with scintillation counters a major difficulty has been encountered by many investigators due to the presence of small pulses at the multiplier output in the absence of any external excitation. These pulses are called Noise or Dark Current Pulses and can be traced to the following causes :-

(a) Emission of thermal electrons from the cathode and dynode surfaces with subsequent amplification in passing down the tube to the collector.

(b) Positive ions formed by the ionisation of the residual gas in the tube causing electrons to be emitted from the cathode, when they strike it.

(c) Cold emission of electrons from projecting metallic parts inside the tube. This effect is only pronounced at high working voltages.

Many investigations on the properties of the noise pulses in photo-multiplier

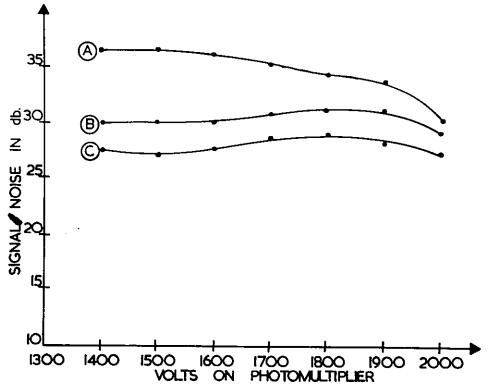

(A) V_{c1} = 2V

(B) V_{c1} = V

(C) V_{c1} = $\frac{1}{2}$V

V = Volts on other sta

FIG. II.7 VARIATION OF CATHODE - 1ST DYNODE VOLTAGE

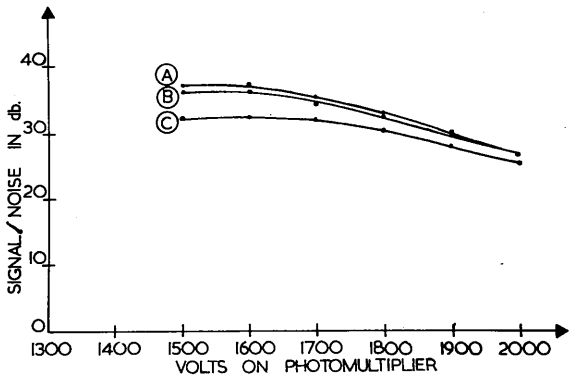

(A) 1ST DYNODE VOLTAG

(B) CATHODE VOLTAGE

(C) 100V W.R. TO CAT

FIG. II.8 VARIATION OF ELECTROSTATIC SHIELDING VOLTAGE

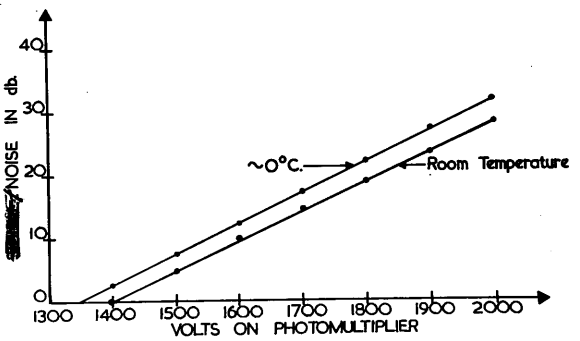

FIG. II.9 TEMPERATURE VARIATION

tubes have been performed. Morton (2) and Engstrom (3) are among many workers who have considered the effects of noise in R.C.A. type 931A tubes. The author decided that the noise properties of E.M.I. 5311 tubes, on which no work had previously been published, would be useful when operation of the tubes in the detection of small scintillations was made. In a case of this kind it has been found that the size of noise pulses is comparable with the signal pulse from the scintillations. It is thus clear that methods of reduction of noise pulses are very important.

The following series of experiments was performed to find, under what conditions, the number and size of the noise pulses was a minimum.

The apparatus consisted of liquid scintillator, multiplier, cathode follower, amplifier, discriminator, and scaler. The experimental method was the following:-

A "standard" pulse height was noted by setting the discriminator at a fixed value throughout, and varying the gain of the amplifier until the scaler counting rate was 100 per sec. This "standard" pulse height was obtained from the scintillation produced in a quartz standard cell (FIG.II.1.) by Co^{60} X-rays. As an indication of both noise pulse height and number of noise pulses, the amplifier gain setting was altered until the counting rate, in the absence of the Co^{60} source was 100 per sec. with the same fixed discriminator setting as before. (This setting is fixed so that at no time is noise from the amplifier, when working at high gain, counted.) The difference in the amplifier gain was taken as a measure of the relative value of noise and the "standard" signal pulses. The difference of gain in decibels gave a measure of the signal to noise ratio.

EXPERIMENTS PERFORMED

I. The graphs of FIG.II,7 show the variation of signal to noise ratio as the voltage between the cathode and the first multiplying dynode is varied. From these results it emerges that :-

(1) the best permissible operating condition is that in which the voltage drop across the first stage is double that across any other stage,

(2) from the slope of the graphs it is clear that at high operating voltages, not all the noise pulses originate at the photo-cathode, because if this were the case the signal to noise ratio would be constant.

The variation of voltage across other stages of the tube does not appreciably affect the signal to noise ratio.

II. Electrostatic Shielding near the cathode.

Morton (2) in his experiments on the noise pulses in a 931A photo-multiplier attempted to find the effect of an electrostatic shield placed near the photo-cathode. A similar type of experiment was performed by the author using an E.M.I. 5311 photo-multiplier. The graphs of FIG.II.8 show the variation of signal to noise ratio with E.H.T. voltages and change of potential of the electrostatic shielding (obtained by using a conducting band of Aquadag painted round the upper part of the tube). From these graphs it appears that the shield should be held at the same voltage as the first dynode to give best signal to noise ratio. It was found that, for higher voltages on the shield, although the signal to noise ratio did not alter appreciably, the effective signal pulse height was reduced. This effect of reduction of noise is probably due to the attraction, by electrostatic potential existing on the inside wall of the photo-multiplier, of noise electrons originating from the outside edge of the photo-cathode. These results are similar to those obtained by Morton for the RCA 931A tube.

III. Temperature Variation on the Multiplier

The most satisfactory method of reduction of the noise level in a photo-tube has been found, by various authors, to be cooling of the photo-cathode. In an attempt to perform an experiment of this type the author encountered serious difficulties, namely :-

(a) condensation of moisture resulting in breakdown of electrical insulation,

(b) fear of cracking the glass envelope of the multiplier,

(c) fear of stripping of the photo-cathode material if the tube was cooled so that the unequal expansion of the glass and the cathode material became apparent,

(d) freezing of the scintillating liquid if the cell was brought too close to the cooling agent, and also crystallisation of the solution.

A simple qualitative experiment was, however, performed to determine the effect of cooling the tube, through a few degrees. The atmosphere inside the sealed multiplier container was dried for a day using a silica-gel drying agent.

The graph of FIG.II.9. gives the effects on noise level of cooling through a few degrees. The graphs are sufficient to show the importance of this cooling on the elimination or reduction of noise in photo-multipliers.

From the results of these experiments it is clear, that, by far, the most important effects are produced by alterations in the temperature and distribution of potential between the multiplier dynodes.

II.(4) COLLECTION OF LIGHT FROM VOLUMES OF LIQUID SCINTILLATORS

II.(4) COLLECTION OF LIGHT FROM VOLUMES OF LIQUID SCINTILLATORSnd measure the energies of radiations from sources of low strength or at large distances from a source. In order to provide reasonable efficiency in these experiments one requires the use of scintillators of large volume.

The development of liquid scintillators has made the construction of scintillators of any size or shape an easy matter. This is indeed a great step from the limitations encountered with crystals for which it is very difficult to obtain large non-opaque volumes. The main difficulty in the case of liquids in large volumes is that of collection of light from a scintillation.

In collection of light from a volume of liquid two points must be noted :-

(a) is the light collected merely sufficient to allow one to say that a particle has passed through the liquid?;

(b) is the light collected proportional to the energy which has been dissipated by the event which has taken place in the scintillator?

In case (a) the amount of light collected need only be sufficient to cause a pulse to appear at the output of the photo-multiplier, which is large enough to distinguish it from photo-tube noise. In case (b), however, the light collection must be uniform over the volume of the liquid and also that enough light is obtained from each event so that statistical fluctuations in the pulse height are unimportant.

It was decided, therefore, to investigate the variation in pulse height from scintillators of different sizes when a fixed energy of γ-rays was incident. (In this case the 1.28 MeV γ-rays from Na^{22}.) The variation of pulse height resolution was determined by observation of the Compton distribution of these γ-rays. The method of determination of resolution will be discussed in the next section.

The results obtained are shown in Fig.II.10. In order to discuss this rapid variation in resolution we must consider the factors influencing the collection of light from a scintillation.

APPROXIMATE THEORETICAL TREATMENT OF LIGHT COLLECTION

Let us consider a particle of energy E incident on the liquid scintillator; then we have :-

the number of photo-electrons per scintillation = $\frac{E.A.C.B.T.G.}{E_{PH}}$

where A = Amount of Energy absorbed ~1 unit

C = Energy Conversion Efficiency in scintillator ~1%

B = Efficiency of Photo-cathode ~5%

T = Coefft. of Transmission of radiation ~1

E_{PH} = Energy of photon of light emitted by the scintillator ~3eV

G = Geometrical Factor in light collection.

It is thus obvious that in most cases the important factor is G. The following analysis is an attempt to explain the variation in resolution by variation of this factor, assuming, as unimportant the statistical variations introduced by the photo-multiplying process.

We consider a liquid scintillator surrounded by MgO powder and of length ℓ ins and diameter 1" where collection of light is obtained from one of the flat ends.

Suppose x = fraction of surface from which collection is made

S = fraction of light absorbed at each reflection.

Then if we consider the light emitted isotropically and uniformly in a scintillator surrounded with MgO powder.

Then fraction of light collected

$$= x + x(1-x)(1-S) + x(1-x)^2(1-S)^2 +$$

i.e. = Direct light + 1st Reflection + 2nd Reflection +

$$= x(1 + (1-x)(1-S) + (1-x)^2(1-S)^2 +$$

$$= \frac{x}{1-(1-S)(1-x)}$$

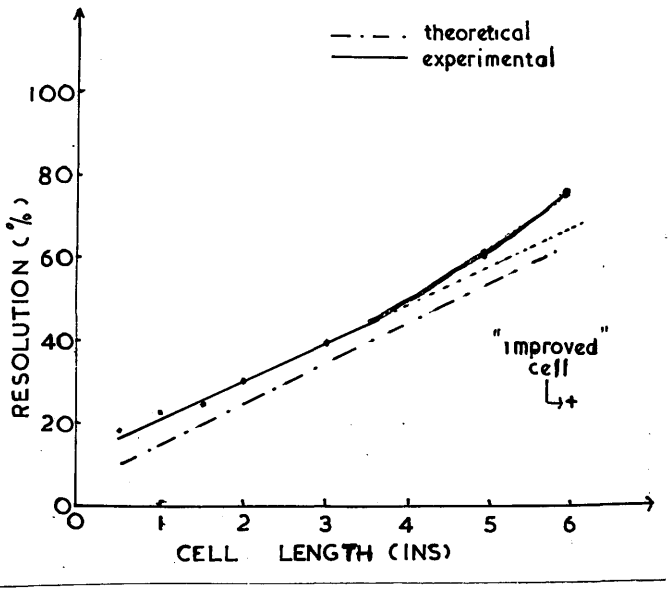

FIG.II.10 VARIATION OF RESOLUTION WITH SIZE OF SCINTILLATOR

SOLVENT	ABSORPTION LENGTH (cm.)
TOLUENE	25
BENZENE	30
XYLENE	15

TABLE II.2

If now we consider a cell in which a scintillation is emitted at a point, and y is the fraction of this light directly incident on the window, and if we assume that after the first reflection the light is uniformly distributed throughout the volume, then the fraction of light collected is given

by $F = y + \frac{(1-y)(1-S)x}{1-(1-S)(1-x)}$

The spread in resolution is determined by the maximum and minimum values of y.

For $o < y < \frac{3}{4}$ then

$$\frac{Fmax - Fmin}{Fmin} = \frac{3\,S}{4(1-S)x}$$

but $x^{-1} = 2(1 + 2\ell)$

$$\therefore \quad \frac{Fmax - Fmin}{Fmin} = \frac{3S.2(1+2\ell)}{4\,(1-S)}$$

S = 0.03 for MgO powder at ~4000A

Giving as % Resolution = $10\ell + 5$

This approximate relationship is shown in FIG. II.10. The agreement with the experimental results is quite good up to the order of 3". At larger volumes, however, the effects of T , the transmission factor, be comes more important. It has been noted by Harrison (4), that liquid scintillators absorb their own radiation. Table II.2 gives the absorption lengths for various liquids. It is this factor which influences greatly the resolution at larger volumes.

Another factor which is not quite so important to the resolution for a fixed incident energy is the variations introduced by the amplication process in the photo-multiplier. It has been shown by Garlick and Wright (5) that this is a comparatively unimportant factor in comparison with the fluctuations introduced by non-uniformity in light collection in scintillation cells at the energy of X-rays which we have considered.

With a $\frac{1}{2}$" liquid scintillator the author has observed the effects of the

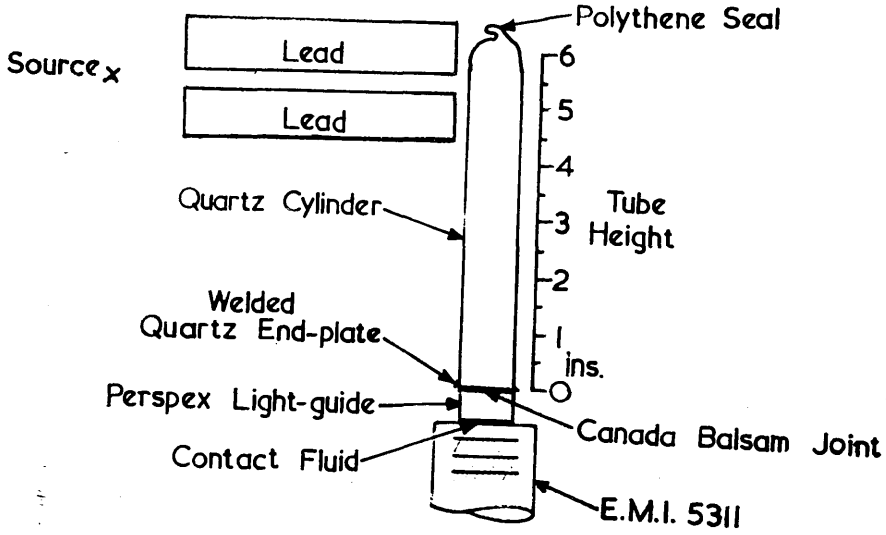

FIG. II.11

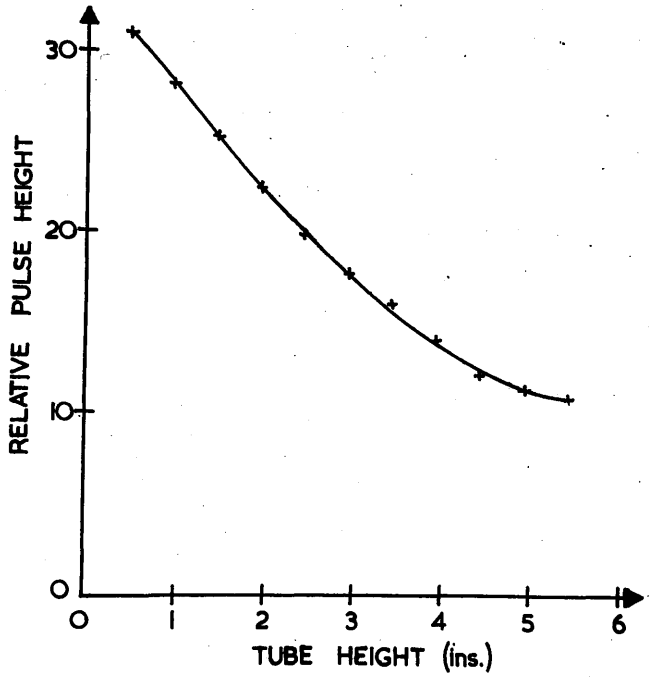

FIG. II.12

multiplier on the resolution of different energies of X-rays. The results obtained agree with the law $R \propto E^{-\frac{1}{2}}$ which has been observed by other investigators such as Garlick and Wright (5).

From the above discussion we have noted that in a large volume of scintillator absorption of light takes place in the liquid itself and at reflection from the walls of the container. This implies that the efficiency of light collection depends very much on the place of origin of the scintillation in the volume. The measurement of particle energies using a large volume of scintillator is thus impossible because of the adverse effect on the pulse height distribution of non-uniformity in light collection.

Accordingly an attempt was made by the author to investigate the possibility of collecting uniformly light from a quartz cell 6" long and 1" in diameter filled with a solution of 5g/l terphenyl in xylene.

The apparatus consisted of the cell, EMI 5311 phototube, cathode follower, amplifier, discriminator and scaler. The method used to compare pulse heights from different positions in the cell was as follows (FIG. II.11).

A well collimated beam of Co^{60} X-rays was incident on the cell in a direction normal to the cylindrical axis, at any selected point, and the setting of the discriminator for which the scaler counting rate was 100 per sec. was noted. This bias setting was taken as a measure of the pulse height produced by a Co^{60} X-ray at that part of the tube in the line of the incident beam. (This assumes that the shape of the pulse height distribution does not depend on beam position, a reasonable assumption provided the bias setting is much lower than the Compton edge). By varying the position of the beam along the length of the cell it was thus possible to obtain a graph of pulse height against position of origin of the scintillation along the tube.

Fig. II.12 shows the results obtained when the cell was surrounded with closely packed MgO powder. Losses in transmission and reflection provide an attenuation

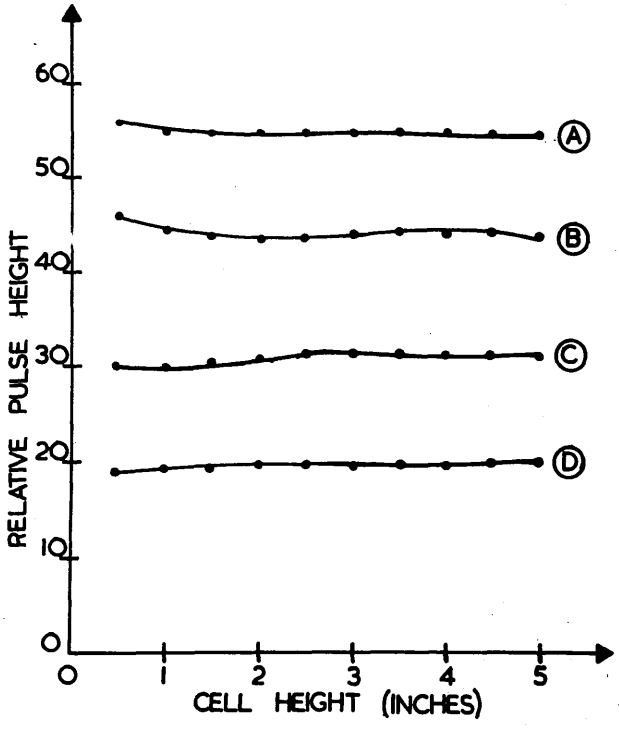

FIG.II.13 LONG CELL RESPONSE

(A) CELL WITH $\frac{1}{2}$" PERSPEX LIGHT GUIDE + SECOND SOLUTE

(B) CELL WITH $\frac{1}{2}$" PERSPEX LIGHT GUIDE

(C) CELL WITH 3" PERSPEX LIGHT GUIDE

(D) CELL WITH 3" DISTRENE LIGHT GUIDE

of a factor of, nearly, 3 in the light originating from the far end of the cell. It was, therefore, decided to attempt to obtain better uniformity of light collection by a deliberate sacrifice in the efficiency of light collection from the nearer end of the cell.

The tube and photomultiplier were separated and light pipes consisting of 3" lengths of perspex and distrene, 1" in diameter, introduced to convey light from the tube to the photo-cathode. These light pipes reduce the pulse height from the nearer parts of the cell by reducing the solid angle of acceptance of light between the end of the cell and the photo-cathode. In these experiments it was found by the author that the perspex light guide was more transparent to the radiation than that of distrene. (FIG. II 13.C & D).

The final arrangement which gave very uniform light collection was one in which the top 3" of the cell was packed with MgO powder and the bottom 3" with Aluminium foil (a reasonably efficient reflecting material although not as good as MgO), together with a $\frac{1}{2}$" perspex light guide (FIG. II 13.B). Comparison of this result with FIG. II.12 shows the greatly increased uniformity which has been obtained. Admittedly some sacrifice of overall pulse height was necessary to achieve this result. Further experiments on the addition of phenyl alpha-naphthalamine as a secondary solute to the terphenyl solution, to a concentration of the order of 0.1 g/l, have shown that the uniformity of light collection can be maintained with increase in pulse height to the initial high level (FIG. II.13.A.) The resolution of this improved cell for 1.28 MeV γ-rays is shown in FIG. II.10.

In this section we have seen that the advantages of liquids in case of construction of large volumes, is rather offset by the difficulty in uniformity of response. The initial research described in this section shows clearly the degree to which this uniformity is present. The second experiment gives one

method by which this problem may be solved. Other methods, notably the use of a large number of photomultipliers, as used by Harrison (6), have been employed in this type of light collection problem.

These previous sections have been devoted to the description of the development work carried out by the author in the preparation of liquid scintillation counters for practical applications. The subsequent section in this part of the thesis describes their performance in detection of nuclear radiations.

II.(5) RESPONSE OF LIQUID SCINTILLATORS TO NUCLEAR RADIATIONS

The most notable difference between inorganic and organic scintillators is the relatively poor response of organic phosphors to heavily ionising radiations, such as protons. This featureof organic scintillators was first noted by Broser et alia (7) and is extremely important in considering the response of liquid scintillators to neutrons, with which the author is primarily concerned. It has also been noted by Kallmann and Furst (1) that liquid scintillators show a saturation of light output as the concentration of the solution is increased. In the case of a solution of terphenyl in xylene the maximum light output is given at a concentration of 5 g/l. In this section the interest is mainly centred in the practical implications of this poor response in neutron spectrometry, although an attempt has been made to correlate the present research with that of those investigators who are aiming at the elucidation of the problem of the fluorescent mechanism.

The author has investigated the type of response, energy dependence, and efficiency of a solution of terphenyl in xylene of concentration 5 g/l, to X-rays and neutrons. From these experiments the energy response of electrons and protons has been derived.

II.(5) (a) Response to X-rays

In order to prepare the liquid scintillation counters for neutron spectrometry the author has found extremely valuable the use of X-ray sources, such as Na^{22} (0.5 MeV and 1.28 MeV), Co^{60} (1-17 MeV and 1.33MeV) and ThC" (2.64 MeV). These sources have provided an adequate range over which pulse height investigations in the counter can be carried out. To make full use of these results it was necessary to consider in some detail the interactions of X-rays in organic liquids.

From the absorption coefficients shown in FIG. II.14, it is obvious that the principal interaction in the energy range from 20 KeV to 20 MeV is Compton Effect.

FIG. II. 14

$$K_{Compton} = \frac{K_{co}A_o}{\rho_o Z_o} \cdot \rho\frac{Z}{A}$$

$$K_{Pair} = \frac{K_{po}A_o}{\rho_o Z_o^2} \cdot \rho\frac{Z^2}{A}$$

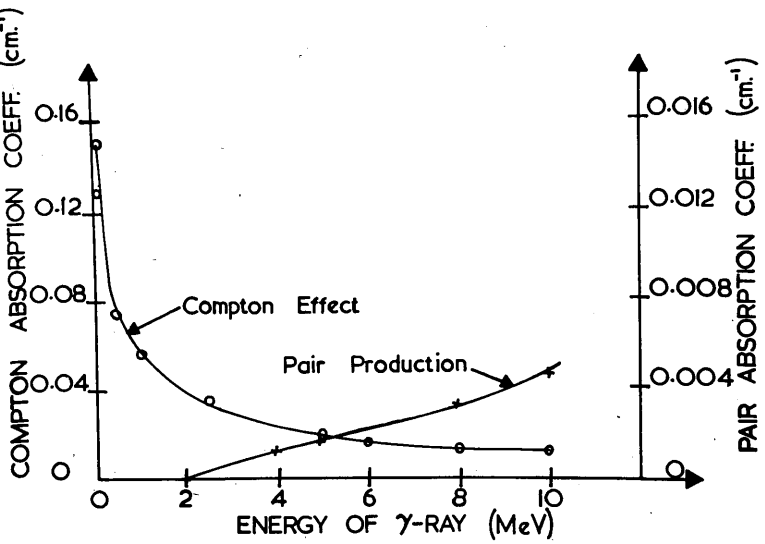

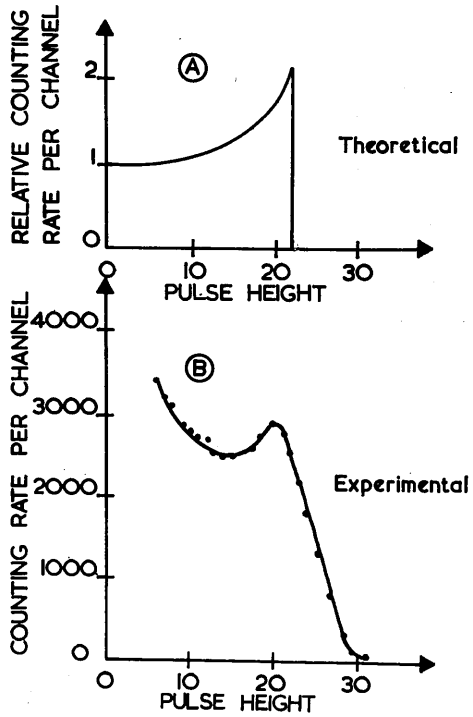

FIG. II.15

RESPONSE OF SCINTILLATOR TO γ-RAYS

(These coefficients have been calculated from the data on lead, given by Heitler (8) using the formulae in FIG.II.14). The efficiency per cm. of solution can easily be obtained from this curve and is found to be the same order of magnitude as for neutrons (q.v.).

Type of Response

The expected distribution of electron energies in Compton scattering of γ-rays is given by the Klein-Nishina formula and is shown graphically in FIG.II.15A. The experimental pulse height distribution from a 1" liquid scintillator, of the type in FIG.II.1B, from a source of Co^{60} γ-rays, is shown in FIG.II.15B. The distribution has been obtained using the single channel kicksorter described in Appendix II.

The large number of small pulses and slope on the high energy edge, which distort the theoretical distribution, can be traced to a number of causes such as wall effects, background, light collection, photo-tube statistics, and the finite channel width of the analyser. A more detailed analysis of these factors will be given later in this section when reference is made to neutron detection.

Resolution

The maximum energy given to an electron in Compton Scattering of γ-rays is :-

$$E = \frac{2\alpha h\nu_o}{2\alpha + 1} \quad \text{where } \alpha = \frac{h\nu_o}{m_o c^2} \qquad m_o = \text{electron rest mass.} \quad h\nu_o = \text{incident energy}$$

The method used by the author, similar to Jordan (9), to determine the position of the maximum electron energy, and therefore the γ-ray energy, is to find the point of inflexion of the Compton edge, by differentiation of the pulse height distribution of FIG.II.15B. This method also serves to indicate the energy resolution of the counter by measurement of the full width at half height of this differential curve. (This method is also applied in the case of neutron spectra q.v.)

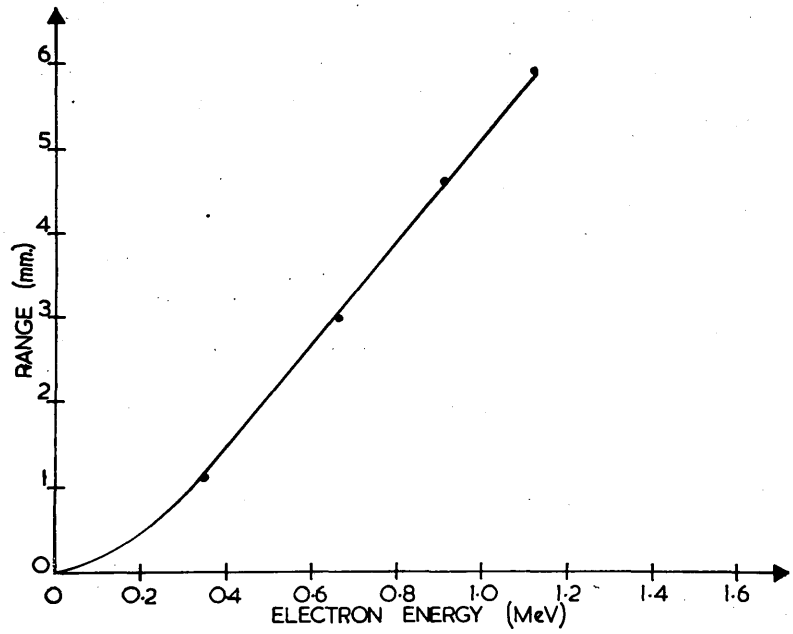

FIG.II.16 RANGE v ENERGY FOR ELECTRONS IN XYLENE

In the case of FIG.II.13B the two Co^{60} γ-ray lines at 1.17 MeV and 1.33 MeV are not resolved and the effective resolution is 30%. With a single line the counter's resolution is 20%, see FIG.II.10 for the case of Na^{22} 1.28 MeV γ-ray.

Later in Part III mention will be made of a double scattering γ-ray spectrometer, of a type similar to that described by Hofstadter (10), using two liquid scintillation counters. It was thought useful to compare the results of the pulse heights from various γ-ray energies and from these to estimate the response of liquid scintillators to electrons.

II.(5) (b) Response to Electrons

(i) Electron Range-Energy Relationship in Organic Liquids

In the construction of a counter to stop electrons it is important to know the range-energy relationship in liquid scintillators. This is shown in FIG.II.16, the data having been obtained from that on aluminium by conversion on a density scale.

(ii) Pulse Height v Energy for Electrons in Organic liquids

FIG.II.17A gives the pulse height-energy distribution for electrons in a solution of 5 g/l terphenyl in xylene. Although no direct experiments were performed on electrons, the relationship has been obtained by correlation of the data from single and double scattering of γ-rays in the solution. The legend to FIG.II.17A gives the experiments from which the points in the curve have been derived. In the range from 0.5 MeV to 2.4 MeV the response to electrons is found to be linear. Comparison with results from a 1 cm cube crystal of anthracene shows the distribution to be similar with the effective pulse height ratio of anthracene to the solution of the order of 3.

No investigations have been carried out by the author to investigate the low energy region of the curve ($<$ 100 KeV) where it is expected that, as has been found by Taylor (11) for anthracene and stilbene FIG.II.17B, the relation

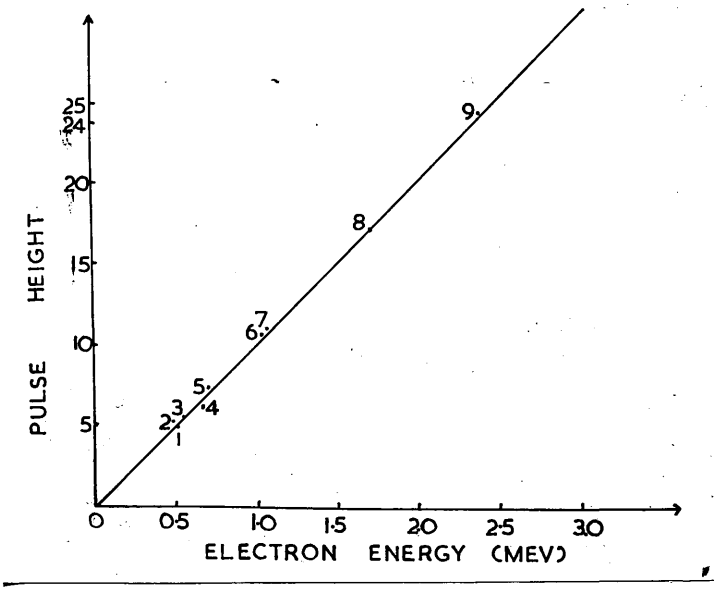

1. Na^{22} at 0.5 MeV
2. } Co^{60} γ-rays 1.17 & 1.13
3. } Scattering at 56°
4. Cs^{137}
5. Na^{22} 1.28 MeV Scattering at 52°
6. Na^{22} Compton Edge for 1.28 MeV
7. Co^{60} Compton Edge
8. ThC'' 2.62 MeV Scattering at 52°
9. ThC'' Compton Edge

FIG. II.17A PULSE HEIGHT v ENERGY FOR ELECTRONS IN SOLUTION OF TERPHENYL IN XYLENE

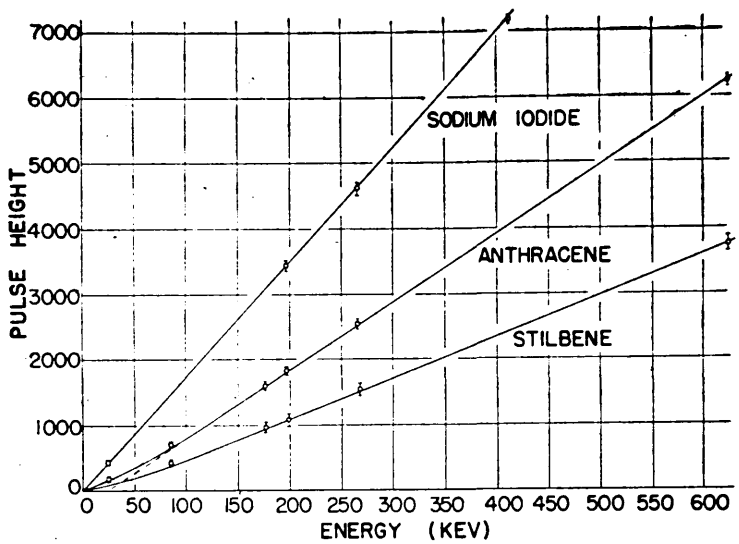

FIG. II.17B PULSE HEIGHT v ENERGY FOR ELECTRONS (TAYLOR (11))

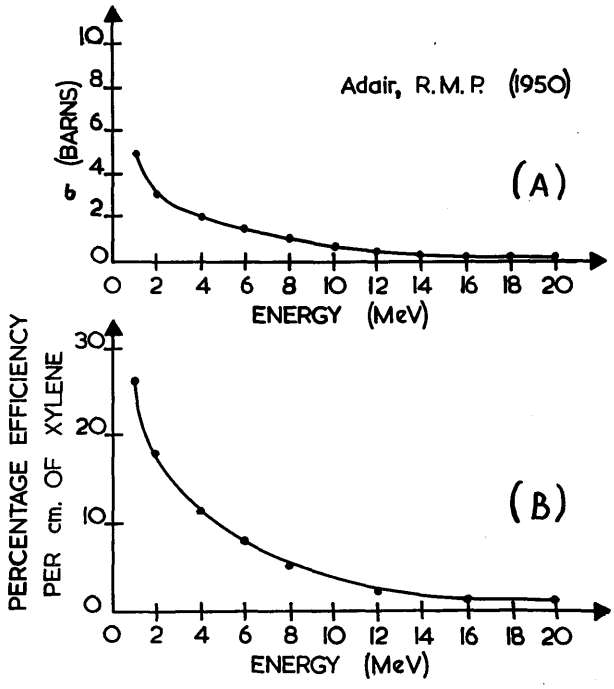

FIG. II.18(A) CROSS-SECTION FOR NEUTRON-PROTON SCATTERING

FIG. II.18(B) EFFICIENCY OF XYLENE FOR STOPPING NEUTRONS

deviates from linearity. This linearity of response to electrons in the energy range 0.5 MeV to 2.4 MeV has greatly simplified the author's work on counter calibration for neutron spectrometry.

II(5) (c) Response to Neutrons

Fast neutrons produce scintillations by the formation of proton recoils in these liquid scintillators.

(i) Efficiency to Neutrons

The efficiency of the solution of terphenyl in xylene to fast neutrons can easily be calculated from the cross-section for elastic scattering of neutrons by protons given by Adair (12) and shown in FIG.II.18A. It has been concluded by various investigators, e.g. Draper (13) that the effects of Carbon in organic scintillators is negligible. The percentage efficiency of xylene, and thus, to a good approximation, the solution, in stopping neutrons is shown in FIG.II.18B.

(ii) Pulse Height distribution for neutrons

It is well known that the scattering of neutrons by protons is practically isotropic, in the centre-of-mass system, for neutrons in the energy range from 0 to 20 MeV. We must thus consider, firstly, the elastic collision of neutrons and protons. FIG.II.19 gives, in the laboratory system, the collision diagram.

From this we have

$$E_n = E_o \cos^2\theta \quad (= \text{Scattered neutron energy})$$

$$E_p = E_o \sin^2\theta \quad (= \text{Scattered proton energy})$$

It follows that the distribution of proton recoil energies is given by

$$\frac{dN}{dE} = \frac{No}{E_o} \quad \text{for } E < E_o \quad \ldots\ldots (1)$$

$$= 0 \quad \text{for } E > Eo$$

where dN is number of proton recoils in energy interval E to E + dE.
and Eo is energy of incident neutrons
and No is total number of scattered neutrons.

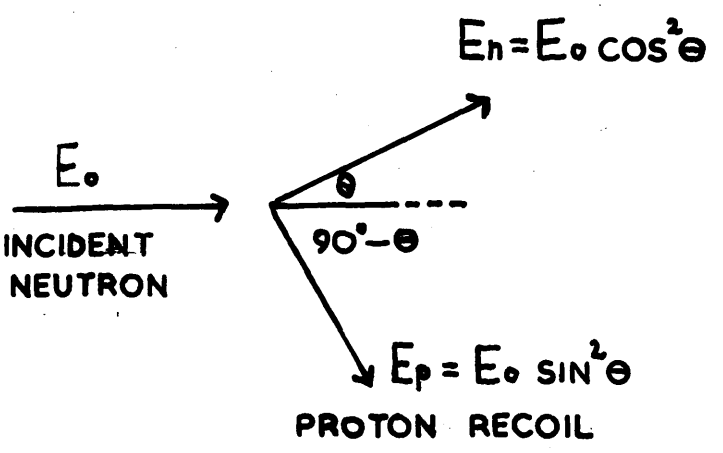

FIG. II.19 COLLISION DIAGRAM FOR NEUTRON AND PROTON (LAB. SYSTEM)

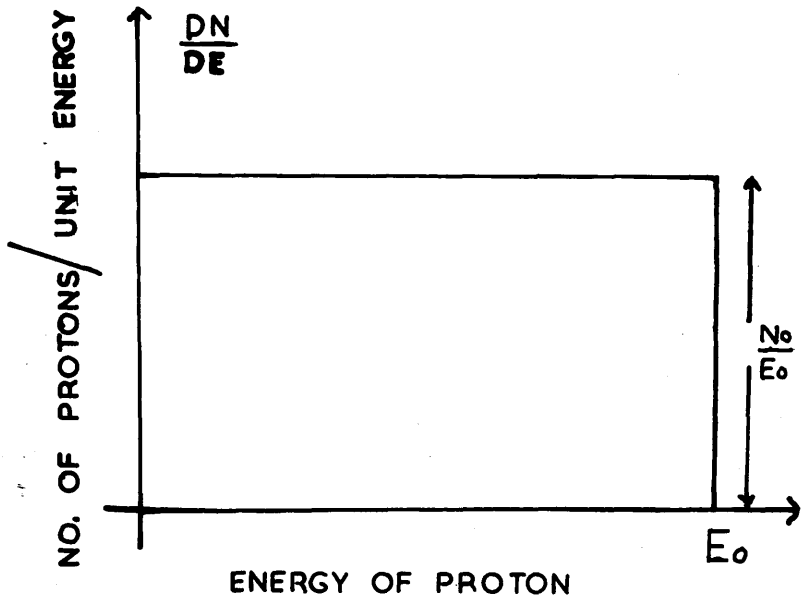

FIG. II.20. PROTON RECOIL DISTRIBUTION FROM ONE NEUTRON GROUP

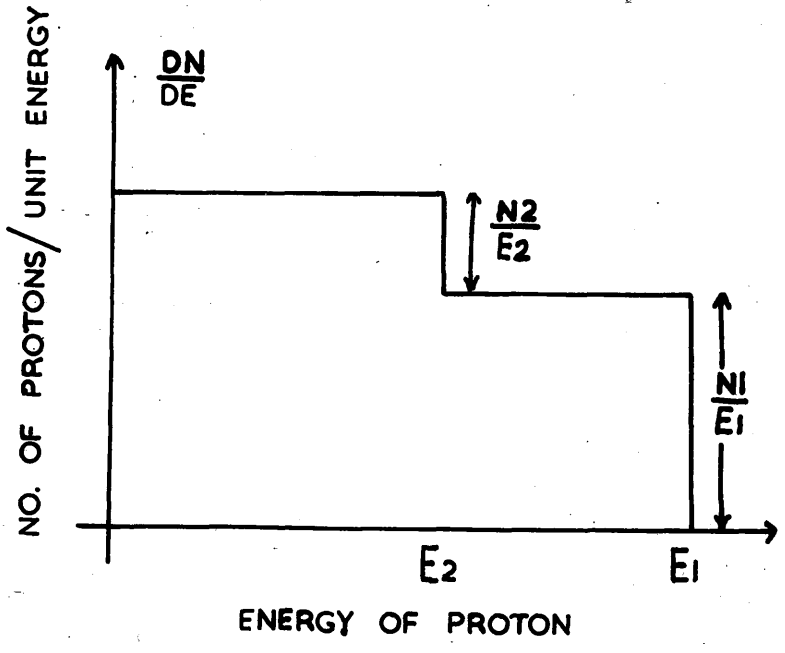

FIG. II.21 RECOIL DISTRIBUTION FOR TWO NEUTRON GROUPS

This gives the step function shown in FIG.II.20. For an incident beam of energies E_1 and E_2 and total scattered intensities N_1 and N_2 the distribution would take the form shown in FIG.II.21.

In practice, the recoil proton energies are measured by observing the pulse height distribution from a liquid scintillator. Several factors are responsible for the distortion of the theoretical distribution of FIG.II.20. The major effects are the following.

(a) Non-linearity of the pulse height v energy distribution for protons in organic scintillators.

The author, in considering this problem in its initial stages, assumed that the pulse height v energy distribution for protons in the solution was similar to that observed by Taylor et alia (11) for anthracene. (Later the distribution was derived from results obtained by the author, see part II(5) (d)).

The law can be written to a first approximation as

$$L = K E^{1.3} \quad \ldots (2)$$

L = light output

E = proton energy

K = constant

The effect of the non-linearity to protons on the response to neutrons is obtained from equation (1) and (2), giving $\frac{dN}{dL} = \text{const.} L^{-\frac{1}{4}}$ and shown in FIG.II.22.

(b) Multiple Scattering

In the case of crystals having efficiencies greater than about 10%, multiple scattering can cause a change in the pulse height spectrum for neutrons. The effect on the distribution of FIG.II.20 is to cause a peak to appear at the high-energy end of the spectrum. Segel (14) has made an estimation of this effect for (D-D) neutrons incident on a 2 cm x 2 cm x 1 cm stilbene crystal. FIG.II.23 clearly shows the change in shape obtained in these calculations. This effect

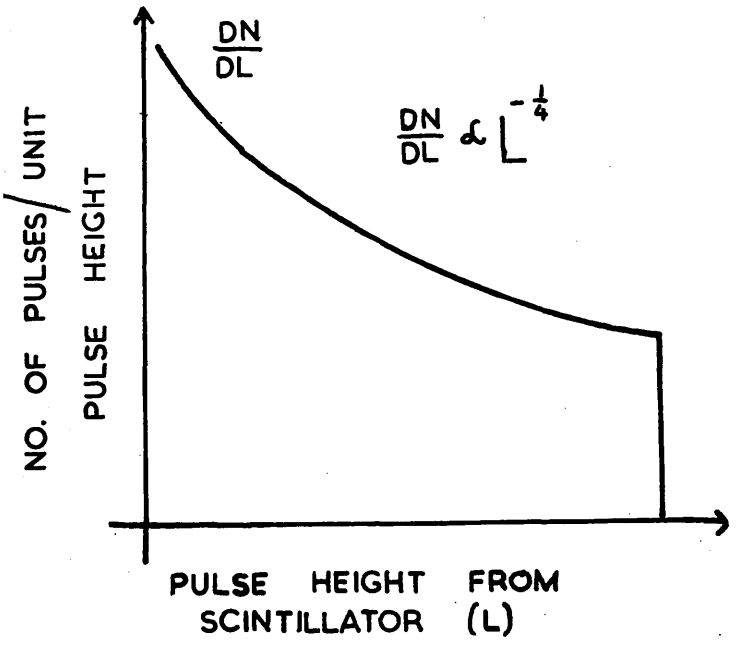

FIG. II.22 RECOIL DISTRIBUTION WITH NON-LINEARITY TAKEN INTO ACCOUNT.

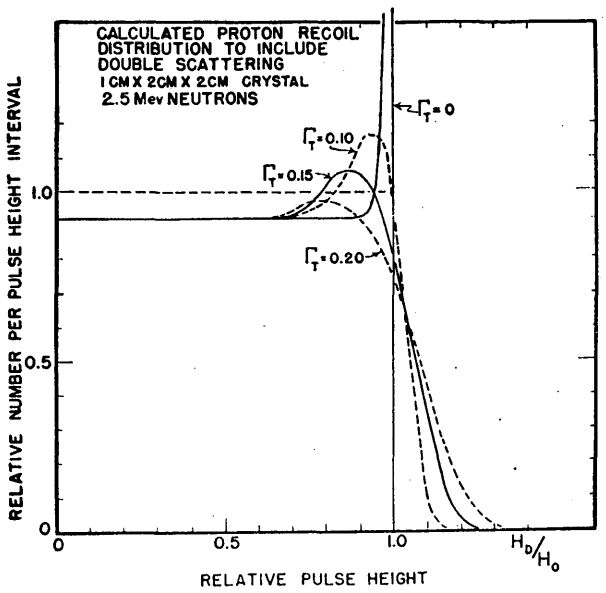

FIG. 23. Calculated energy distribution of recoil protons due to 2.5-Mev neutrons, in a stilbene crystal 2 cm×2 cm×1 cm, including the effects of double scattering.

FIG. II.23 (AFTER SEGEL (14))

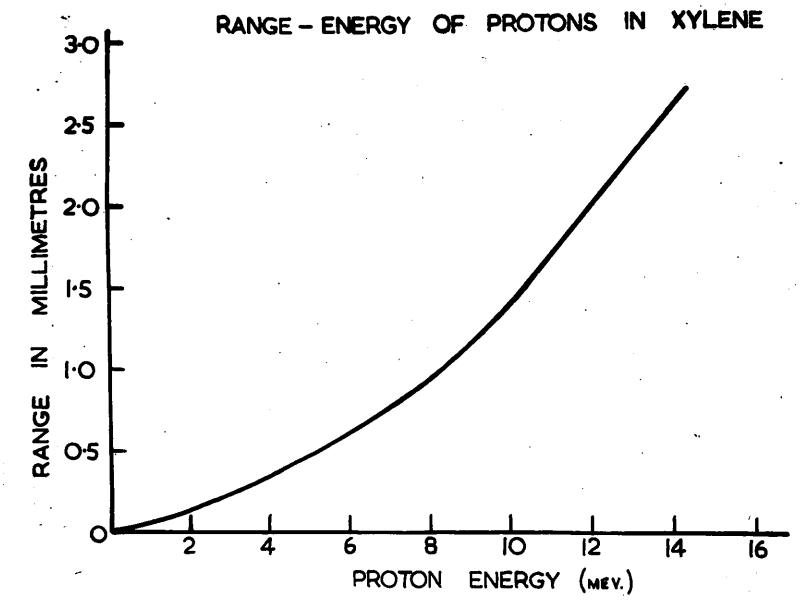

FIG. II.24 RANGE v ENERGY FOR PROTONS IN XYLENE

seems to offer, at first sight, an improvement in definition of neutron energies but it has been found by the author in investigation of the response to (D-D) neutrons, of the liquid scintillators, that the emphasis of the higher energy end is largely masked by the non-linear response of the solution.

(c) Crystal Photo-tube statistics and Channel width

The actual pulse height spectrum from mono-energetic protons incident on a liquid scintillation counter is not an infinitely narrow line of height L but rather a Poisson distribution of finite width which is a varying function of L. This effect is due to variations in the crystal and phototube, already discussed in Part II(4). A similar effect on the pulse height spectrum is found due to the finite width of the channel in the analyser. These factors influence the higher energy end of the spectrum to the greatest extent and cause the edge of the distribution to become less steep.

(d) Edge Effects

The escape of recoil protons from the scintillator before their full energy is expended in the scintillator causes an additional number of small pulses to appear in the pulse height distribution, thus distorting the low energy end of the spectrum. From the range v energy relationship for protons in xylene, FIG.II.24, it is obvious that, unless the scintillator is small or the neutron energy large, these wall effects are negligible.

EXPERIMENTAL PULSE HEIGHT DISTRIBUTIONS FROM LIQUID SCINTILLATORS

SPECTRUM FROM (D-D) NEUTRONS

The 50KV machine, described in Appendix I, was used to produce 50 KeV deuterons to bombard a target of heavy ice and produce a high yield of mono-energetic neutrons of energy 2.5 MeV. These neutrons were incident, on a 1"diameter by 1" long scintillator along the axis of the cylinder. The pulse height distribution, FIG.II.25, was measured using the single channel kicksorter described in Appendix II.

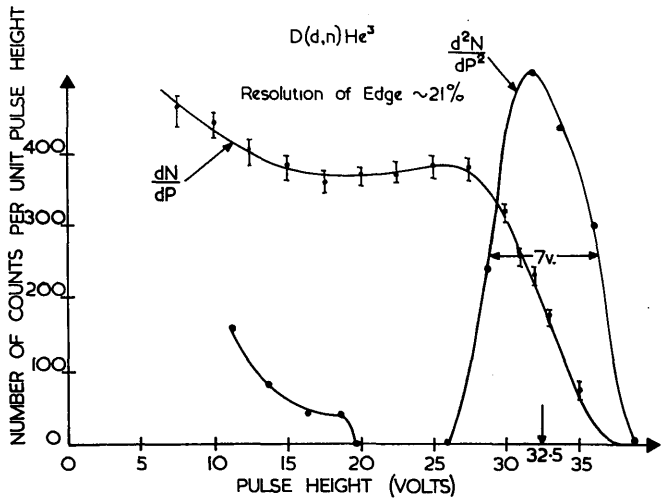

FIG. II.25 EXPERIMENTAL DISTRIBUTION FOR 2.5 MeV NEUTRONS INCIDENT ON LIQUID SCINTILLATOR

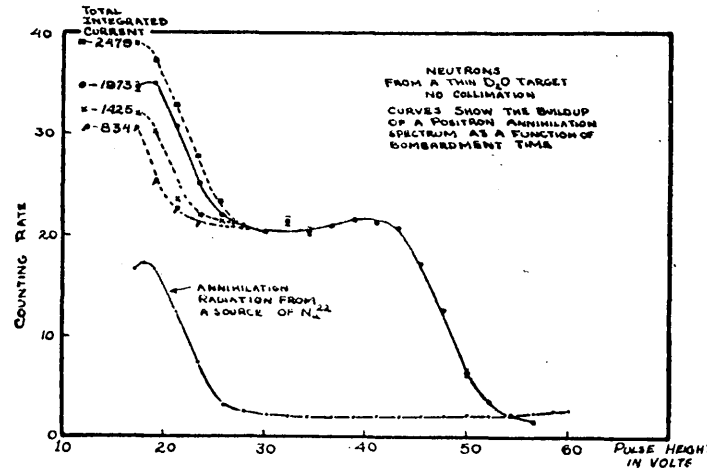

FIG. Pulse-height spectra due to $D-D$ neutrons from a thin target, with no collimation, showing the buildup of annihilation radiation with increasing bombardment time. The spectrum due to annihilation radiation from Na^{22} is shown for comparison.

FIG. II.26 (AFTER SEGEL (14))

RESOLUTION AND ENERGY MEASUREMENT

From the curve of FIG.II.25 it is not easy to calculate the pulse height corresponding to the 2.5 MeV neutrons due to the distortions in the curve. Similar distortions appear in neutron spectra when methane-filled proportional chambers are employed and it is for this reason that the analysis of the scintillation counter curves has been tackled in a similar manner by the author. By differentiation of the curve of FIG.II.25 the author is enabled to a good approximation to define the maximum energy as the position of the peak of this new curve and the resolution as the full width at half height of the peak. From the curve FIG.II.25 the resolution for the (DD) neutrons is 21%.

Comparison of this result with that of Segel (14) using a 2 cm 2 cm x 1 cm stilbene crystal, FIG.II.26, in a similar experiment shows good agreement in shape. The sharper rise in FIG.II.26 at lower energies is due to the greater background radiation in Segel's experiment. In both cases a slight rise is observed at the high energy end of the spectrum, which can be attributed to the effects of multiple scattering. This rise is not as pronounced as would be predicted from Segel's calculations, due to the masking effects of the non-linearity of response of the scintillators to protons.

Efficiency

To estimate the efficiency of the counter to neutrons is also difficult due to the distorted shape of the distribution. By integration of the observed curve of FIG.II.25 the efficiency of the counter to 2.5 MeV neutrons is estimated as 20% in good agreement with calculations from FIG.II.18B.

In Part III, a discussion of the difficulties involved in neutron measurements using this single counter technique will be given.

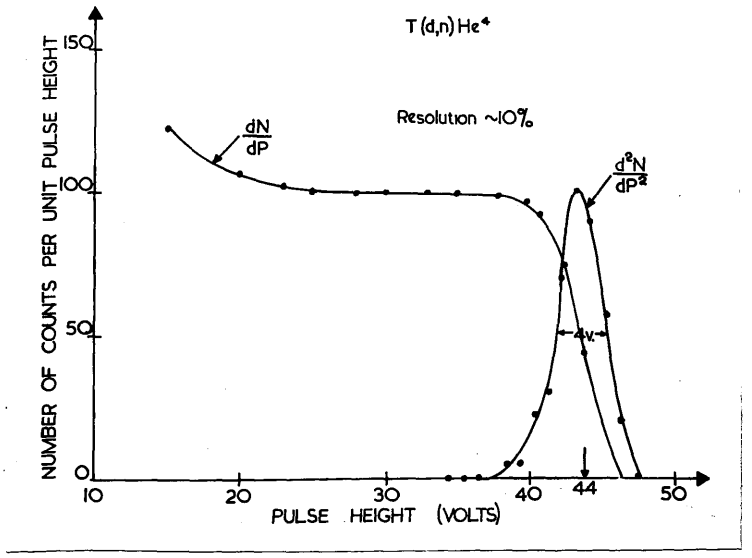

FIG. II.27 EXPERIMENTAL DISTRIBUTION FROM 14 MeV NEUTRONS ON LIQUID SCINTILLATOR

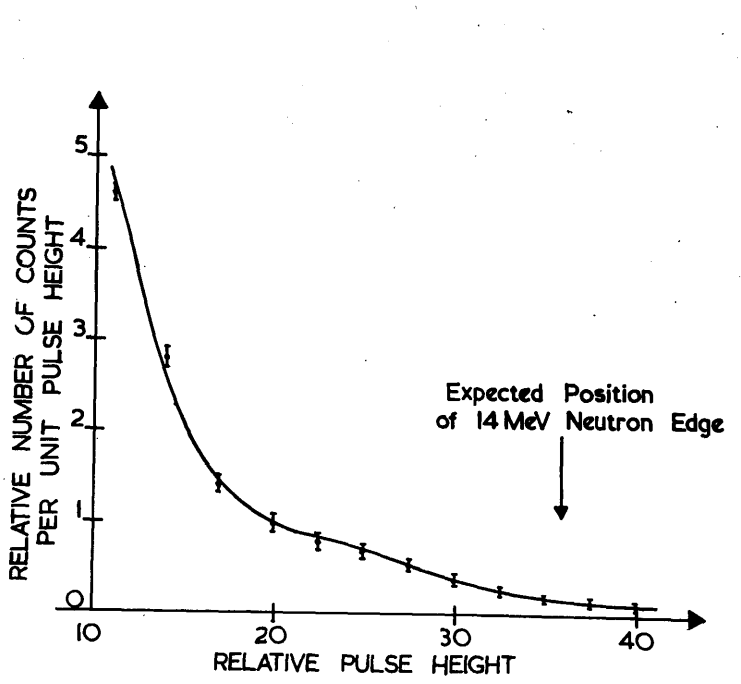

FIG. II.28 RESPONSE TO PRODUCTS OF $B^{11}(d,n)C^{12}$ REACTION

RESPONSE TO (D,D) NEUTRONS OF [illegible] MeV

A similar experiment was carried out using 14 MeV tritium neutrons using the target described in Appendix I.

The result is shown in FIG.II.27. The resolution is calculated as 10%, a figure in good agreement with the law, resolution inversely proportional to the square root of(particle energy)$^{\frac{1}{3}}$. The efficiency in this case is estimated as 5%.

In this case, as is expected, there is no evidence of a rise at higher energies due to multiple scattering, and further the effects of non-linearity are also not as pronounced as for the lower energies of (DD) neutrons. Thus the spectrum in this case is less distorted and resembles the step function of FIG.II.26.

RESPONSE TO NEUTRONS FROM $B^{11}(d,n)C^{12}$ REACTION

In order to investigate the response of this single counter to an inhomogeneous neutron beam it was decided to consider the neutrons of 13,9 and 4 MeV from the reaction $B^{11}(d\ n)C^{12}$ using an incident beam of 500 KeV deuterons from the Glasgow 1 MeV H.T. Set.

The observed distribution, FIG.II.28, shows no evidence of the steps which are illustrated in FIG.II.21 for such cases. Consideration shows that this is due to background radiation and the presence of 4 MeV X-rays, from the above reaction, blurring the neutron distribution.

It is thus obvious that such an arrangement is unsuitable for the resolution of neutron energies when the neutrons are associated with X-rays. In Part III the methods employed by the author to overcome these difficulties are described.

II (5) (d) RESPONSE TO PROTONS

The importance in fast neutron spectrometry, using organic scintillation counters, of the pulse height v energy relation for protons has been made obvious in the preceding section. In the range of proton energies for which information was required by the author no means of direct measurement was available. It was

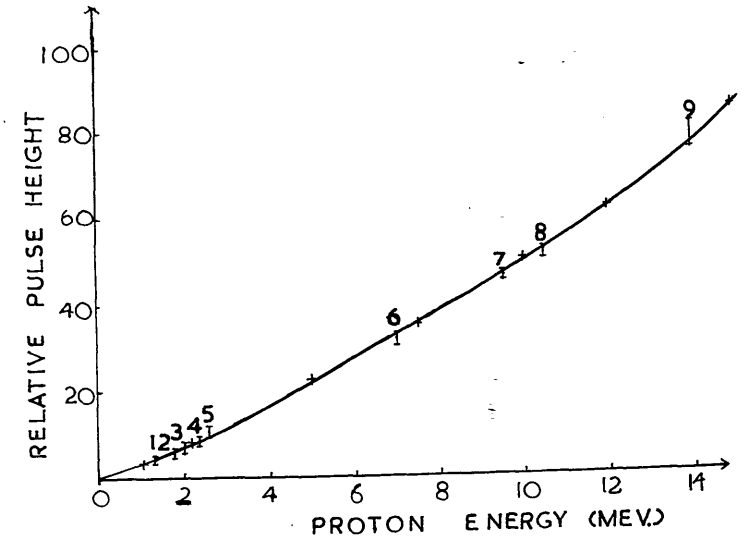

1. Double Scattering (DD) neutr
   at $\theta = 45^\circ$
2. at $\theta = 56^\circ$
3. at $\theta = 64^\circ$
4. at $\theta = 77^\circ$
5. (D-D) single counter edge
6. Double Scattering (D.T.) neut
   at $\theta = 45^\circ$
7. at $\theta = 56^\circ$
8. at $\theta = 60^\circ$
9. (D.T.) single counter edge

+ Points after TAYLOR (11)

FIG. II.29 PULSE HEIGHT v ENERGY FOR PROTONS IN A SOLUTION OF 5 g/l TERPHENYL IN XYLENE

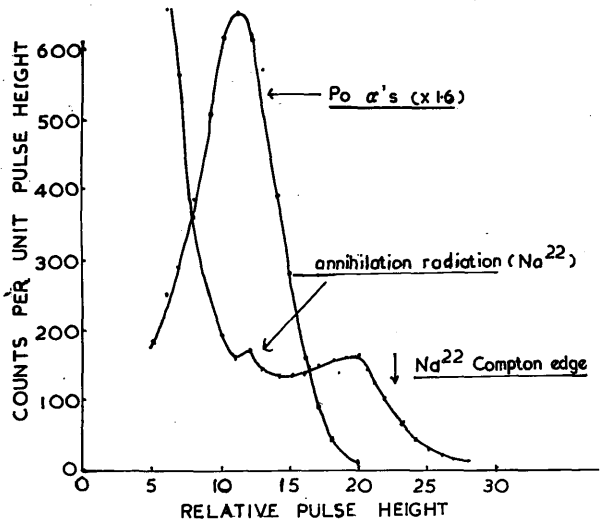

FIG. II.30 RESPONSE OF LIQUID SCINTILLATOR TO Po α's AND Na^{22} γ-RAYS

therefore, decided that, to a good approximation, the pulse height v energy relationship could be derived by measurements on the beams of mono-energetic neutrons from the (Dp) and (D,T) reactions.

From single counter and double scattering measurements, described in Part III, the curve of FIG.II.29, for a solution of 5 g/l terphenyl in xylene, was derived. On this curve are superimposed points at various energies (the crossed co-ordinates), which are normalised from the data on anthracene given by Taylor et alia (11) by allowing for the conversion efficiency of the solution. The agreement between the results on anthracene and a solution of 5 g/l terphenyl in xylene has also been noted by Harrison (4) and Reynolds (15), who report investigations of the response of liquid scintillators of different concentrations, and conclude that the deviation from linearity becomes greater as the concentration is reduced below 5 g/l, being similar to anthracene at 5 g/l. To a first approximation the law for pulse height v energy for protons in a solution of 5 g/l terphenyl in xylene can be written $L = KE^{1.3}$, a relationship which has been used in the previous section.

II(5) (e) RESPONSE TO α-PARTICLES

No systematic experiments were performed to determine the response of liquid scintillators to α-particles. An experiment was, however, performed to determine the pulse height from Po α-particles and compare these results to similar ones obtained from anthracene. The poor response of the organic scintillator to α-particles is clearly seen from the curve in FIG.II.30. The ratio of α-particle pulse height to Na^{22} annihilation radiation is equal to that obtained by Reynolds(15), using terphenyl in toluene, and by Taylor (11), for anthracene.

This section of the thesis shows the similarity of response of the liquid scintillators and other organic scintillators such as anthracene. The results given here shall be used later, in Part III, to illustrate the advantages and disadvantages in the application of liquid scintillators to fast neutron spectrometry.

REFERENCES TO PART II.

1. KALLMANN,H. & FURST, M. :- Phys.Rev.81 p.853 (1951)
2. MORTON, G.A. :- R.C.A.Rev.9 p.632 (1948)
3. ENGSTROM, R.W. :- Jow&Amer.Opt.Soc.37 p.420 (1947)
4. HARRISON, F.B. :- Nuc. Vol.10 No.6 p.40 (1952)
5. GARLICK,G.F.T. & WRIGHT, G.T. :- Proc.Phys.Soc.B65 p.415 (1952)
6. HARRISON, F.B. :- Nuc.Vol.12 No.3 p.44 (1954)
7. BROSER, I. et alia :- Natruf A.4 p.204 (1949)
8. HEITLER, W. :- Quantum Theory of Radiation.Lon. (1936)
9. JORDAN, W.H. :- Nuc. Vol.5 Oct. p.40 (1949)
10. HOFSTADTER, R. :- Phys.Rev.78 p.619 (1950)
11. TAYLOR, C.J. et alia :- Phys.Rev.84 p.1034 (1951)
12. ADAIR, R.K. :- Rev.Mod.Phys.22. p.249 (1950)
13. DRAPER, J.E. :- Rev.Sci.Inst.25 p.558 (1954)
14. SEGEL, R.E. et alia :- Rev.Sci.Inst.25 p.140 (1954)
15. REYNOLDS, G.T. :- Nuc. Vol.10, No.7 p.46 (1952)

PART III THE FAST NEUTRON SPECTROMETERS

III.1 THE POSSIBILITY OF THE APPLICATION OF LIQUID SCINTILLATION COUNTERS IN FAST NEUTRON SPECTROMETRY.

III.1(a) The difficulties involved in the application of liquid scintillation counters.

A fast neutron spectrometer, to perform the experiments, which are required in neutron measurements, should have properties of

(a) fast response,

(b) high efficiency,

(c) energy proportionality,

(d) resolution of neutron groups,

and (e) discrimination against γ-rays.

The liquid scintillation counters, which have been described in Part II, have fast response, the order of 10^{-9} sec. as measured by Post (1), and high efficiency, as shown in Fig.II18B. Thus they satisfy the properties (a) and (b) of the first paragraph. Difficulties are however encountered in the direct application of the simple liquid scintillation cells in the measurements of neutron groups from nuclear reactions. It is clear from Part II5 that they comprise :-

(a) the practically uniform distribution of pulse heights from proton recoils from zero to the maximum neutron energy, coupled with the distortion of this spectrum due to the non-linearity of the proton "light output versus energy" relationship in the liquid scintillator, light collection,etc., and,

(b) the blurring of the neutron spectrum by the presence of γ-rays, which, generally, accompany neutron groups from nuclear reactions.

The curves given in FIGS.II.25 and II.27 for 2.5 MeV and 14 MeV neutrons incident on a liquid scintillation counter illustrate the difficulties associated with the determination of the energies and intensities of neutron groups even in the absence of a γ-ray background. At 2.5 MeV the overall detection efficiency was 20% and a calculation showed that, of these scattered neutrons, 40% were scattered more than once, and that approximately 30% of the multiple scattered neutrons were initially scattered through angles greater than 60°. The latter neutrons gave rise to protons which produce the peak in the pulse height distribution.

For the 14 MeV neutrons, which produce a flat pulse height distribution, on first consideration, it would be tempting to assume that the response of the liquid to protons was linear. Calculation showed, however, that 10% of the scattered neutrons were scattered more than once and 20% suffered edge effects. It was clear, therefore, that the distribution, assuming linearity of response, should have had a peak near the maximum pulse height. The observed distribution can only be explained by the addition of the effects of non-linearity, multiple scattering and edge-effects.

These two examples clearly illustrate the different shape of distribution which may be obtained when neutrons of different energy are incident on a simple scintillation counter, and the calculation which is necessary if the intensities and energies of the groups in a complex neutron spectrum are desired. It should be mentioned, however, that, provided the size of the scintillator is chosen to record predominantly single scattering events, rough measurements of neutron energies can be obtained. Considerable calculation is still necessary if the relative intensity of groups of neutrons is required. In the presence of γ-rays the results are further complicated.

III.1(b) METHODS CAPABLE OF OVERCOMING THESE DIFFICULTIES

The inability of organic scintillation counters to discriminate against γ-rays has proved the major obstacle in their application to fast neutron spectrometry. In the following discussion of the methods, considered by the author in the development of a satisfactory neutron spectrometer, it will become evident that several simple methods, suitable for measurement of neutron groups, are rendered inadequate in the presence of a high energy γ-ray background. The methods are divided into two main groups.

Group A :- Single Counter Methods

(1) Collimating tube spectrometer

(2) Large scintillation - cell spectrometer.

Group B :- Double Scattering Coincidence Methods

(1) Double scattering with pulse height analysis in the primary counter, designated the (E_p, θ) method.

(2) Double scattering with pulse height analysis in the primary counter and time discrimation between the counters, designated (E_p, θ, t) method.

(3) Double scattering with pulse height analysis in the primary counter, with observation of delayed coincidences in the secound counter which acts as an epithermal neutron detector, designated (E_p, E_n) method.

(4) Double scattering with time-of-flight analysis between the counters, designated (t) method.

A short introduction to these methods follows.

Group A (1) The Collimating tube spectrometer.

By elimination of those proton recoils which are not due to "head-on" neutron-proton collisions in the liquid scintillator, it is possible to overcome the difficulty of uniform distribution mentioned in Part III.1(a). The technique depends on the collimation of the recoil protons in a small diameter quartz tube filled with the scintillating solution. It is an inherent property of the design that the background due to γ-rays is reduced. This method is an extension of the type of neutron proportional chamber, employing a similar collimating action, developed by Giles(2). The experiments on this spectrometer are discussed in Part III.2.

Group A (2) Large Volume Scintillator

A high energy neutron, incident on a large liquid scintillator, will be reduced to thermal velocities after successive collisions with protons in the counter. The pulses of light from these recoil protons will be recorded as one pulse at the cathode of the photomultiplier, since the time taken by the neutron to reach thermal velocities is the order of 10^{-8} secs. This multiple scattering of the neutrons results in a pulse height distribution in which there is a peak corresponding to the energy of the neutron.

It is possible to distinguish between neutrons and γ-rays by the introduction into the scintillator of a second solute which contains a nucleus of high slow neutron cross-section, suchaas B^{10} or Cd. The presence of this nucleus in the scintillator results in the appearance of a pair of pulses at the output of the photomultiplier when a fast neutron is incident. The primary pulse is caused by the slowing down of the incident neutron, as described above. The secondary pulse, which is delayed in time, is due to the α-particle or γ-ray, from B^{10} or Cd, respectively, produced in the capture of the "slowed-

down" neutron. Observation of delayed coincidences between these two pulses in the scintillator results in the detection of neutrons in the presence of a γ-ray background.

This method is discussed later in Part III.4. Several investigators, (Meuhlhause (3) and Harrison (4)) have recently considered this spectrometer for high energy neutrons.

Group B (1) Double Scattering with pulse height analysis in the counter. (E_p, Θ)

This spectrometer is based on the simultaneous recording in two liquid scintillation counters of the successive scatterings of the same neutron through a definite angular interval. The idea is to isolate, by coincidence measurements, recoil protons of a specific energy. It is thus possible by analysis of the recoil distribution spectrum in the primary counter, to specify a proton energy, E_p , corresponding to an angle, Θ , between the counters. The incident neutron energy is easily calculated from the knowledge of the values of E_p and Θ. The experimental distributions obtained by the author using this spectrometer are given in Part III.3.

(In principle this technique is identical to that developed by Hofstadter (5) to overcome a similar difficulty in the application of organic scintillators to γ-ray spectrometry.)

Although this method, (designated by the author (E_p, Θ) method), is satisfactory for the determination of the energies of neutrons, unaccompanied by γ-rays, it is inadequate when γ-rays are present. Several variations on this (E_p, Θ) method, will now be described, in which it is possible to discriminate against γ-rays in the measurement of neutron spectra.

Group B (2) Double scattering with time-of-flight discrimination (E_p, θ, t).

This technique is, in principle, similar to (E_p, θ) but, in this case, a fast coincidence unit of resolving time, $\sim 3 \times 10^{-8}$ secs. is used, replacing the slower unit of resolving time $\sim 10^{-6}$ secs. of (E_p, θ). This faster coincidence unit allows discrimination between γ-rays and neutrons by utilising the difference in time-of-flight of the particles between the counters.

Draper (6) and Chagnon (7) have discussed and tested this type of neutron spectrometer. It is included in this section for completeness but has not been investigated, experimentally, to any great extent, by the author.

Group B (3) Double scattering with detection of scattered neutrons of epithermal energies. (E_p, E_n)

By observations of the pulse heights of recoil protons in the primary counter corresponding to scattered neutrons of epithermal energies on detection in the secondary counter, it is possible by delayed coincidence measurements between the counters to obtain neutron spectra in the presence of γ-rays. Beghian (8) has tested this (E_p, E_n) method, using as an epithermal neutron detector, a NaI crystal surrounded by silver foil.

The author has performed experiments, which are described in Part III,4, using as the slow neutron detector a liquid scintillator to which a compound containing B^{10} has been added.

Group B (4) Time-of-flight analysis in double scattering (t).

The measurement of the time-of-flight of neutrons scattered between the two counters is sufficient to determine the energies of the neutrons, and, at the same time, to discriminate against γ-rays. The unique geometrical properties of this technique affords the possibility of an efficiency very much higher than in alternative techniques. This method will be described later in more detail, to show its advantages over all other techniques.

PART III. 2. THE COLLIMATING-TUBE NEUTRON SPECTROMETER.

III.2 (a) THE PRINCIPLE OF THE TECHNIQUE

The spectrometer is based on the collimation of the proton recoils originating in the scintillating liquid. By this method only "head-on" or nearly "head-on" collisions are recorded. The collimating action is obtained by the use of a thick wall quartz tube, filled with scintillating liquid, whose radius is such that a proton recoiling at an angle different from the "head-on" recoil, will strike the wall of the tube. Thus, the pulse height from all but "head-on" proton recoils is appreciably reduced.

It is obvious that the narrower the tube the greater is the collimation and consequently the energy resolution of the spectrometer is increased. However a narrow bore results in low efficiency. The choice of a particular resolution fixes the radius and the efficiency of detection of the tube.

γ-ray pulse heights are reduced in this spectrometer since electrons have longer ranges in the liquid and are, therefore, more efficiently collimated than the recoil protons. Multiple scattering of the electrons in the liquid is also considerable. These two effects result in a very large number of the recoil electrons losing most of their energy in the walls of the quartz tube.

The final form of this spectrometer consists of a number of tubes mounted as one scintillation cell on a photo-multiplier. The difficulties involved in light collection from this final form of spectrometer will be considered later in this section.

III.2 (b) CALCULATION OF THE ENERGY RESOLUTION, EFFICIENCY, AND PULSE HEIGHT DISTRIBUTION FROM A SINGLE COLLIMATING TUBE, IRRADIATED WITH NEUTRONS.

The following approximate analysis involves the determination of the expected distribution of pulse heights from a collimating tube when it is

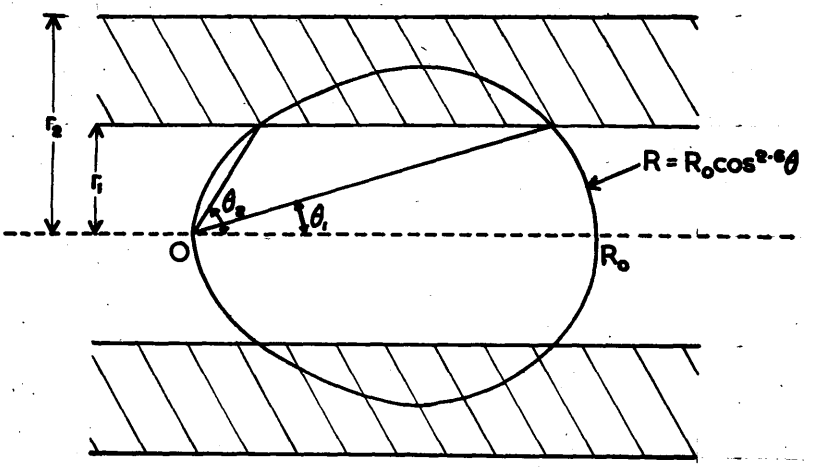

FIG. III.1 COLLIMATING TUBE ARRANGEMENT

irradiated with mono-energetic neutrons. In order to simplify the analysis, but to give a reasonable estimate of the expected distribution, all proton recoils are assumed to originate along the axis of the tube.

We have shown in Part II.5 that the distribution of recoil energies when mono-energetic neutrons of energy E_o, are incident on a liquid scintillation counter is :-

$$\frac{dN}{dE} = \frac{N_o}{E_o} \quad \text{where } E \leq E_o \quad \text{and } N_o \text{ is the number of scattered neutrons.}$$

$$= o \quad \text{for} \quad E > E_o \text{ ------(1)}$$

We also have that, in the laboratory system,

$$E_{proton} = E_o \cos^2\Theta \text{------(2)}$$

where θ is angle between recoil and incident neutron.

Then $$\left|\frac{dE}{E_o}\right| = \text{Sin } 2\theta \; d\theta$$

ie $$\left|\frac{dN}{N_o}\right| = \text{Sin } 2\theta \, d\theta \text{ ---(3)}$$ where dN is number of recoils netween angles θ and $\theta + d\theta$.

Protons of energy E, have ranges R in a liquid scintillator given approximately by $R = kE^{1.3}$. ---(4), thus we have from equations (2) and (4)

$$R = R_o \cos^{2.6}\theta \text{ -- (5)}$$

where R_o = range of recoil of maximum energy

and R = range of proton recoiling at an angle θ to the line of flight.

The experimental quartz tube of internal radius = r_1, external radius = r_2, and lengths $l \gg R_o$, filled with a solution of 5g/l terphenyl in xylene, is shown in Fig.III.1. The range of recoils at all angles is shown in the polar diagram of Fig.III.1.

Suppose this tube is bombarded with neutrons which have energy E_o, whose lines of flight are parallel to the axis of the tube, and consider proton recoils which originate on the axis of the tube. Those recoils, which proceed between the angles θ_1 and θ_2. will strike the tube wall and have a range in

the liquid given by $R^1 = r_1 \operatorname{cosec}\theta$ ----(6) where $\theta_1 \leq \theta \leq \theta_2$

Recoils protons, which are scattered at an angle θ where $0 \leq \theta \leq \theta_1$ and $\theta_2 \leq \theta \leq \frac{\pi}{2}$, will have range R where

$R = R_o \cos^{2.6}\theta$ --- (5)

Now when $\theta = \theta_1$ and θ_2

$r_1 \operatorname{cosec}\theta = R_o \cos^{2.6}\theta$

i.e. $r_1 = R_o \cos^{2.6}\theta . \sin.\theta$ ----- (7)

We have from Part II.5 that the relationship between light output, L^1, and proton energy E, in a liquid scintillator is given by

$L^1 = K^1 E^{1.3}$ ----- (8)

Thus if L is a relative measure of pulse height, then for $0 \leq \theta \leq \theta_1$, and $\theta_2 < \theta \leq \frac{\pi}{2}$, we have using equations (4) and (5) that,

$L = R_o \cos^{2.6}\theta$

$\therefore |dL| = 2.6\ R_o \cos^{1.6}\theta . \sin.\theta . d\theta$

but from equation (3)

$$\left|\frac{dN}{N_o}\right| = \sin 2\theta . d\theta$$

Thus $$\frac{dN}{dL} = \frac{N_o}{1.3\ R_o} \cdot \frac{1}{\cos^{0.6}\theta}$$

But $$\cos\theta = \left(\frac{L}{R_o}\right)^{\frac{1}{2.6}}$$

$$\therefore \frac{dN}{dL} = \frac{N_o}{1.3 R_o^{10/13}} \cdot \frac{1}{L^{3/13}} \quad -----(9)$$

For , $\theta_1 \leq \theta \leq \theta_2$ we have from equation (6)

$L = r_1 \operatorname{cosec}\theta$ ----(10)

$dL = r_1 \cot\theta \operatorname{cosec}\theta . d\theta$

and $$\frac{dN}{N_o} = 2 \sin\theta \cos\theta\ d\theta$$

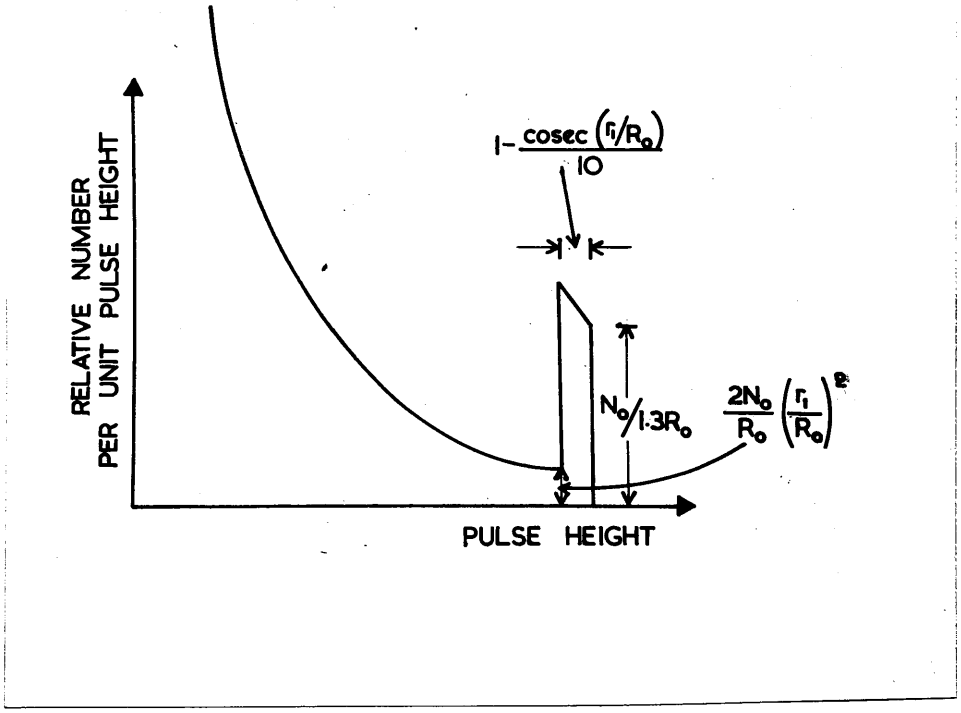

FIG. III.2 THEORETICAL DISTRIBUTION

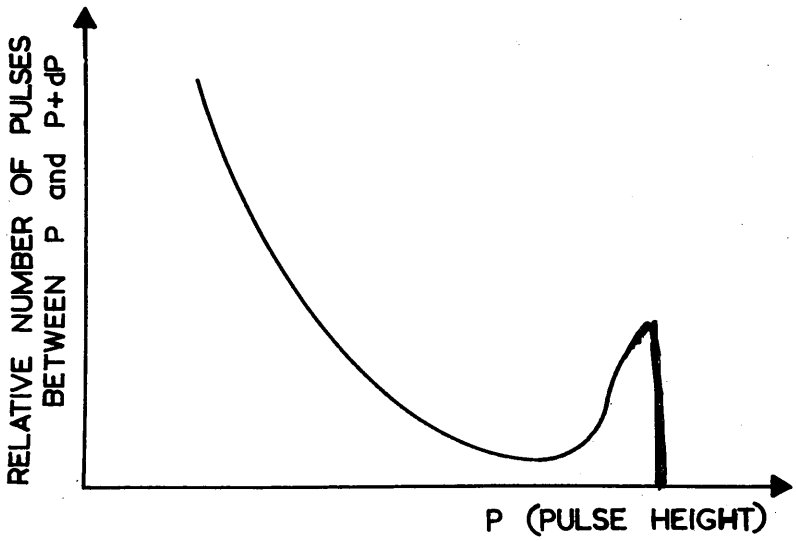

FIG. III.3 EXPECTED DISTRIBUTION

thus $\frac{dN}{dL} = \frac{2}{r_1} \sin^3\theta \cdot N_o = \frac{2\, r_1^2\, N_o}{L^3}$ ---(11), using equation (10)

We have, from equation (9) when $\theta = 0$

then $L = R_o$

and $\left|\frac{dN}{dL}\right| = \frac{N_o}{1.3\, R_o}$

and from equation (11) when $\theta = \theta_1$

$$\left|\frac{dN}{dL}\right| = \left|\frac{2r_1^2\, N_o}{L^3}\right|$$

$$\doteq \frac{2\, N_o}{R_o} \left(\frac{r_1}{R_o}\right)^2 \quad \text{assuming } \theta_1 \text{ is small thus } L_{\theta 1} \doteq R_o$$

The width of the distribution of pulse heights between $\theta = \theta_1$ and $\theta = 0$ is given by,

$$R_o - r_1 \operatorname{cosec} \theta_1 ,$$

if θ_1 is small then $\theta_1 \doteq \frac{r_1}{R_o}$

$\therefore$ Width of the distribution $= R_o \left\{1 - \frac{r_1}{R_o} \operatorname{cosec} \frac{r_1}{R_o}\right\}$

From this analysis, the shape of the theoretical distribution is shown in Fig. III 2., in which the width of the peak is determined by the value of i.e. r_1, the radius of the tube. 1

Calculation of Tube Efficiency

The fraction of recoils appearing in the Peak, F

$$= \int_{\theta=0}^{\theta=\theta_1} \frac{dN}{N_o}$$

$$= \int_0^{\frac{r_1}{R_o}} \sin 2\theta \cdot d\theta$$

$$= \left(\frac{r_1}{R_o}\right)^2 \text{ when } \theta_1 \text{ is small.}$$

For $F = \frac{1}{100}$

then $\frac{r_1}{R_o} = \frac{1}{10}$

Thus for a ratio of tube radius to the range of maximum recoil of $\frac{1}{10}$ the effective efficiency for recoils appearing in the peak is 1%. This gives the efficiency of a single tube as the order of 10^{-3} to 10^{-4} per incident neutron in the range of energies from 1MeV to 20 MeV, using the detection efficiency derived in curve Fig. II 18B.

The energy resolution of the tube

$$\text{Pulse Height Resolution} = \frac{\text{Width of the peak of distribution}}{\text{Max. Pulse Height}}$$

$$= \frac{R_o(1 - \frac{\pi}{R_o} \operatorname{cosec} \frac{r_1}{R_o})}{R_o}$$

$$= 1 - \frac{r_1}{R_o} \operatorname{cosec} \frac{r_1}{R_o}$$

for $\frac{r_1}{R_o} = \frac{1}{10}$ to give an efficiency of 10^{-3} to 10^{-4} per incident neutron.

Then Resolution $= 1 - \frac{1}{10} \times 9.568$

$\doteq 0.04$

i.e. % Resolution = 4

This analysis does not however take into account various factors, already mentioned in Part II5, which contribute to a decrease in the resolution of the spectrometer. The effects are :-

(a) variations in light output from a given proton energy due to the difficulty of uniform light collection in the scintillation cell.

(b) photo multiplier variations,

and(c) the finite channel width of the pulse height.analyser.

These factors broaden the peak of Fig.III 2, so that the final expected distribution will be of the form shown in Fig.III.3.

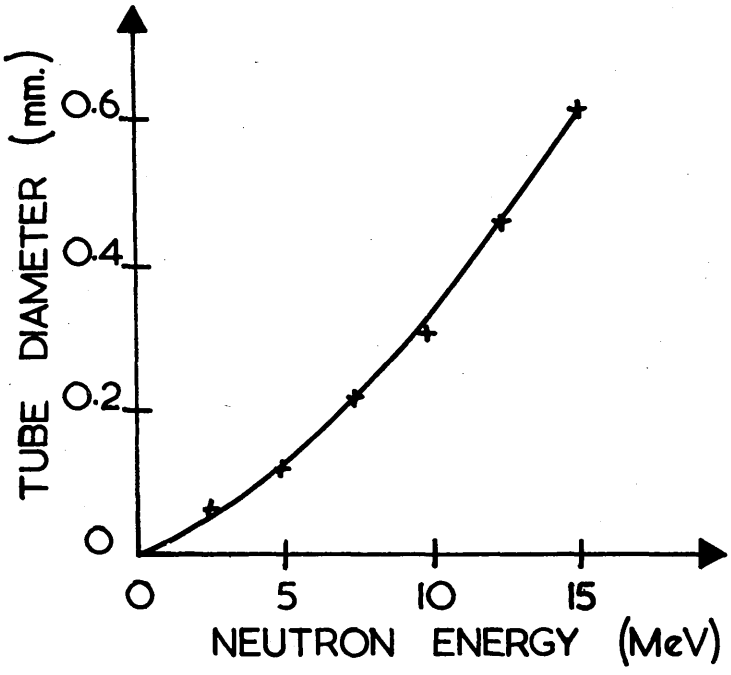

FIG.III.4 VARIATION OF TUBE DIAMETER WITH NEUTRON ENERGY

Variation of tube diameter with neutron energy

One serious disadvantage of this type of spectrometer lies in the necessity for different tube diameters if the resolution of the instrument is to be maintained over a range of neutron energies. Fig.III.4. shows the variation of tube diameter with neutron energy, to give a resolution of 4% and an efficiency of the order of 10^{-3} per incident neutron. From this it is clear that a single tube could cover fairly satisfactorily, with only a small variation in resolution, a range of 3 to 4 MeV in neutron energy.

III2(c) Response Time of the spectrometer

The response time of the spectrometer is limited mainly by the speed with which the photomultiplier can respond to pulses of light from the scintillator. By using suitable electronic arrangements, rise times of pulses as good as 10^{-8} sec. can be obtained. This makes the spectrometer very suitable for fast coincidence experiments, required in angular correlation investigations.

III.2(d) Experimental Arrangements

(1) Scintillation Cells

Some prelimiary experiments were performed on this type of spectrometer by Mr. R. Giles, in this laboratory, but no satisfactory results were obtained, because of the unsuitable arrangements of collimating tubes. The author, in tackling this problem, decided that, before proceeding to the use of a large number of quartz tubes, packed together as a single scintillating cell, it seemed desirable to make a specific investigation of a single tube, as a clearer and more definite indication of the possibilities of this collimating spectrometer.

For this investigation the quartz tube was placed in a hole in a perspex light guide and good optical contact between tube and perspex obtained using

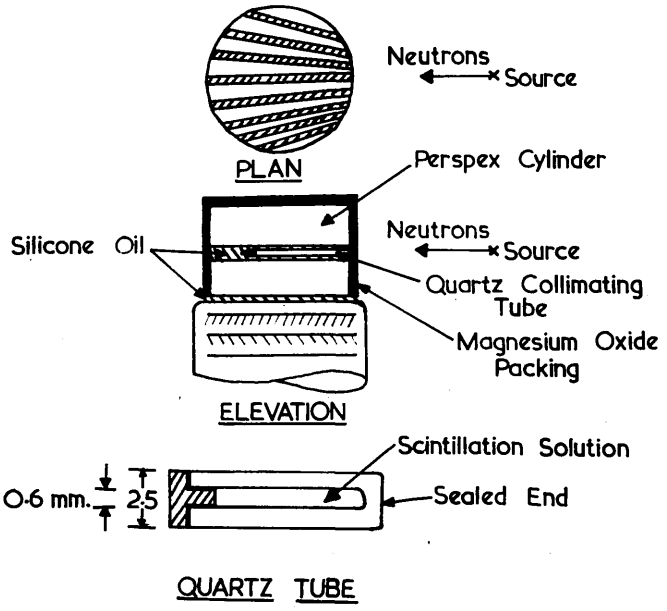

FIG. III.5 EXPERIMENTAL ARRANGEMENT OF COLLIMATING TUBES

silicone oil as a contact fluid. Several light guides, which could accommodate up to 60 collimating tubes, were made. A typical arrangement is shown in Fig.III.5.

It is clear from the calculations of Part III.2(b) that for the proper operation of this spectrometer it is essential for the incident neutron beam to be accurately parallel to the axis of the scintillation tube. This necessitates the careful alignment of the tubes and the source.

(2) Electronic Equipment

The apparatus for this spectrometer is extremely simple comprising a phototube, cathode follower, amplifier, and pulse height analyser. Two types of analyser have been employed (a) Photographic method (see Appendix II), and (b) 100 channel pulse height analyser of Hutchinson (9). The initial experiments were performed using the photographic method, but after the development of the 100-channel analyser in the laboratory this was the method employed to analyse the pulse height distribution.

III.2(e) Neutron Experiments

(1) 14MeV neutrons from T(d,n) reaction

The initial experiment was undertaken using a single collimating tube, of diameter 0.6 mm. and filled with a solution of 5 g/l terphenyl in xylene, placed in a perspex light guide as described in a foregoing paragraph. This scintillator was placed close (2cm) to a Tritium target, which was bombarded with 50 KeV deuterons from the Cockcroft-Walton generator described in Appendix I. The distribution obtained in this experiment showed some success and it was decided to extend it by increasing the number of collimating tubes to 8, as in the arrangement of Fig.III5. This second experiment gave a pulse height distribution as shown in Fig.III.6.

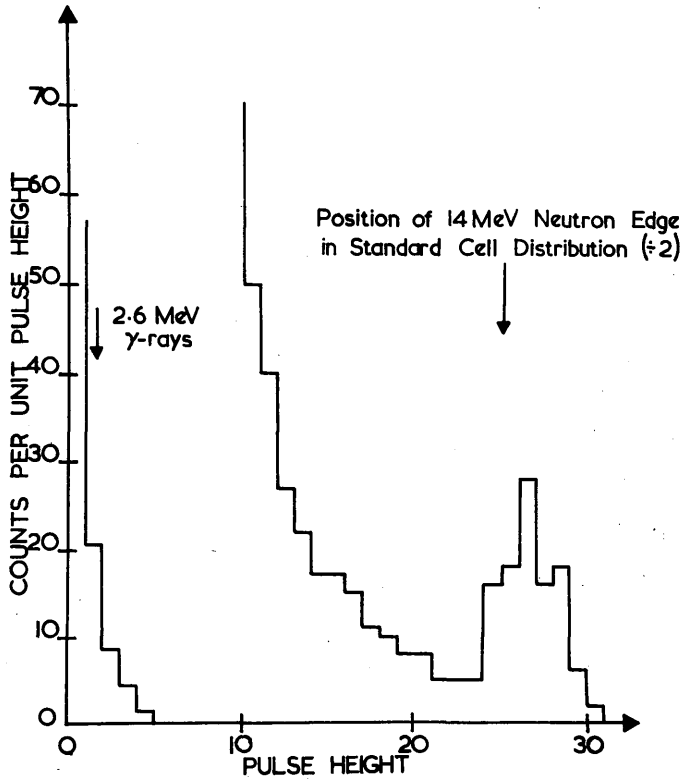

FIG.III.6 DISTRIBUTION FROM 14 MeV NEUTRONS AND 2.64 MeV γ-RAYS

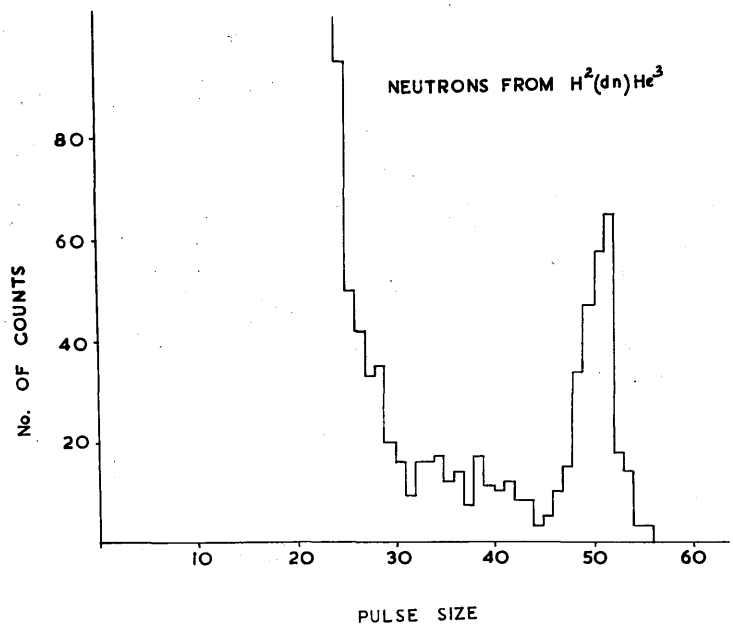

FIG.III.7

2.5 MeV NEUTRONS ON GILES (2) PROPORTIONAL COUNTER

On the same electronic settings the spectrum of the 14 MeV neutrons from a single scintillation cell, of the type shown in Fig.II.1b., was analysed. The pulse height corresponding to the maximum neutron energy is noted in Fig.III.6. From these results it is clear that there is a reduction of pulse heights in the collimating tube arrangement of the order of 60%. This reduction is to be expected from the light collection difficulties involved in the manner of mounting the collimating tubes.

γ-ray distribution

In order to estimate the pulse height from γ-rays, a ThC" 2.64 MeV γ-ray source was placed in the position of the target and the spectrum analysed. This distribution is shown in Fig.III.6. In this analysis the γ-ray pulse height has been reduced by a factor of 4, when compared to the maximum pulse height in a scintillating cell of Fig.II.1b. It is thus possible to discriminate against γ-rays in this spectrometer by selection of pulse height discriminator level in analysis of spectra.

Resolution and Efficiency

The resolution in the peak of the distribution is 22%. The increase over the theoretical factor can be attributed to the factors of light collection, photo-tube variations and finite channel width mentioned in Part III.2(b). The efficiency is calculated to be 10^{-4} per incident neutron. This is the efficiency of detection in the peak of the distribution.

Comparison with Giles Proportional Counter Method.

Giles (2) has applied the collimating technique, using a methane filled proportional chamber, to the analysis of the D(d,n) 2.5 MeV neutrons. The distribution is shown in Fig.III.7. This spectrometer is most suitable for the measurement of low energy neutrons but the similarity of the action of the two instruments can clearly be seen from the curves of Fig.III.6 and 7.

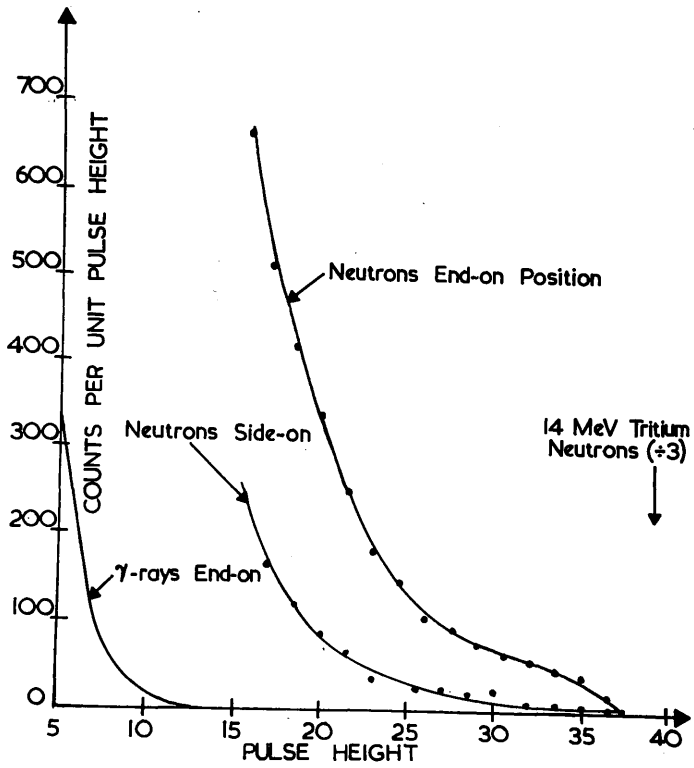

FIG.III.8 NEUTRONS FROM $B^{11}(dn)C^{12}$ REACTION AND γ-RAYS FROM $B^{11}(p,\gamma)C^{12}$ REACTION

At higher energies, 14 MeV, Giles has calculated the resolution of the instrument to be the order of 20% and the efficiency $\sim 10^{-5}$ per incident neutron. The response time, 10^{-6} sec, of this instrument is however much longer than in the scintillation collimating spectrometer.

Response to $B^{11}(dn)C^{12}$ neutrons

Spectrometer Arrangement

In order to increase the overall efficiency of the spectrometer in detection of neutrons from the $B^{11}(d,n)C^{12}$ reaction, which has a smaller yield than the T(d,n) reaction, the number of collimating tubes was increased to the order of 60. These tubes were mounted as before, in a perspex light guide. This light guide was designed so that the tubes lay on the radii of a sphere with its centre at the centre of the target which was made as small as possible. In this way it was ensured that neutrons from the target were incident along the axes of the scintillating tubes. The diameter of the tubes was 0.5 m.m. so that the resolution of the two high energy neutron groups of 13 and 9 MeV would be possible.

Neutron Distribution

The deuterons of energy 0.5 MeV were derived from the Glasgow 1 MeV H.T. set and observations on the neutrons were carried out at an angle of 90° to the incident beam. After careful alignment of the spectrometer with the target the spectrum of Fig.III.8 was obtained using the 100-channel pulse height analyser. Resolution of the neutron groups at 13 and 9 MeV has not been obtained. All that remains of the higher energy group is a slight discontinuity in the distribution. For comparison, the position of pulse height from the tritium neutron group on a single scintillation cell of Fig.II.1b is shown. The poorness of the spectrometer resolution is attributed to the light collection efficiency from the light guide. This is verified from

the position of the 14 MeV tritium neutron pulse height. A further experiment was performed with the spectrometer aligned so that the neutrons were incident at right angles to the tube axis. The spectrum in this case is also shown in Fig.III.8. This clearly shows the sensitivity of the instrument to the direction of the incident neutrons.

Response to γ -rays

A further experiment was performed by observing the pulse height spectrum from the high energy γ-rays in the $B^{11}(p,\gamma)C^{12}$ reaction, incident on the spectrometer in the "end-on" position. The spectrum in this case is also shown in Fig.III.8. It is clear that the γ-ray pulse height has been considerably reduced thus making it possible to discriminate against high energy γ-rays, while detecting efficiently high energy neutrons.

III.2 (f) CONCLUSIONS

These results are disappointing from the point of view of realisation of a good fast neutron spectrometer, due to the inability of the instrument to resolve neutron groups with high efficiency because of the difficulties of light collection. They show, however, some very interesting properties of the instrument as a fast neutron detector.

The instrument has :-

(a) High Efficiency of detection of fast neutrons $\sim 10^{-2}$ to 10^{-3} per incident neutron (after electronic discrimination against γ rays), compared to 10^{-4} to 10^{-3} for those techniques discussed in Part I.3.

(b) Fast Response to the passage of neutrons, of the order of 10^{-9} secs.

(c) Directional Properties: It is clear from Fig.III.8 that the spectrometer is very sensitive to the direction of incidence of neutrons.

(d) Simplicity of arrangement both mechanically and electronically. Later work described in this thesis will make more clear the advantage of this property of the present instrument.

(e) Discrimination against γ-rays. Although the instrument will detect γ-rays, discrimination can be obtained by the choice of electronic bias level, since the pulse height from the γ-rays is considerably reduced.

(f) Neutron Energy Discrimination. Although resolution of neutron groups is not possible, it is feasible in a neutron spectrum to separate, by electronic means, those pulses which are due to the highest energy neutrons. This degree of discrimination is of some consequence in the applications of the instrument in neutron detection.

(g) In a foregoing section we noted that a limitation of the instrument as a fast neutron spectrometer appeared in the necessity for changing the tube diameter for different neutron energy ranges. This requirement does not present itself in using the technique in fast neutron detection since, in this case, the important factor is the effectiveness of the tube in reducing the γ-ray pulse height. Efficiency of detection can thus be raised by increasing the tube diameter.

In the light of these observations it is possible to assess the probable success of the instrument in applications in fast neutron physics. (No such investigations have been carried out by the author since the other types of spectrometers, described later, showed more promise in the resolution of neutron groups.)

With this instrument of high efficiency, fast response and discrimination against γ-rays, we can perform those neutron experiments in which energy resolution is not essential.

The type of experiment which can be considered are :-

(a) measurement of excitation functions in (p,n) and (d,n) reactions,

(b) measurement of angular distributions of the highest energy group of neutrons, using the property (f) mentioned above,

(c) measurement of angular correlation between a fixed energy γ-ray and simultaneously emitted neutrons, e.g. in (d,n) reactions from light nuclei and inelastic scattering of neutrons from "medium-heavy" nuclei. For a particular example in this case we could consider the correlation between the 4 MeV γ-ray and 9 MeV neutrons emitted in coincidence in the $B^{11}(d,n)C^{12}$ reaction, or the neutrons and γ-rays emitted in the $Fe^{56}(n,n^1)Fe^{56*}$ reaction.

III.3 THE DOUBLE SCATTERING SPECTROMETER. (E_ρ, Θ) METHOD

III.3 (a) INTRODUCTION

In Part III.2 was described a method by which the difficulty of the uniform distribution of pulse heights from a liquid scintillation cell, on bombardment with neutrons, could be overcome. In this (E_ρ, Θ) method this difficulty is solved by the selection of the angle of scattering of a neutron between two scintillation cells operated in coincidence and the observation of pulse sizes in the primary scattering cell.

To achieve good energy resolution in this spectrometer, however, requires either (a) small scattering cells or (b) a large separation of these cells. Both of these requirements automatically tend to reduce the efficiency of the spectrometer. In the following analysis of the problem the interdependence of resolution and efficiency will be considered and from this the best geometrical arrangement deduced.

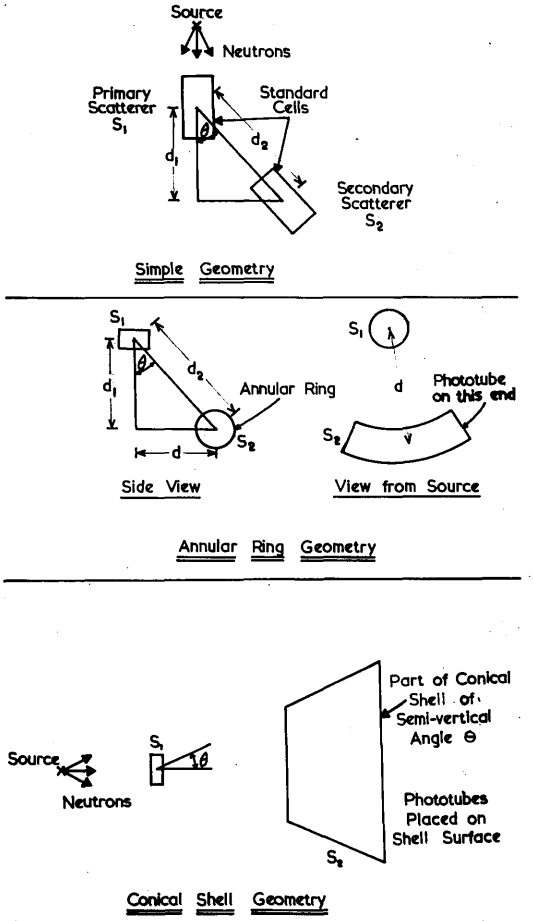

FIG.III.9 THE GEOMETRIES OF THE DOUBLE SCATTERING METHOD.

III.3(b) ANALYSIS OF THE PULSE HEIGHT DISTRIBUTION, RESOLUTION AND EFFICIENCY FOR THE (E_p, θ) METHOD.

If a neutron of energy E_o, is scattered at an angle θ by a proton in a liquid scintillator the energy of the recoil proton E_p is $E_o \sin^2 \theta$ and of the scattered neutron E_n, is $E_o \cos^2 \theta$. Thus scattering at a fixed angle, by selection of coincidences between recoil protons and scattered neutrons, should lead to a proton pulse height distribution corresponding to an energy $E_o \sin^2 \theta$, i.e. a line distribution. In practice, however, no such simple distribution is observed. Instead a peak is obtained for which the width is determined by the following factors :

(a) the geometry of the scintillating cells, used to observe the recoil protons and scattered neutrons;

(b) the statistical fluctuations in the photomultiplier in which the pulses from the proton recoil counter are amplified;

(c) the light collection in theproton recoil counter;

(d) the variations in the electronic devices following the "proton recoil" photomultiplier;

(e) the channel width of the analyser in which the pulse height distribution from the proton recoil counter is finally measured.

The ratio of the full width at half height of this peak to the peak height is called the resolution, R, of the spectrometer.

In the following paragraphs we shall determine the importance of these factors on the resolution of the (E_p, θ) method.

FIG.III.9 shows three types of geometry which have been considered by the author in testing the spectrometer arrangements. For this discussion we shall use the "annular-ring" geometry of FIG.III.9, since it is easy to deduce from it the properties of the other geometries.

In this arrangement we have :-

r_1 - radius of target

r_2 = radius of primary scatterer S_1

r_3 = radius of secondary scatterer S_2

a = distance from centre of target to centre of S_1

d_2 = distance from centre of S_1 to centre of S_2

d_3 = length of primary scatterer S_1

θ = angle between line of centres of target and of S, and line of centre of S_1 and S_2.

In the following analysis we assume that the peak obtained is approximately a Gaussian distribution for which the standard deviation (ΔL_ρ) is related to the resolution R, by $\frac{2\Delta L_\rho}{L_\rho} = R$

As we have already noted the resolution is determined by effects (a), (b), (c), (d), (e) which themselves are assumed to produce Gaussian distributions for which the standard deviations are $(\Delta L_\rho)_{Geom}$, $(\Delta L_\rho)_{counter}$, $(\Delta L_\rho)_{ELEC.}$, $(\Delta L_\rho)_{ANAL.}$ ((ΔL_ρ) counter includes effects (b) and (c))

By a theorem in the calculus of probabilities then

$$R = \frac{2\Delta L_\rho}{L_\rho} = \frac{2}{L_\rho}\left[(\Delta L_\rho)^2_{GEOM.} + (\Delta L_\rho)^2_{COUNTER} + (\Delta L_\rho)^2_{ANAL.} + (\Delta L_\rho)^2_{ELEC.}\right]^{1/2}$$

Geometrical Resolution

We have $$E_\rho = E_0 \sin^2\theta \quad \ldots\ldots (1)$$

then by differentiation

$$\Delta E_\rho = \frac{2E_\rho}{\tan\theta} \cdot \Delta\theta \quad \ldots (2)$$

For a detailed evaluation of $\Delta\theta$ we must consider the factors which lead to variation of the scattering angle θ :-

A. The scattered neutron may pass into any part of the secondary counter.

The distribution of the angle of scatter is in this case, proportional to $\frac{r_3}{d_2}$. This condition states simply, that for small variations in angle of scatter it is necessary to have the cross-sectional radius of the annular ring small and the separation between S_1 and S_2 large.

B. The scattered neutron may come from any part of the primary scatterer S_1.

The distribution of angle of scatter is proportional to $\frac{d_3}{d_2}$. In this case, small variations are ensured by having the length of primary scatter small and the separation between S_1 and S_2 large.

C. The incident neutron may come from any part of the target.

The distribution in angle of scatter is proportional to $\frac{r_1}{a}$, i.e. the variations in angle are small if the radius of the target is small and the distance from target to S_1 large.

D. The incident neutron may be scattered in any part of S_1.

The distribution in angle of scatter is proportional to $\frac{r_2}{a}$ i.e. the variations in angle are small if radius of S_1, is small and the distance between the target and S_1 large.

Hence $$(\Delta\theta)^2 \doteq \left[A\left(\frac{d_3}{d_2}\right)^2 + B\left(\frac{r_1}{a}\right)^2 + C\left(\frac{r_3}{d_2}\right)^2 + D\left(\frac{r_2}{a}\right)^2 \right]$$

where A, B, C and D are the effective weighting factors for the angular variations.

A more detailed analysis gives

$$(\Delta\theta)^2 \doteq \left[\frac{1}{8}\left(\frac{d_3}{d_2}\right)^2 + \frac{1}{2}\left(\frac{r_1}{a}\right)^2 + \frac{1}{4}\left(\frac{r_3}{d_2}\right)^2 + \frac{1}{12}\left(\frac{r_2}{a}\right)^2 \right] \quad \cdots\cdots (3)$$

Using equation (2), the contribution to the spread in recoil energies due to geometrical variation $(\Delta E_p)_{Geom}$, is given by

i.e. $$(\Delta E_p)^2_{GEOM.} \doteq \left(\frac{2E_p}{\tan\theta}\right)^2 \left[\frac{1}{8}\left(\frac{d_3}{d_2}\right)^2 + \frac{1}{2}\left(\frac{r_1}{a}\right)^2 + \frac{1}{4}\left(\frac{r_3}{d_2}\right) + \frac{1}{12}\left(\frac{r_2}{a}\right)^2 \right] \cdots (4)$$

We have, from Part II.5(d) that $L_p \doteq K E_p^{1.3}$ ..... (5)

where L_p is light output from proton of energy E_p.

From equation (4) and (5) we have,

$$(\Delta L_p)^2_{GEOM} = 1.7 \left(\frac{2L_p}{\tan\theta}\right)^2 \left[\frac{1}{8}\left(\frac{d_3}{d_2}\right) + \frac{1}{2}\left(\frac{r_1}{a}\right)^2 + \frac{1}{4}\left(\frac{r_3}{d_2}\right)^2 + \frac{1}{12}\left(\frac{r_2}{a}\right)^2\right]$$

Counter Variations. Fluctuations in the number of quanta incident on the cathode of the photomultiplier, due to variations in the light collection in the primary scatter, lead to deviations in pulse height denoted by $(\Delta L_p)_{counter}$.

Electronic Variations. denoted by $(\Delta L_p)_{ELEC}$.

Channel width of Analyser denoted by $(\Delta L_p)_{ANAL}$.

These variations lead to the resolution of the complete instrument defined as R where

$$R = \frac{2}{L_p}\left[(\Delta L_p)^2_{GEOM} + (\Delta L_p)^2_{COUNTER} + (\Delta L_p)^2_{ELEC} + (\Delta L_p)^2_{ANAL}\right]^{1/2}$$

The factors $(\Delta L_p)^2_{counter}$, $(\Delta L_p)^2_{ELEC.}$ and $(\Delta L_p)^2_{ANAL.}$, although difficult to determine separately, can be obtained as one factor $(\Delta L_p)^2_{S.C.}$ by observations on the resolution of a single counter arrangement when bombarded with neutrons. Thus we can write,

$$\text{Resolution, } R = \frac{2}{L_p}\left[(\Delta L_p)^2_{GEOM} + (\Delta L_p)^2_{S.C.}\right]^{1/2} \quad ..... \quad (6)$$

Efficiency

If N_o = number of neutrons scattered in S_1,

then $dN = N_o \sin 2\theta . d\theta$.

= number of neutrons scattered between the angles θ and $\theta + d\theta$

Further,
the solid angle subtended between θ and $\theta + d\theta$

$= 2\pi \sin\theta . d\theta$

If $d\Omega_2$ = solid angle subtended by the counter S_2 we have

the number scattered into the counter S_2

$$\doteq \frac{N_0 . d\Omega_2 . 2 . \sin\theta . \cos\theta . d\theta}{2\pi \sin\theta . d\theta}$$

$$\doteq \frac{N_0 . d\Omega_2 . \cos\theta}{\pi}$$

The number of neutrons scattered in S_2

$$\doteq \frac{N_0 . d\Omega_2 . \cos\theta \; K . t' . \sigma(E_0 \cos^2\theta)}{\pi}$$

where t' = length of counter S_2 parallel to the line of centres of S_1 and S_2

$\sigma(E_0 \cos^2\theta)$ = cross-section of neutron-proton scattering for neutron energy, $E_0 \cos^2\theta$,

K = no. of atoms in the scintillator/cm-barn

i.e. Efficiency $\doteq \frac{N_0}{\pi} . d\Omega_2 . \cos\theta . K . t' . \sigma(E_0 . \cos^2\theta) . F.$

where F is the fraction of the total neutron scatterers in the secondary scatterer which are recorded by the electronic equipment.

But $N_0 \doteq \frac{N_1}{4\pi} . d\Omega_1 . K . d_3 . \sigma(E_0)$

where N_1 = total number of neutrons from the target

$d\Omega_1$ = solid angle subtended by S_1 at the target

$\sigma(E_0)$ = cross section for neutron proton scattering for an incident neutron of energy E_0.

Thus the overall efficiency

$$\doteq \frac{N_1 . d\Omega_1 . K . d_3 . \sigma(E_0) . d\Omega_2 . \cos\theta . K . t' . \sigma(E_0 \cos^2\theta) . F}{4\pi . \pi}$$

$$\doteq \frac{N_1 . r_2^2 . 2r_3 . l . K^2 . d_3 . t' . \cos\theta . \sigma(E_0) . \sigma(E_0 \cos^2\theta) . F}{4 a^2 . d_2^2}$$

where l = length of secondary counter.

III.3(c) DESIGN CONSIDERATIONS

The dependence of resolution and efficiency of the instrument on the choice of angle of scattering and the design of the scattering cells will now be considered.

Choice of Scattering angle

It is clear from equation (7) that the angular dependence of efficiency is governed by two factors, viz., $\cos\theta$ and $\delta(E_0\cos^2\theta)$. Analysis of their variation with angle shows that the latter is the more critical term, favouring large values of θ. Although $\delta(E_0\cos^2\theta)$ is greatest for $\theta \simeq 90^\circ$, the efficiency will clearly be dependent on the pulse height in S_2. This pulse height dependence sets the upper limit of angle θ, usually θ is made less than 75°.

From equations (4) and (6) the resolution is determined by a function of $\cot\theta$, thus favouring large angles. In the case when $(\Delta L_\rho)^2_{Geom.} < (\Delta L_\rho)^2_{S.C.}$ then the resolution is dependent mainly on the pulse size produced by recoil protons in S_1, i.e. proportional to $E_0\sin^2\theta$. This factor favours large scattering angles.

From these considerations the range of angles for the satisfactory practical operation of the spectrometer is taken as $30^\circ \leq \theta \leq 75^\circ$.

Design of Scintillating Cells

From equations (6) and (8) the geometrical factors on which the resolution and efficiency depend, are derived. It is clear that the resolution is increased by reduction of $\frac{1}{d_1}; \frac{1}{a} : t_1 : t_2 : t_3 : d_3$ whereas the efficiency is increased by having large values of these same factors, with two additional factors ℓ and r^1 which, although they considerably affect the efficiency, do not influence the resolution of the instrument. The interdependence of

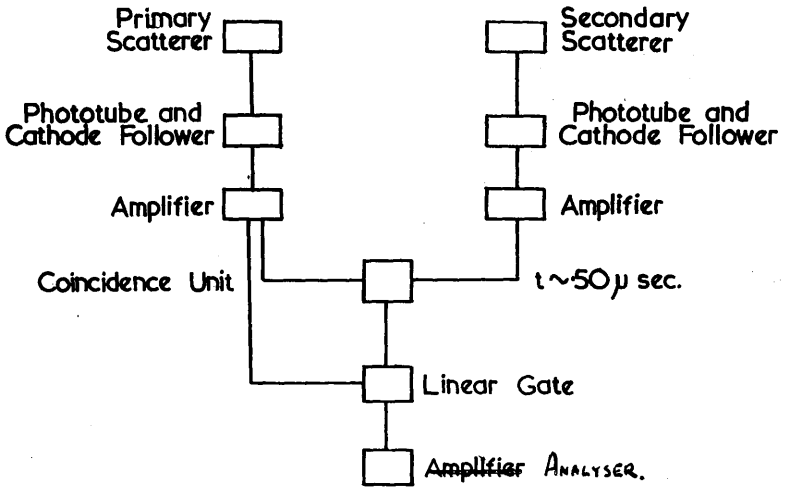

ELECTRONIC BLOCK DIAGRAM
FOR
DOUBLE SCATTERING EXPERIMENTS

FIG. III.10

resolution and erficiency is such that efficiency must be sacrificed to obtain good resolution.

The best resolution is not however determined, solely, by these geometrical considerations. In equation (6) it is clear that any attempt to reduce $(\Delta L_\rho)^2_{Geom}$ to a value very much less than $(\Delta L_\rho)^2_{S.C.}$ does not appreciably affect the pulse height resolution but only reduces the efficiency of the arrangement.

The method of scintillator design is clearly exemplified from the three geometrical situations shown in FIG.III.9. From the simple geometry, with a suitable choice of θ, the separation of the scintillators can be determined to give a geometrical resolution such that $(\Delta L_\rho)^2_{Geom} \doteq (\Delta L_\rho)^2_{S.C.}$ With no deterioration in resolution the efficiency can be increased by extension to the annular ring geometry i.e. an increase in ℓ in S_2. The final and most efficient geometry in this instrument is shown in the conical shell arrangement, i.e. an increase in r^1 combined with the increase in ℓ of the annular ring geometry.

III.3(d). ELECTRONIC ARRANGEMENT

The block diagram of FIG.III.10 illustrates the simplicity of the electronic equipment required for measurements in this (ϵ_ρ, θ) method. The light pulses from the two scattering cells, S_1 and S_2, are converted in the photo-tubes, amplified and mixed in a coincidence unit of resolving time 5×10^{-7} secs. The output pulses from the coincidence unit are then used to select pulses from the primary scattering cell in the linear gate. These selected pulses are then analysed using either the photographic method or 100 channel kicksorter as previously outlined in Part III.2. The problem of light collection in the secondary scattering cell is considerably eased since

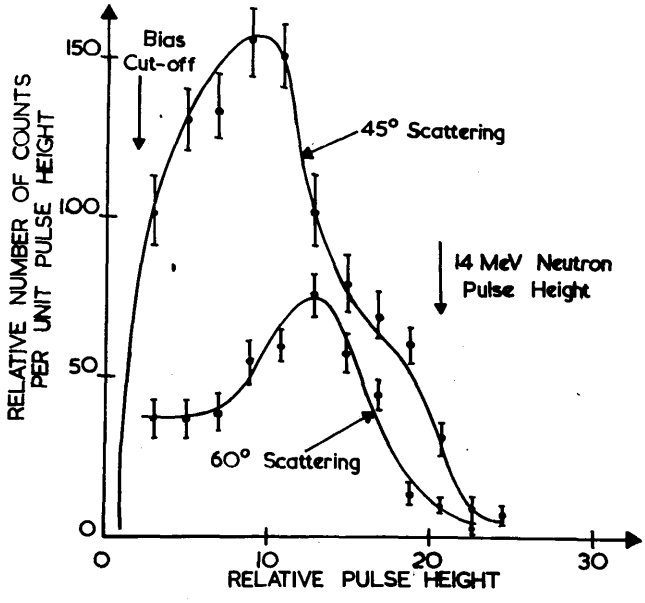

FIG.III.11 OBSERVED SPECTRA FROM DOUBLE SCATTERING OF (D,T) NEUTRONS IN SIMPLE GEOMETRY ARRANGEMENT

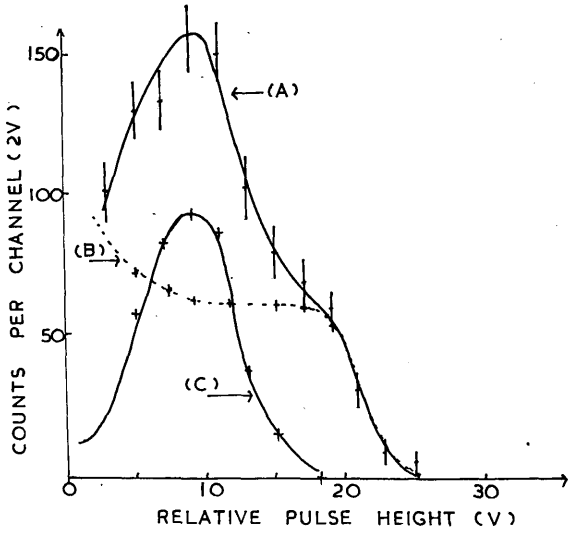

FIG.III.12.

(A) OBSERVED SPECTRUM AS IN FIG.III.11.

(B) RANDOM COINCIDENCES.

(C) REAL NEUTRON DISTRIBUTION

the pulses from it do not require to be proportional to the energy of the scattered neutron. In the channel containing the primary scatterer, however, proportionality and linearity are essential.

III.3(e) EXPERIMENTS (1) Simple Geometry

The initial experiments to test the instrument were performed using two similar standard scintillation cells in the simple geometry arrangement of FIG.III.9. In this case, $t_1 = \frac{1}{4}"$; $t_2 = \frac{1}{2}"$; $t_3 = \frac{1}{2}"$; $d_2 = 4"$; $a = 4"$; $d_3 = 2"$; and two angular settings of 45° and 60°. The arrangement was constructed to provide efficiency at the cost of resolution. (In this experiment the coincidence unit had a resolving time of 10^{-6} sec.)

Neutron Spectra

The source of neutrons was the (D T) reaction, using the 50 KeV deutrons from the Cockroft-Walton machine described in Appendix I. The recorded Spectra at 45° and 60° are shown in FIG.III.11. The ratio of real to chance coincidence rates in this experiment was 1/3.

FIG.III.12 shows the spectrum observed at $\theta = 45°$, together with the "chance" pulse height distribution. FIG.III.12C gives the "real" neutron distribution.

Resolution and Efficiency

Good agreement has been obtained between the observed and calculated values (from equations (6) and (8)) of the resolution and efficiency for this arrangement. The observed values are resolution 80% and an efficiency of 10^{-6} per neutron from the source. It should be noted that in calculating the resolution the value for $(\Delta L_\rho)^2_{S.C.}$ was obtained from single counter experiments on neutrons of the type described in Part II.5(c) and in this case a value of 0.015 L_ρ was calculated for $(\Delta L_\rho)^2_{S.C.}$

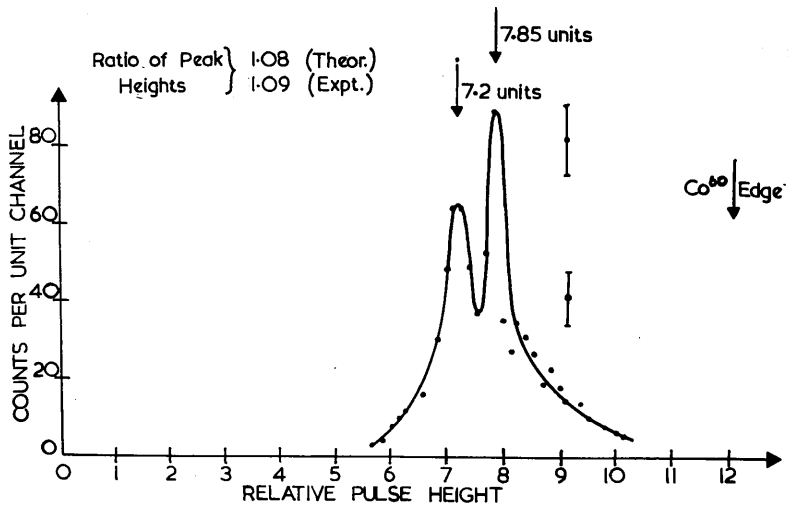

FIG. III.13 DOUBLE SCATTERING OF Co^{60} γ-rays at $\theta = 60^{\circ}$ IN ANNULAR RING GEOMETRY OF FIG. III.~~12~~9

Energy response

The main purpose of this preliminary investigation was to test, in addition to the properties of resolution and efficiency, the sensitivity of the arrangement to variation in the scattering angle and thus the proton pulse heights in the primary counter. The pulse heights of the peaks in the distributions of FIG.III.11 agree well with the law assumed in Part II.5(d) giving $L_p = K E_p^{1.3}$ where E_p is the proton energy, in this case $E_p = E_o \sin^2 \theta$.

(2) Annular-ring Geometry

The experiments using the "simple geometry" described above were sufficiently successful to attempt to increase the resolution of the instrument. To do this, two new scintillating cells were constructed. The primary scatterer was reduced to a length of 1/2", thus causing both $(\Delta L_p)^2_{Geom}$ and $(\Delta L_p)^2_{S.C.}$ to be reduced. The second scatterer was made in the form of an annular ring of internal radius 9-1/2" and external radius 10-1/2" and of length 10".

The experiments were performed using with these scintillators, a coincidence unit with resolving time = 5×10^{-7} secs.

The geometrical situation of the scintillators is shown in FIG.III.9 . The arrangement is such that for $\theta > 45^o$ the resolution is determined mainly by $(\Delta L_p)^2_{S.C.}$ since the geometrical factor $(\Delta L_p)^2_{Geom}$ is smaller than $(\Delta L_p)^2_{S.C.}$ The efficiency of detection of neutrons from the source is the same order as in the "simple geometry" arrangement.

Experimental results. Co^{60} γ -rays

To test the resolution of the spectrometer a Co^{60} source (γ -rays of energy 1.17 and 1.34 MeV) was placed in the target position, with "a" = 4" and collimation of the γ -ray beam obtained using lead. The scattering angle

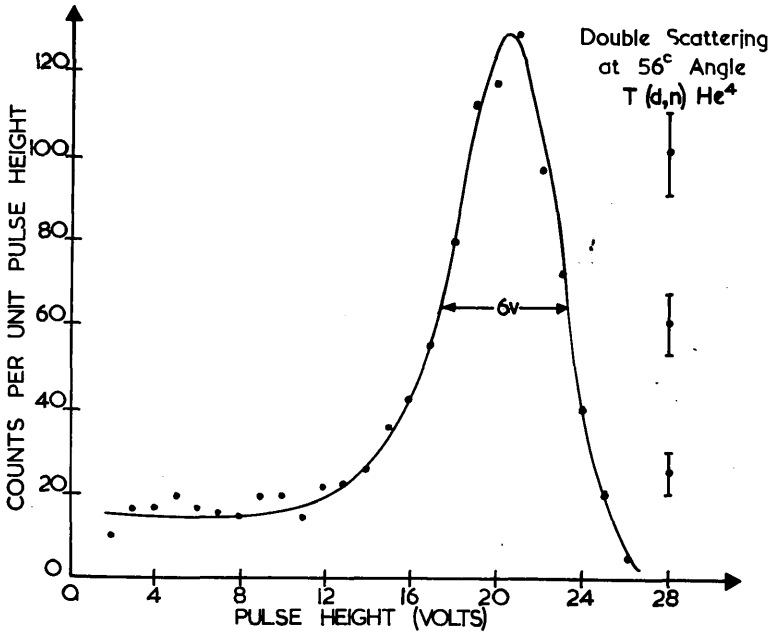

FIG.III.14 SPECTRUM FROM (D - T) NEUTRONS

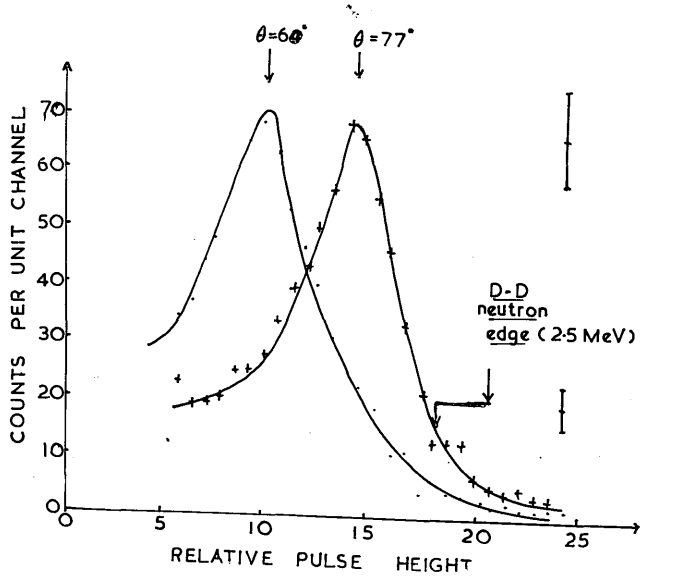

FIG.III.15 SPECTRA FROM (D - D) NEUTRONS

was fixed as $\theta = 60^{\circ}$. The pulse height spectrum is shown in FIG.III.13. Single counter measurements do not resolve the two groups, while the spectrometer technique clearly yields two distinct lines. The resolution in this experiment is estimated as 20%.

NEUTRON EXPERIMENTS

14 MeV neutrons

With the scatterers in approximately the same positions as in the γ-ray experiment (in this case $\theta = 56^{\circ}$) the spectrum shown in FIG.III.14 was obtained when the 14 MeV (D,T) neutrons were incident on the spectrometer arrangement. In this case the resolution is 28%. The decrease in the resolution compared to γ-ray case in this case is mainly due to the non-collimation of the incident neutron beam, and the multiple scattering of the neutrons in S_1.

The efficiency is calculated as 1 in 10^{+6} of the neutrons from the source in good agreement with that calculated from equation (8).

2.5 MeV neutrons

FIG.III.15 gives the spectra, for a similar geometrical situation as above, for the 2.5 MeV (D,D) neutrons. In this case the resolution is 40% and the efficiency of the order 1 in 10^{+5} neutrons from the source. The increase in efficiency is due to the dependence of the cross-section for scattering on energy involved in equation 8. The decrease in resolution is due mainly to the smaller pulse heights in the primary scatterer due to the lower neutron energy involved.

III.3(f) CONCLUSIONS

In the light of these experiments a review of the properties of this technique will now be outlined.

(1) Efficiency. The overall efficiency in these experiments for 14 MeV

neutrons is 1 in 10^6 of neutrons from the course. By further extension to the complete conical shell geometry this efficiency can easily be increased to the order 1 in 10^4 of the neutrons from the source. This is, at least, a factor of 100 better than the conventional methods of neutron spectrometry mentioned in Part I, such as photographic plates, proportional counters etc.

(2) High speed of response. The response time of the instrument to fast neutrons is determined by the electronic equipment employed in the experiments discussed above. In these experiments the response time is of the order of 10^{-7} secs.

(3) Good energy resolution. The experiments both on γ-rays and neutrons, clearly show that the energy resolution is independent of geometry employed in the final arrangements, being governed mainly by the statistics of (a) light collection in the primary scatterer and (b) the associated electronic equipment. The resolution, although poor compared with photographic plates, proportional chambers etc. is adequate for many of the applications mentioned in Part I.

(4) Energy proportionality. Although the response of the liquid scintillators to protons is not linear the distribution in pulse heights can be translated into an energy scale using the relationship shown in FIG.II.29. (Further consideration of the light output - proton energy relationship is given at the end of this section).

(5) Sensitivity to γ-rays

FIGS.III.14 and 15 show that, in its present form, the spectrometer is sensitive both to neutrons and γ-rays. It is thus inadequate for experiments in which the neutrons to be measured are accompanied by γ-rays.

These investigations of the response of this (E_p, θ) spectrometer to neutrons and γ-rays show the properties of this type of instrument.

It is clear, however, that, in its present form, although having many advantageous properties, the sensitivity of the instrument to γ-rays prevents its direct application in neutron experiments of the type discussed in Part I. In subsequent sections of this thesis, however, the refinements to this technique to overcome the effects of γ-rays will be considered in some detail.

III.3(g) APPLICATIONS OF THIS (E_p, θ) SPECTROMETER

Some simple applications of the spectrometer have been performed by the author, and the results presented previously in Part II.5. Although not accurate they are of interest since they constitute the only available data on the calibration of the scintillation cells to protons and electrons.

LIGHT OUTPUT v ENERGY RELATIONSHIP FOR PROTONS AND ELECTRONS IN A SOLUTION OF 5 g/l TERPHENYL IN XYLENE

In the double scattering experiments, previously mentioned, the energy of the scattered proton is $E_p = E_o \sin^2\theta$. It is thus possible, by observing the variation of light output with the angle of scatter of a beam of neutrons of fixed energy, to obtain a relationship between light output and the energy of a proton incident on a scintillator.

The results obtained from a series of investigations using the 14 MeV and 2.5 MeV neutron sources, previously mentioned, have already been presented in Part II of this thesis in FIG.II.29. In this series of experiments the pulse height spectra, in the primary counter in the annular ring geometry for angles of scatter of 45°, 56° , and 60° for 14 MeV neutrons and angles of 45°, 56°, 60°, and 77° for the 26 MeV neutrons, were analysed.

Birks (10) showed that the variation of light output along the path of an ionizing particle in an organic crystal, could be expressed in the form :

$$\frac{dL}{dr} = \frac{A \frac{dE}{dr}}{1 + B \frac{dE}{dr}}$$

where A and B are constants, and

where $\frac{dL}{dr}$ = light output in a path element, dr.

and $\frac{dE}{dr}$ = rate of loss of energy

For organic crystals B has the value 8.8×10^{-2} gm cm^{-2} MeV^{-1}. Harrison (11), although he has performed no measurements on the response of liquids to protons has considered the pulse height in a terphenyl solution of alpha particles and found the value of B to be approximately that derived by Birks.

The data presented here for a 5 g/l terphenyl solution agrees well with that deduced by Harrison for a solution of terphenyl from data presented by Taylor (13) on the response of anthacene to fast protons. A more detailed investigation by Harrison, using alpha particles, has suggested that the deviation from linearity of liquid scintillators increases as the concentration of the solution is decreased. These results, presented by the author, on the response of organic liquid scintillators to protons constitute the first experimental evidence of the similarity of response of anthracene and liquid scintillators to protons.

In a similar manner the response of the liquid scintillators to electrons has been obtained using various sources of γ-rays. The results, in this case, have been presented earlier in Part II in FIG.II.17A. For electrons in the range of energies investigated, the light output is proportional to the energy of the incident particle. The results are in good agreement with those derived by Harrison (11).

The mechanism of this most important feature of the behaviour of organic crystals and solutions as phosphors has been studied in detail by many experimenters and a good account of the processes of importance is given by Reynolds (12).

III.(3)(h) THE DOUBLE SCATTERING METHOD INCLUDING TIME OF FLIGHT DISCRIMINATION - (E_p, θ, t) METHOD

At this point, it is of interest to consider briefly the extension of the (E_p, θ) method suggested by Neiler et alia (14) and investigated by Chagnon et alia (7) and Draper (6). It is clear from the analysis of the (E_p, θ) method that the inability of the technique to discriminate against γ-rays, prevents the application of the instrument in general neutron experiments.

The (E_p, θ, t) technique is, in essence, a combination of the (E_p, θ) method and the (t) method to be described later in Part III.5. The geometrical situation, and thus the analysis of efficiency and resolution, is similar to the (E_p, θ) technique. The additional factor, the time of flight, is introduced by altering the electronic system of the (E_p, θ) method by the replacement of the slow coincidence unit of resolving time 10^{-6}, by one having a resolving time $\sim 3 \times 10^{-8}$ secs.

The faster coincidence unit allows discrimination between γ-rays and neutrons by utilising the difference of time of flight of the neutrons between the two scattering crystals. The pulses from the primary scatterer S_1, see FIG.III.9, are artificially delayed by a time equal to the average time of flight of a neutron between S_1 and S_2. These delayed pulses from S_1 and the pulses from S_2 are mixed in a coincidence unit and the coincidence pulses used to select, for pulse height analysis, the delayed pulses from S_1. In the form of spectrometer described by Chagnon the coincidence unit has a resolving time of 3×10^{-8} secs, $\theta = 45^{\circ}$, and the distance apart of the scintillators equal to 140 cm. The resolving time is such that the range of neutron energies accepted is restricted and in order to cover efficiently a spectrum of energies from 1 MeV to 14 MeV a series of different delays would be required in this present arrangement.

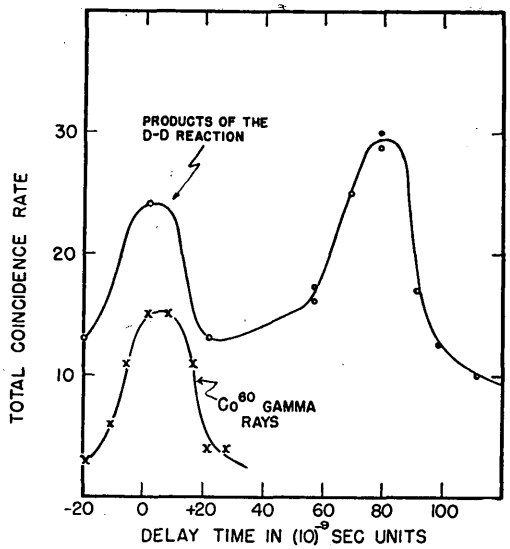

FIG. 8. Delayed coincidence rate *versus* delay between pulses from the primary and secondary counters, for Co^{60} gamma-rays and for the products of the D, D reaction.

FIG. III.16 AFTER CHAGNON (7)

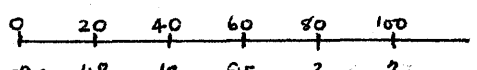

TIME OF FLIGHT
OVER 140 cm

ENERGY (MeV)

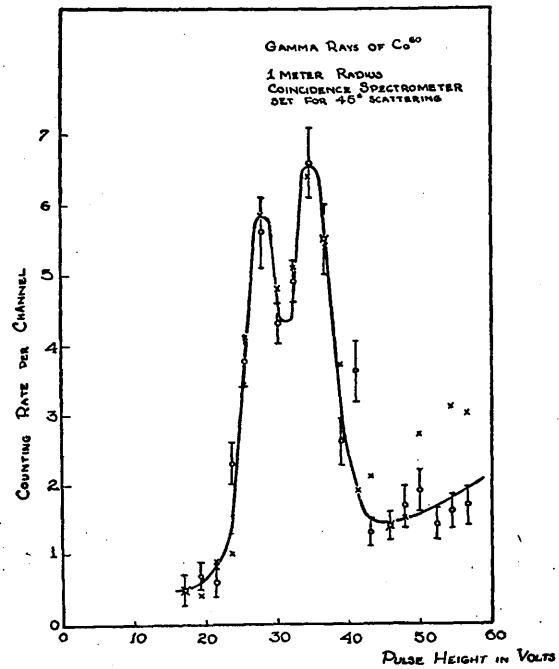

FIG. 6. Gamma-ray spectrum of Co^{60}. (Two runs of 1 hour each.) The peaks correspond to gamma energies of 1.17 and 1.34 Mev. The delay between counters is 4×10^{-9} sec in this case.

FIG. III.17

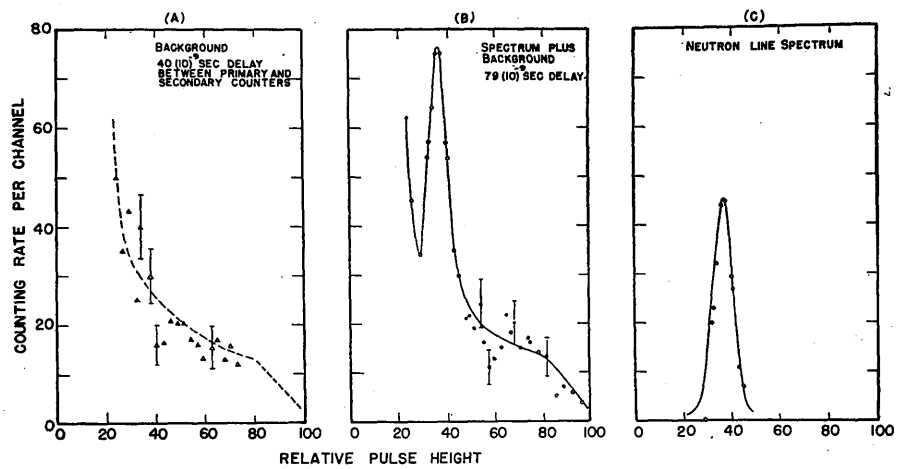

FIG. 7. (A) Background distribution, with delay too short for true coincidences. (B) Over-all pulse-height distribution observed for the products of the D, D reaction. (The points of curve *B* are from two separate runs. (C) Subtracted points, fitted with theoretical curve.

FIG. III.18

OPERATION OF THE SPECTROMETER AND EXPERIMENTAL RESULTS

FIG.III.16, which shows the total coincidence rate against delay time for the instrument operating on Co^{60} γ-rays and the products of the (D - D) reaction plus contamination, illustrates the operation of the spectrometer. It is clear that when the delay line is set for neutrons of a given energy range, of maximum energy ~ 10 MeV, no γ-rays will give true coincidences. (The approximate incident neutron energies corresponding to the times of flight are noted under FIG.III.16 for the geometry of the experiment).

The experimental results on Co^{60} γ-rays and (D - D) neutrons observed by Chagnon are illustrated in FIGS.III.17 and 18. They are very similar to those obtained by the author in FIGS.III.13 and 15. For comparison also is included Draper's result on (T - D) neutrons, using a similar geometrical arrangement. They are similar to those presented by the author in FIG.III.14 and are shown in FIG.III.19.

CONCLUSIONS

This method, although offering an advantage over the (E_p, θ) method, is still limited by the requirement that, in order to measure a spectrum of neutron energies, from a few MeV upwards, a series of delays would be required. It is also clear from FIG.III.16 that, for high neutron energies, complete discrimination against γ-rays could not be obtained since the resolving time employed is such that for neutron times of flight $\leq 2 \times 10^{-8}$ secs. the delay inserted would not be sufficient to exclude true coincidences due to γ-rays.

The use of a faster coincidence unit of resolving time less than 10^{-8} secs, although it solves the difficulty of measuring energies greater than 10 MeV, would accentuate the difficulty of covering a complete neutron spectrum at one

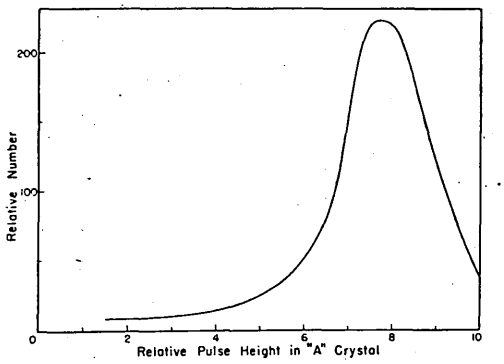

FIG. 6. $T-d$ neutrons. The difference of curves 5(a) and 5(b) corrected for the energy dependence of the spectrometer efficiency.

FIG.III.19 (AFTER DRAPER (6)

FOR $\theta = 45^{\circ}$)

delay setting, i.e. the reduction of the resolving time would require the use of a larger number of delays.

Later in Part III.5 a discussion of this method in the light of the more simple time of flight method will be given.

TABLE III.1

COMPOUND	ACTUAL BORON CONTENT %
Tri-methyl borate	9.32
Tri-ethyl borate	7.24
Tri-propyl "	5.31
Tri-butyl "	4.70
Tri-amyl "	3.97
Tri-hexyl "	3.44
Tri-octyl "	2.71
Tri-cresyl "	3.25
Tri-2-cyclohexyl--cyclohexyl borate	1.90
Tri-hexylene glycol biborate	5.82

III.4 DOUBLE SCATTERING WITH THE DETECTION OF THE SCATTERED NEUTRON IN THE EPITHERMAL RANGE OF ENERGIES (E_p, E_n) METHOD

III.4(a) INTRODUCTION

Before proceeding to a detailed discussion of this double scattering method a brief survey of the investigations carried out by the author in the development of a convenient epithermal neutron detector using a Boron-loaded liquid scintillator will be given. In Part III.1 the boron-loaded scintillator has been discussed in the detection of fast neutrons using a large volume of scintillator. It is proposed to outline briefly at the conclusion of this section the properties of such a method in the measurement the energies fast neutrons since, up to the present, no results have been published using this technique.

III.4(b) BORON-LOADED LIQUID SCINTILLATORS

THE PREPARATION OF THE SCINTILLATOR

By the addition of a nucleus, having a high slow neutron cross-section, to a liquid scintillator an efficient slow neutron detector with a very fast response time can be obtained. The problem of introducing such a nucleus is one of finding a suitable compound which, on addition to the scintillator, does not appreciably reduce its fluorescent efficiency. Compounds of boron have been tested by the author and found suitable. Such compounds have been considered by other investigators. (Muehlhause and Thomas (3), Cleland (15) and Kirkbride (16).) Compounds of cadmium have been preferred by others when larger volumes of scintillator have been employed. (Harrison(4)).

The boron compounds comprise the family of liquid borate esters shown in Table III.1. The lower alkyl borates hydrolyse readily but stability

tends to increase as the length of the carbon chain increases. Thus tri-n-butyl borate does not hydrolyse quite as rapidly as the methyl compound, though it does decompose quickly in the presence of water. Tri-methyl borate, the lowest of the series, forms an azeotrope with methanol and is therefore difficult to obtain in a state of high purity. This compound, which has been used by Muehlhause (3), hydrolyses even on exposure to air. The author, however, found by investigation of a number of liquid borates that a new compound Tri-hexylene glycol bi-borate could be more easily incorporated in the scintillator than the others, because of its greater stability. In the compounds of boron used by the author no enrichment of the quantity of B^{10}, the active component of natural boron, has been attempted.

B^{10}, which is present in ~ 18.8% in normal boron, has a high capture cross-section (4000 barns at thermal energies of the neutrons) which follows a $\frac{1}{v}$ law from thermal energies to 300 KeV. The capture results in an exothermic reaction yielding two energetic charged particles.

$$B^{10} + n \rightarrow Li^{7*} + He^4 + 2.3\ MeV \quad (93\%)$$
$$B^{10} + n \rightarrow Li^{7} + He^4 + 2.8\ MeV \quad (7\%)$$

The predominant reaction produces an α-particle which, because of the poor response of organic scintillators to heavy particles, is equivalent to a 120 KeV electron in the liquid scintillator. Thus, if the γ-ray from the de-excitation of Li^{7*} is captured in the liquid scintillator, the total pulse height from the capture process is equivalent to a 0.6 MeV electron. (The mean free path of the γ-ray in the liquid is however of the order of 10 cm. suggesting that, in the case of small scintillators the probability of capture is small).

The investigations have been carried out using as a counter filling a solution of equal volumes of the standard scintillating liquid (5 g/l terphenyl

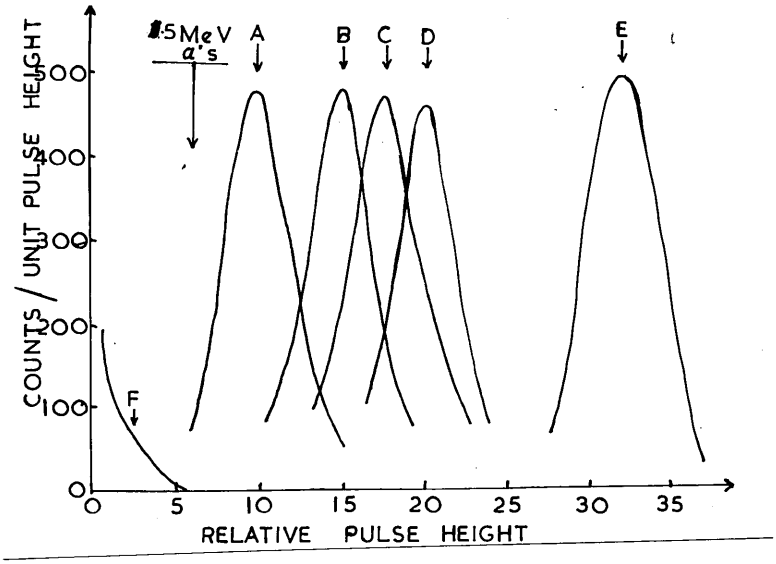

FIG.III.20 Po α'S ON LIQUID SCINTILLATOR

A - SOLUTION OF TERPHENYL + ADDED SOLUTE + BORATE IN XYLENE

B - PURE TERPHENYL IN XYLENE

C - SAME AS -A- WITH BUBBLING OF SOLUTION

D - TERPHENYL + ADDED SOLUTE

E - SAME AS -D- WITH BUBBLING

F - NOISE LEVEL

in xylene + 0.1 g/l phenyl - α - napthylamine) and the clear, colourless borate, tri-nexylene - glycol biborate.

PULSE HEIGHTS FROM THE BORON-LOADED SCINTILLATOR

A standard scintillation cell of the type shown in FIG.II.1 (a) and (b) and of length 2" was filled with the borate solution indicated above and its response to 5.3 MeV α-particles from a Po source investigated. The spectra for these α-particles were measured under various conditions using the 100 channel kicksorter and are shown in FIG.III.20. (The conditions, under which spectra A to F were observed are noted under the figure). The observed spectra of the α-particles and noise from the photo-multiplier are shown in A and F respectively.

Since the light output from the α-particle of the boron capture reaction are smaller, by a factor of three, than the 5.3 MeV α-particles it is clear from A and F that the pulse heights from multiplier noise and the B^{10} capture α's will be of the same order. It was noted, however, from the work of Pringle et alia (17) that, removal of oxygen from the liquid scintillator, by bubbling nitrogen through it, caused an increase in the light output from the solution. On treatment of the borate solution in this way the pulse height from the Po α's was increased to the value shown in C. In this solution the position of the peak from the capture reaction α-particles should appear in the position shown in FIG.III.20, a value slightly greater than that for the maximum pulse height from noise. Thus the choice of a suitable electronic bias, in this case 4 pulse height units, will enable discrimination against noise pulses without reducing to any considerable extent the efficiency of detection of the α-particles from the capture reaction. Muehlhause and Thomas (3) have used two multipliers in coincidence to eliminate the effects

of noise in these counters. A further method is to cool the multiplier to a temperature of $\sim -10^{o}C$.

EFFICIENCY OF DETECTION

The efficiency of detection of slow neutrons in this boron-loaded scintillator is important in considerations of the (E_p, E_n) spectrometer for fast neutrons. Although no direct measurements have been made by the author, mainly due to the lack of a suitable source of slow neutrons, the results of Muehlhause and Thomas (3) have been used to indicate the probable efficiency in this case. The efficiency is governed mainly by the processes of scattering, moderation and escape from the scintillator before capture. The results suggest that for neutrons of thermal energies the efficiency of the scintillator used by the author is $\sim 90\%$ and for epi-thermal neutrons $\sim 60\%$.

LIFETIME OF NEUTRONS IN THE SCINTILLATOR

In the region ($E_n < 300$ KeV), where the $\frac{1}{v}$ capture law holds the time spectrum for neutron capture is exponential. The life-time associated with this exponential function depends on the number of boron atoms in the scintillator. For the recipe of scintillator used by the author the lifetime is calculated as $\sim 2.5\ \mu$secs.

III.4c THE DOUBLE SCATTERING METHOD (E_p, E_n)

THE PRINCIPLE OF THE METHOD

In the analysis of resolution and efficiency of the (E_p, θ) method discussed in Part III.3, it was noted that the optimum values of these factors was obtained when the angle of scattering approached 90^{o}. To detect the scattered neutrons in an organic scintillator was, however, shown to be impossible because of the very poor response of the scintillator to low energy protons. In this (E_p, E_n) method, however, the problem is solved by

substituting for the second simple organic scintillator, a boron loaded scintillator which has a high detection efficiency for slow neutrons and which produces a pulse from the slow neutrons detectable above photo-multiplier noise.

Most of the pulses from the boron loaded scintillator are, however, delayed with respect to the pulses from the primary counter, since the capture time-spectrum for slow neutrons is exponential with a lifetime of 2.5 μsecs. This property can be used to advantage in discriminating against γ-rays which produce prompt coincidences when scattered between the counters.

Observation of delayed coincidences between the counters, in this instance in the time interval from 1/2 μ sec. to 2-1/2 μsecs. after the appearance of a pulse in the primary counter, enables the measurement of fast neutron energies and at the same time discards prompt coincidences due to γ-rays.

RESOLUTION

In the analysis of the resolution of the double scattering method (E_p, θ) given in Part III.3, it was noted that this factor comprised two terms $(\Delta L_p)_{Geom}$, and $(\Delta L_p)_{S.C.}$ both of which had a minimum for $\theta \doteqdot 90^o$ for a fixed energy of the incident neutron. It is thus clear that this (E_p, E_n) method in which $\theta \doteqdot 90^o$ has the best resolution possible in a double scattering method employing pulse height analysis. The resolution is determined mainly by $(\Delta L_p)_{S.C.}$, since $(\Delta L_p)_{Geom.}$ is dependent on $\omega t \theta$ and tends to 0 as θ tends to 90^o. This term is governed mainly by the optical and electronic properties of the primary scattering channel.

EFFICIENCY

Although the detection efficiency of the boron loaded scintillator is 60% for epithermal neutrons its effective efficiency in the (E_p, E_n) arrangement is reduced to 30%, since half of the pulses from the scintillator are rejected

- ELECTRONIC BLOCK DIAGRAM -
- FOR BORATE DELAYED -
- COINCIDENCE SPECTROMETER -

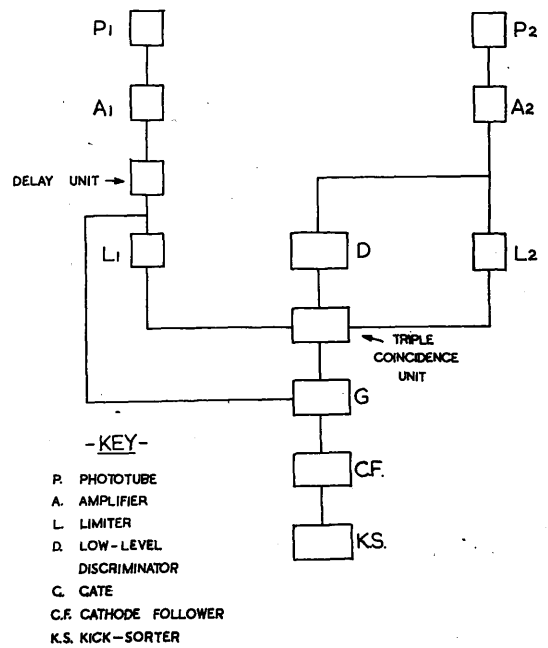

FIG. III.21

in the delayed coincidence measurements. The overall efficiency of the (E_p, E_n) method is greater than in the (E_p, θ) method giving its best resolution since the separation of the scatterers can be reduced without affecting the resolution of the instrument and further since the detection efficiency of the second scatterer is higher.

Using an arrangement of scatterers of the simple geometry of FIG.III.9, with $\theta \doteq 90^\circ$ and $d_1 = 2''$ and scintillators P_1 1" long and 1" in diameter and P_2 2" long and 1" in diameter the overall detection efficiency has been calculated as 1 in 10^{+4} per incident neutron. This is an order of magnitude greater than in annular ring geometry of the (E_p, θ) method for a resolution of 20%. By extending the second scatterer to an annular ring scintillator the efficiency could be further increased by an order of magnitude.

ELECTRONIC ARRANGEMENT

The block diagram for the electronic equipment is shown in FIG.III.21. Pulses from the primary scatterer P_1, are amplified, delayed and limited in L, before being applied to the triple coincidence unit. Pulses direct from P_2 are treated in a similar manner. (These pulses are also fed into a low level discriminator which operates the third channel of the coincidence unit. The discriminator is inserted to reject noise pulses from P_2). The coincidence unit and low-level discriminator have been considered in more detail in Appendix II.

The delayed pulses from P_1. are shaped to 2 μsec square pulses and the pulses from P_2 to 1/2 μsec. pulses, before application to the coincidence valves. By this means delayed coincidences between the counters in the time interval from 1/2 μsec to 2-1/2 μsec after the appearance of a pulse in the primary counter are registered on the output of the coincidence unit.

These coincidence pulses are then used to operate the linear gate G, and select for pulse height analysis coincident pulses from the primary scatterer.

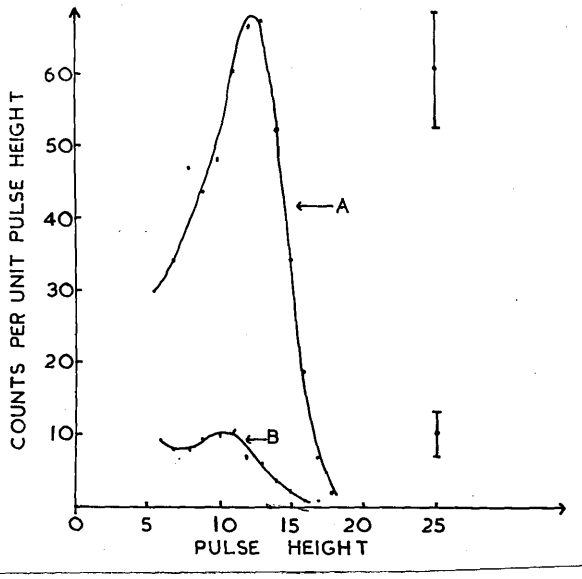

FIG. III.22 DOUBLE SCATTERING Co^{60} γ-RAYS

A - DIRECT COINCIDENCES

B - COINCIDENCES WITH $\frac{1}{2}$ μ SEC DELAY IN PRIMARY SCATTERING CHANNEL

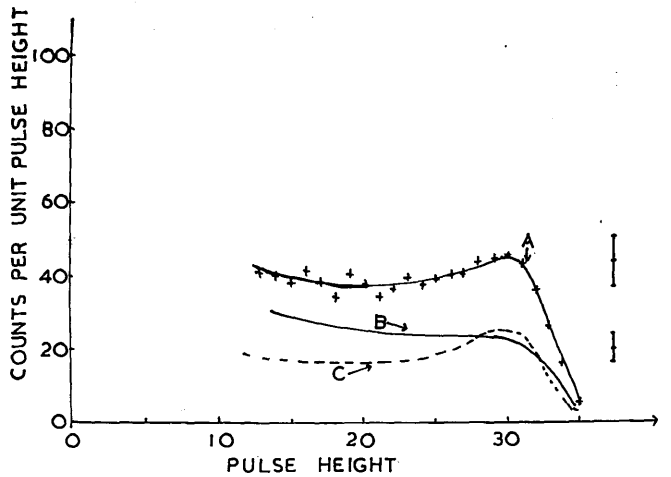

FIG. III.23 DOUBLE SCATTERING 14 MeV NEUTRONS

A - OBSERVED SPECTRUM

B - RANDOM COINCIDENCES

C - SUBTRACTED DISTRIBUTION

EXPERIMENTAL RESULTS

To test the operation of the electronic arrangement and its ability to discriminate against γ-rays, the counters P_1 and P_2 were arranged so that $\theta = 120^\circ$ and $d_2 = 2"$ in the simple geometry of FIG.III.9. and irradiated with Co^{60} γ-rays of mean energy 1.2 MeV. (P_2 was shielded from the direct beam using lead blocks). The distance of P_1 from the source was adjusted to ensure that the random coincidence rate was small compared to the real coincidence rate.

Prompt coincidences were observed and the spectrum is shown in FIG.III.22A. On the insertion of a delay of 1/2 μsec. in the primary scattering channel the spectrum of FIG.III.22B was observed showing that the efficiency of the arrangement under the conditions in which the neutron spectra are to be observed is negligible.

OBSERVATION OF 14 MeV NEUTRONS FROM (DT) REACTION

With the same scatterers and $\theta = 90^\circ$ the overall pulse height spectrum observed from the products of the (D,T) reaction is shown in FIG.III.23A. The random coincidence spectrum, observed by the insertion of a long delay in the primary channel, is given in FIG.III.23B. The subtracted distribution is given in FIG.III.23C. In this case the real to random coincidence rate is rather low. The long tail at pulse heights lower than the peak can be attributed to two main factors :-

(a) multiple scattering in the primary scatterer calculated to be of the order of 20% in crystal P_1 and

(b) neutrons, which are scattered at angles less than 90° being completely stopped in P_2 and thus registered as delayed coincidence.

(This is the more important process in producing the long tail).

The resolution of neutron peak is approximately 25%, considerably poorer

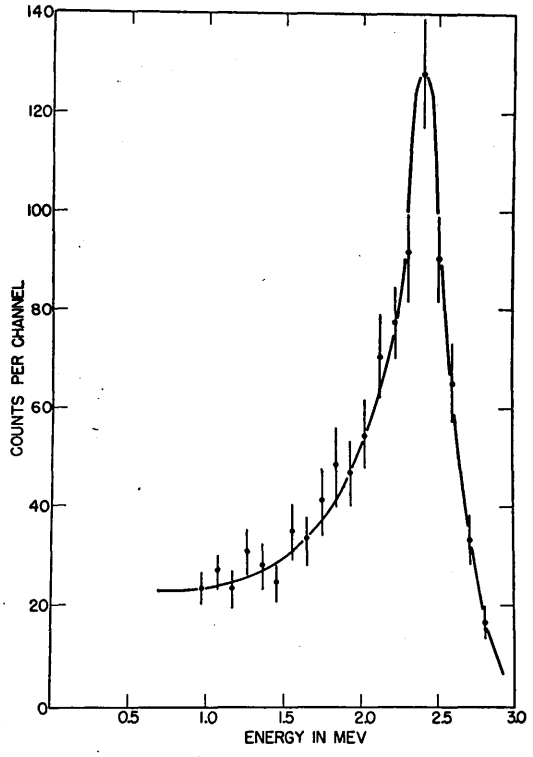

Neutron peak.

FIG.III.24 (AFTER BEGHIAN ET ALIA (8))

than expected, primarily due to the effects of multiple scattering. Reduction of the dimensions of the primary scatterer would improve the resolution and at the same time reduce the effect of the factor (b) mentioned above.

III.4d. AN (E_p, E_n) METHOD DUE TO BEGHIAN

It is interesting to compare the above method due to the author and a similar geometrical method due to Beghian et alia (8). The latter differs in using as an epithermal neutron detector a NaI crystal surrounded by silver foil and, also, in the selection of the energy the epithermal neutrons, generally in the range from 3 KeV to 50 KeV. Discrimination against γ-rays is obtained by a time-of-flight method of the type described earlier in the (E_p, θ, t) method.

The spectrum of 2.5 MeV (D, D) neutrons obtained by this technique is shown in FIG.III.24. The resolution of the peak is 18% and the efficiency of the order of 1 in 10^{+6} per incident neutron. The poor efficiency can be attributed to two main factors. Firstly, the epithermal neutron detector has about 6% efficiency compared to 60% for the boron loaded scintillator; secondly, the epithermal neutron detector and the coincidence circuitry select a very narrow band of neutron energies. This latter factor reduces considerably the overall efficiency of the arrangement without improving the resolution, since the primary scatterer and its associated electronics are incapable of reproducing the narrow energy band of recoil protons as a narrow band of pulse heights.

This technique could be improved by replacing the secondary scatterer by the boron loaded detector, which would have a larger efficiency and a faster response time than the "silver-encased" sodium iodide detector. The main advantage of this type of technique over that investigated by the author lies in the improvement in resolution due to the selection of the energy of the scattered neutrons.

III.4e. A LARGE VOLUME DETECTOR

Using a large cylinder of scintillator 75 cm in diameter and 75 cm high, incorporating a compound of cadmium Reines et alia (18) have efficiently detected neutrons in the presence of a high background of γ-rays. The discrimination against γ-rays has been performed using a delayed coincidence technique, the primary pulse corresponding to a recoil proton and the secondary pulse due to the γ-ray due to the capture of the slowed-down neutron in cadmium.

This detector has been applied by these investigators to the measurement of the energies of the 1.1 MeV and 1.3 MeV γ-rays from Co^{60}. The resolution is sufficient to distinguish between the two energies. The principle of operation of such a detector in the measurement of fast neutron energies has been given earlier in Part III.1. Analysis of the expected distribution however shows that instead of a narrow peak corresponding to the total neutron energy, it is considerably broadened due to the ill-effects of the non-linear pulse height v energy relationship for protons in the liquid scintillator. The resolution of the peak for 14 MeV neutrons is calculated to be approximately 50%, rather poor for most applications.

Reduction of the dimensions of the scintillator to ensure that the neutrons, registered as delayed coincidences, have lost most of their energy in their first collision in the liquid, although reducing the efficiency per incident neutron by an order of magnitude increases the expected resolution by a factor of 2. Thus the smaller detector may prove quite useful in many applications in fast neutron spectrometry.

III.4(f) CONCLUSIONS

The boron loaded scintillator is a considerable advance in technique in the detection of slow neutrons with high efficiency. Trihexylene glycol biborate, because of its stability, simplifies the preparation of this type of scintillator. The main advantages of this type of scintillator over conventional methods such as BF_3 counters are its very fast response time $\sim 10^{-9}$ secs, very high efficiency $\sim 90\%$ and its small detecting volume. Boron loaded scintillators are ideally suited for slow neutron time-of-flight measurements for which high efficiency and fast response are desirable.

In the fast neutron spectrometer, employing a boron loaded scintillator, investigated by the author, although the energy resolution is rather poor, the geometry can be adjusted to improve this factor and the efficiency increased by the extension of the secondary scatterer to an annular ring. By substituting a boron loaded scintillator for the silver-encased sodium iodide crystal in the Beghian method, the efficiency, its most inadequate property, could be considerably increased since a larger energy band of scattered neutrons could be accepted without impairing its resolution.

The large volume scintillator loaded with cadmium has been shown to be satisfactory in the detection of fast neutrons in the presence of γ-rays but inadequate in its resolution of neutron energies due to the non-linear response of the organic scintillator to protons. In a smaller volume, however, this type of spectrometer could provide adequate resolution for many experiments. In these smaller volumes boron compounds would be preferred since the high energy γ-ray from the cadmium capture reaction, unlike the α-particle from the boron reaction, has a small probability of stopping in the scintillator.

PART III.5 THE TIME OF FLIGHT FAST NEUTRON SPECTROMETER (THE (t) METHOD)

III.5(a) INTRODUCTION

The methods of fast neutron spectrometry, which have been discussed in the preceding sections of Part III, have relied on pulse height analysis for the measurement of the neutron energies. The non-linearity of organic scintillators to protons however mitigates against the quality of the results. Measurement of neutron energies by a time of flight method only requires the detection of the neutrons and is therefore independent of this non-linearity. A further advantage of a time-of-flight method lies in its ability to discriminate against γ-rays by utilising the difference in time-of-flight between neutrons and γ-rays. Satisfactory neutron detectors for such a technique must have high efficiency and fast response. It must also be possible to construct large volume detectors so that the efficiency can be maintained over long flight paths. The liquid scintillator counter is ideal for this purpose.

The method to be described in this section utilises to the fullest extent the exceptional qualities of liquid scintillation counters and at the same time surmounts the difficulties associated with the methods of fast neutron spectrometry described earlier. The greatest efficiency in any of the double scattering methods of fast neutron spectrometry is also achieved in this technique by virtue of its unique geometrical properties.

The success of this method in resolving the high energy neutron groups in the $B^{11}(d,n)C^{12}$ reaction shows its adequacy to perform many of the experiments outlined in Part I.

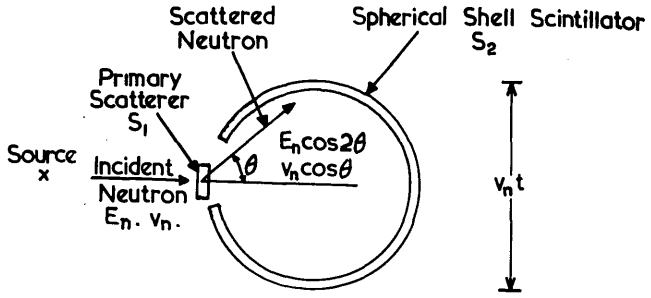

- A -

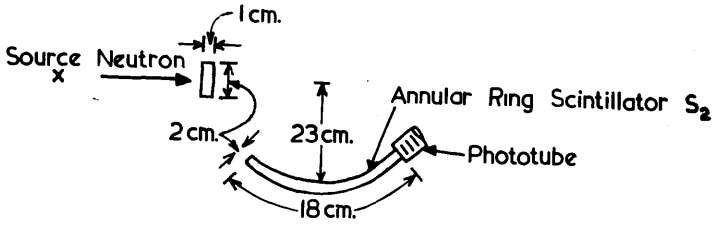

B - GEOMETRY — S_2 IN MERIDIAN POSITION

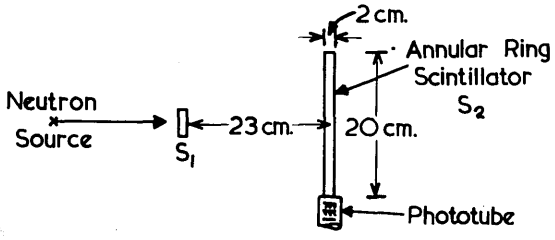

C - GEOMETRY — S_2 IN AZIMUTHAL POSITION

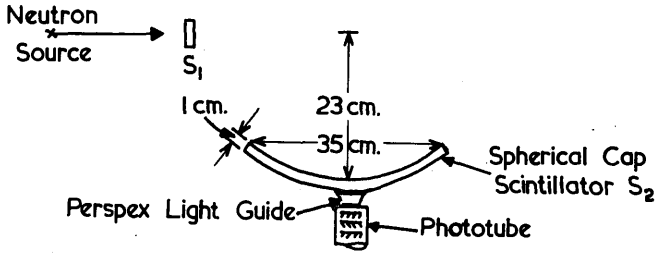

D - GEOMETRY — S_2 IN SPHERICAL CAP POSITION

FIG. III.25 SCINTILLATOR ARRANGEMENTS

III.5(b) THE PRINCIPLE OF THE METHOD

In FIG.III.25 is shown the geometries associated with this method. When a neutron of energy E_o and velocity v_o is scattered at an angle θ in the primary scatterer S_1, the energy and velocity of the scattered neutron are $E_o \cos^2\theta$ and $v_o \cos\theta$ respectively. The distance from the point of scatter assuming S_1, is small to any point on the surface of the sphere of radius a, is $2a\cos\theta$.

Thus the time of flight between the primary scatterer S_1, and the spherical shell scintillator S_2 is :

$$t = \frac{2a\cos\theta}{v_o \cos\theta} = \frac{2a}{v_o}$$

i.e. the time of flight between S_1 and the surface of the sphere of radius a, is independent of the angle of scattering and depends only on the velocity of the incident neutron and the diameter of the sphere.

Thus by measuring the time of flight of neutrons between a small primary scatterer S_1, on the extremity of the diameter of the sphere along which the neutrons are incident, and a thin spherical shell scintillator S_2, the energies of the incident neutrons can be calculated. This measurement is made by observing coincidences between delayed pulses from S_1 and direct pulses from S_2.

For a sphere of diameter 50 cm, the time of flight of a neutron of energy E_o is :

$$t = 3.6 \times 10^{-8} . E^{-1/2} \text{ secs} \quad \text{-----} \quad (1)$$

In the energy range of 1 MeV to 20 MeV the time of flight is of the order of 10^{-8} secs, thus requiring coincidence resolving times of the order of 10^{-9} secs. to give adequate energy resolution. The methods of millimicro-second coincidence measurement will be considered in more detail in Part III.5(e).

III.5(c) RESOLUTION AND EFFICIENCY

For a neutron group of energy E_n incident on the spectrometer arrangement shown in FIG.III.25(A) there results not a unique time of flight T_n but a distribution of times of flight. The factors which cause this spread in time of flight are the finite resolving time of the coincidence unit and the finite size of the scattering cells. The following approximate analysis of spread in time of flight indicates the most important factors influencing the resolution of the spectrometer.

(1) The resolving time of the coincidence unit

The resolving time, t, of the coincidence unit is equal to $\frac{N_c}{N_1 N_2}$ where N_c = chance coincidence rate and N_1 and N_2 are the counting rates of unrelated events in the two counters of the coincidence system. In practice this resolving time is measured by observing the prompt coincidence resolution curve for the coincidence circuit, i.e. the curve of coincidence rate as a function of the delay time artificially inserted in series with each counter in turn. The full width at half height of this curve gives approximately the resolving time of the unit.

The ultimate resolving time of coincidence units using organic phosphors such as terphenyl in xylene has been considered in detail by Post and Schiff (19) and Post (20). These authors show that for small scintillators, resolving times better than 3×10^{-10} secs., cannot be achieved with the photomultipliers at present in existence. This figure is appreciably increased when large scintillators are employed or when the energy expended by the radiation in the scintillator is small.

In thepresent experiments the resolving time of the coincidence unit is 5×10^{-9} secs. With such a resolving time the effect of photon transit

time in large scintillators is not appreciable. The coincidence unit will be referred to in more detail in Part III.5(e). The effect of photon transit time on the photon collection-time spread at the photocathode of the multiplier will, however, limit the best obtainable resolution to a value of 10^{-9} secs.

(2) The geometrical factors contributing to a spread in the time of flight.

Variations in the time of flight T_n of the neutrons are caused by the finite sizes of the scattering cells. In the following discussion the main factors influencing the spread in time of flight will be considered.

A spread in the time of flight may occur as follows :

(a) The scattered neutrons may have a constant flight path, S, but slight variations in the angle of scattering due to the finite size of the primary scatterer may occur. This introduces a spread in time of flight given by

$$\Delta T_1 = \frac{S}{v_0 \cos^2\theta} \cdot \sin\theta \, d\theta$$

$$= \frac{S}{v_0 \cos^2\theta} \cdot \frac{\sin\theta \cdot r_1}{S}$$

r_1 = radius of the primary scatterer S_1

$$\frac{\Delta T_1}{T_n} = \frac{v_0 \, r_1 \sin\theta}{2R \, v_0 \cos^2\theta} = \frac{r_1 \sin\theta}{2R\cos^2\theta} \qquad \text{..... (2)}$$

(b) The scattered neutrons may be scattered through a fixed angle θ, but have variable flight path, giving

$$\frac{\Delta T_2}{T_n} = \frac{r_2}{2R\cos\theta} \qquad \text{..... (3)}$$

$2r_2$ = length of S_1 parallel to the incident neutron beam.

(c) The scattered neutrons may be scattered at any point in the secondary scatterer at a fixed angle of scatter θ, due to the finite thickness of S_2, giving

$$\frac{\Delta T_3}{T_n} = \frac{r}{2R\cos^2\theta} \qquad \text{.... (4)}$$

where r = thickness of S_2

From these factors it is clear that if r_1, r_2 and r are small with respect to R and the angle of scattering is chosen so that $\cos\theta > 0$ i.e. angles in the range $0 < \theta < 70^\circ$, the spread in time of flight due to these geometrical factors is small compared to the resolving time of the coincidence unit. In the experiments to be described r_1 = 1 cm r_2 = 1/2 cm r = 1 cm and R = 25 cm. and thus the spread in time of flight for $\theta = 60^\circ$ are $\Delta T_1 = T_n \times \frac{1}{20}$; $\Delta T_2 = T_n \cdot \frac{1}{50}$; $\Delta T_3 = T_n \times \frac{1}{25}$. For 14 MeV neutrons $T_n = 10^{-8}$ secs. Thus the spread due to these geometrical factors is less than 10^{-9} secs. These geometrical factors, however, set a lower limit to the resolving time which is higher than that suggested in the section on the time resolution of the coincidence unit. The energy resolution of the spectrometer derived from equation (1) is given by,

$$R = \frac{2\Delta E}{E} = \frac{4\Delta T}{T_n} \qquad \ldots\ldots (5)$$

where ΔT is the time resolution which is governed by the resolving time of the coincidence unit. In the energy range 1 MeV to 14 MeV the resolving time of the coincidence unit is constant and therefore the energy resolution is governed by T_n^{-1}, i.e. by $E_o^{+1/2}$, from equation (1). Thus this time of flight method has its best resolution at low energies of the incident neutron unlike the pulse height methods mentioned in earlier sections which have their best resolution at large energies of the incident neutron.

EFFICIENCY

With the geometry shown in FIG.III.25A and source strength of N_0 neutrons the following calculation gives the efficiency of the arrangement.

Number of neutrons scattered in S_1 = $\dfrac{N_0 \cdot 2\pi \cdot r_1^2 \cdot r_2 \cdot n \cdot \sigma(E_0)}{4\pi d^2}$

$$= \frac{N_0 \cdot r_1^2 \cdot r_2 \cdot n \cdot \sigma(E_0)}{2 d^2}$$

where d = distance from the source to the centroid of primary scatterer

n = number of hydrogen atoms/c.c.

$\sigma(E_0)$ = cross section for $(n\text{-}p)$ scattering of a neutron of energy E_0.

$$\left\{\begin{array}{l}\text{The number of these neutrons} = \dfrac{N_0 \cdot r_1^2 \cdot r_2 \cdot n \cdot \sigma(E_0)}{2d^2} \cdot \sin 2\theta \cdot d\theta \\ \text{scattered into } d\theta \text{ at an angle } \theta\end{array}\right.$$

Therefore the number of these neutrons scattered again in S_2

$$= \frac{N_0 \cdot r_1^2 \cdot r_2 \cdot n \cdot \sigma(E_0) \cdot n \cdot \sigma(E_0 \cos^2\theta) \cdot r \cdot 2\sin\theta \cdot d\theta}{2d^2}$$

If the angle of scattering θ is selected so that the pulses produced in the counter are large enough to operate the coincidence unit, then,

$$\left.\begin{array}{l}\text{the efficiency} \\ \text{of the spectrometer}\end{array}\right\} = \frac{N_0 \cdot r_1^2 \cdot r_2 \cdot n^2 \cdot \sigma(E_0) \cdot r}{d^2} \int_{\theta_2}^{\theta_1} \sin\theta \cdot \sigma(E_0 \cos^2\theta) \cdot d\theta \quad \cdots\cdot (6)$$

where θ_1 is the maximum and θ_2 the minimum permissible scattering angle of the neutrons.

A comparison between the efficiency of this type of spectrometer obtained by integration of (6) employing a spherical shell and that of the pulse height methods employing a complete annular ring shows an increase of efficiency by, at least, an order of magnitude.

III.5(d) DESIGN CONSIDERATIONS

Neutrons of energy E_0 have a time of flight T_n given by $7 \times 10^{-10} \cdot 2R \cdot E_0^{-\frac{1}{2}}$ where R is the radius of the spherical scintillator. Good resolution favours large values of R. This leads to the consideration of the design of very large scintillators.

A considerable number of technical difficulties arise in the construction of such a spherical shell, such as the manufacture of large spherical surfaces

in glass or a suitable metal such as aluminium. Further limits in the size of a large scintillator are self-absorption of the light emitted and poor light collection which both reduce the efficiency of the counter. Although this large scintillator is used as a detector and does not require the uniform collection of light from its volume it is important to collect as large a percentage of light as possible in order to ease the operation of the fast coincidence unit.

A figure of approximately 25 cm for R was chosen as one for which a suitable scintillator could be constructed and for which self absorption effects were small. The spherical cap of dimensions shown in FIG.III.25 was constructed using two pyrex globes of radius of curvature 25 cm. Light collection was obtained by packing the scintillator with magnesium oxide in a light tight box and viewing through a perspex light guide. Better efficiency of light collection could be obtained if a number of photomultipliers were used to observe the scintillations.

In the calculation of the efficiency of the arrangement it was noted that for θ small the energy expanded in the primary scatterer was too small to operate the coincidence unit and for θ large a similar effect was noted in the second scatterer. Thus in designing the spherical scintillator values of θ in the range $10^\circ < \theta < 70^\circ$ should be chosen since the extension to values of θ outside these limits does not add to the overall efficiency but only increases the background counting rate. Values of r_1, r_2 and r should be chosen large to increase the efficiency of the spectrometer but are limited in size by their effect on the resolution. For the scintillator sizes shown in FIG.III.25 these factors do not increase the time resolution as governed by the coincidence unit, and give good efficiency. This efficiency could however be increased, by increasing the dimensions of the primary scatterer, without affecting the resolution.

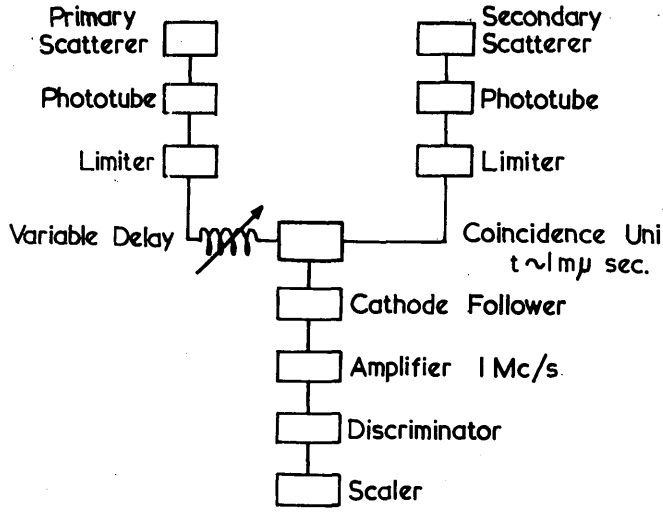

ELECTRONIC BLOCK DIAGRAM
FOR
SINGLE CHANNEL TIME ANALYSER

FIG. III.26

III.5(e) ELECTRONIC EQUIPMENT

The block diagram of the electronic apparatus is shown in FIG.III.26. It is based on the circuitry used by Bell et alia (21) and is described in detail in Appendix II. In this section, therefore, only the principle of operation of the circuit shall be considered.

Pulses from the photo-multipliers (E.M.I. Type 6262) are impressed on the grids of the limiting valves which are built into the multiplier assembly to improve the high frequency response of the circuit. In order that the pulses from these multipliers are sufficient to cut off the limiting valves in the shortest possible time a working voltage of 2000v is applied to the multipliers. The positive pulses from the anodes of the limiting valves are transmitted, along lengths of co-axial cable of characteristic impedance 100 Ω , to the coincidence or mixing unit. These cables serve as connecting leads and also as variable delays to the pulses from the individual counters. The action of the mixing unit is described in Appendix II. In principle it comprises a shaping circuit and a point-contact diode which selects and amplifies, by its action, as a non-linear element, coincident pulses from the shaping unit. The pulses from the mixing unit are then amplified and the larger coincidence pulses selected by the discriminator before being counted by the scaler.

The resolving time of the arrangement is determined by the shaping circuit employed in the mixing unit, the bias setting on the discriminator and the energy expended in the phosphor. For the shaping unit employed in the circuit which should give a minimum resolving time of 2×10^{-9} secs, the slower rising pulses from the limiter produce, after shaping, pulses of smaller amplitude than those produced from pulses of faster rise time. Thus the output pulses from the mixing unit are variable in amplitude and the resolving time will depend on the

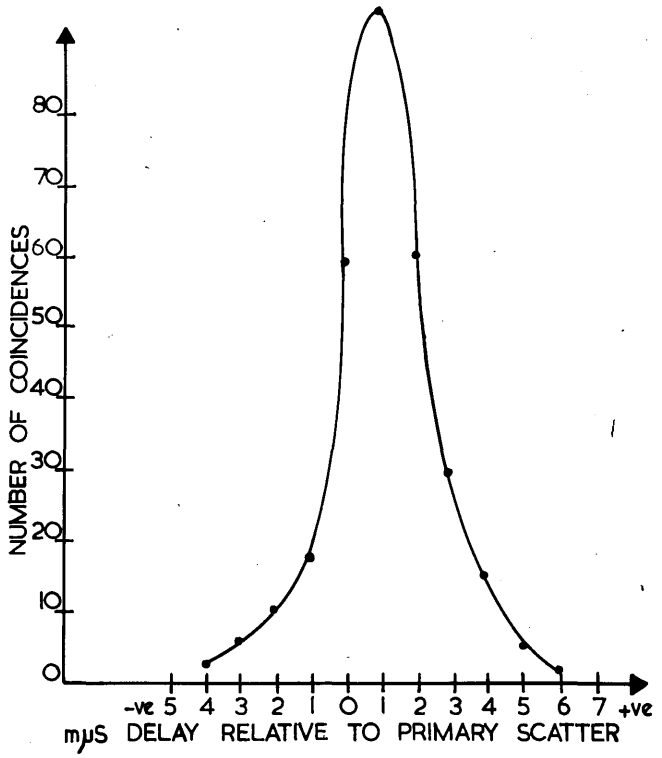

FIG. III.27. RESOLUTION CURVE OBTAINED USING Co^{60} γ-RAYS

discriminator level since a high value of discriminator bias ensures that only those pulses of fast rise-time are counted as coincidences. This effect tends to reduce the efficiency of the circuit when short resolving times are required.

Resolution curves, such as that shown in FIG.III.27 are measured by observing the coincidence counting rate as a function of the delay inserted in series with one of the counters. This curve was obtained when Co^{60} γ-rays were scattered at an angle of 60° between two small scintillators, 2" diameter and 1" long, placed 30 cm apart. In this instance the discriminator bias was set at a fairly high level so that the resolving time of 3×10^{-9} secs could be obtained. The efficiency of the coincidence unit was calculated to be of the order of 50%.

In order to simplify the recording of coincidences a multichannel time delay analyser, shown in detail in FIG.A.13 of Appendix II, was designed. It further incorporates a fast amplifier between the photomultiplier and limiting valve in order to improve the rise-times of the pulses from the limiting valve. This unit, although not employed in any of the experiments to be described in the following section, was successfully operated over three coincidence channels.

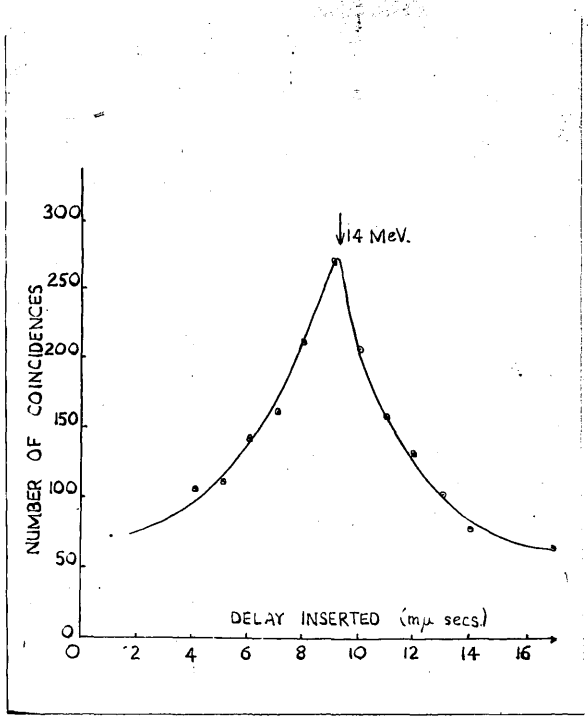

FIG. III.28. TIME OF FLIGHT SPECTRUM FOR $T(d,n)He^4$ NEUTRONS ON ARRANGEMENT OF FIG. III.25B.

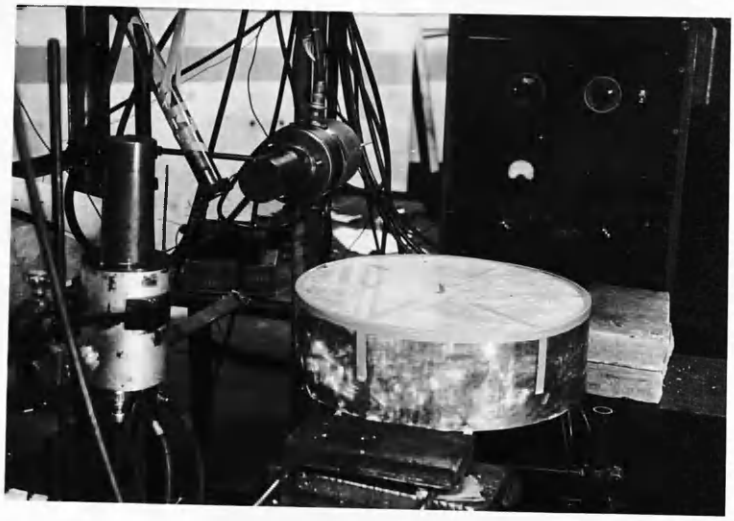

FIG.III.29 SCINTILLATOR ASSEMBLY

SHOWING LARGE SPHERICAL CAP, PRIMARY

SCATTERER AND MONITOR COUNTER

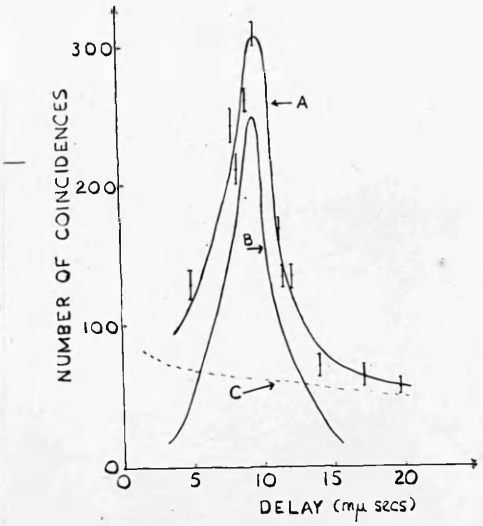

FIG.III.30 TIME OF FLIGHT SPECTRUM FOR T(d,n) NEUTRONS

A - OBSERVED DISTRIBUTION

B - SUBTRACTED DISTRIBUTION

C - SPECTRUM OF RANDOM COINCIDENCES

III.5(e) NEUTRON EXPERIMENTS

(i) Results from the neutrons from $T(d,n)He^4$

A convenient source of high energy neutrons for calibrating and testing the spectrometer was obtained from the interaction of a 350 KeV deuteron beam on a Tritium-Zirconium target. The deuteron beam was provided by the departmental 1 MeV H.T. set. The neutron flux was monitored using a liquid scintillation counter placed at a distance of 100 cm from the target.

With the geometry of FIG.III.25B and the single channel time-analyser, the spectrum shown in FIG.III.28 was observed. (Each point on the curve corresponds to the same total number of counts on the monitor counter.) Observations were carried out at an angle of 45° to the incident beam of deuterons. The observed time of flight is in good agreement with the calculated time of flight of the 14 MeV neutrons of 9.3 μsecs. The energy resolution at this energy is calculated to be 50%.

Although no absolute calculation of the efficiency was made, the time of observation of each point on the curve, approximately 4 minutes, shows the high efficiency of which this spectrometer is capable.

A similar experiment was performed using the arrangement of FIG.III.25D employing the large spherical cap as the secondary scatterer. A photograph of the equipment showing target monitor and spectrometer, is given in FIG.III.29. In this case the spectrum of random coincidences was also observed, by the insertion of the delay in the secondary scatterer channel. The total, random, and subtracted spectra for this arrangement are shown in FIG.III.30.A.C.B. The results are similar to those given in FIG.III.28. In this case the overall

Neutron groups from $B^{11}(d\,n)C^{12}$ (Jo 52a).

Q	C^{12*}
(13.740±0.014)[a]	0
(9.30 ±0.02)[a]	4.44
4.1 ±0.1	9.6
2.9 ±0.1	10.8
2.6 ±0.1	11.1
2.00 ±0.08	11.74
0.98 ±0.08	12.76
0.53 ±0.05[b]	13.21[b]
0.38 ±0.05[b]	13.36[b]
−0.42 ±0.05(?)	14.16(?)
−1.35 ±0.03	15.09
−1.78 ±0.03(?)	15.52(?)
−2.33 ±0.03	16.07

[a] Q values from other disintegration data.
[b] May be one level at 13.3 Mev.

TABLE III.2

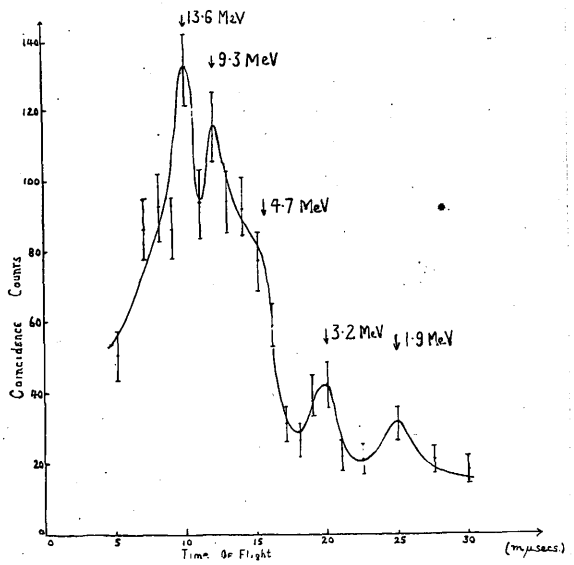

FIG.III.31 TIME OF FLIGHT SPECTRUM OF NEUTRONS FROM B^{11} (d,n) C^{12} REACTION

efficiency was increased by a factor of 4. The increase is a factor of 3 smaller than anticipated, primarily due to poor light collection from the secondary scatterer. The light collection could, however, be improved by increasing the number of photomultipliers on the surface of the large secondary scatterer.

The results presented, however, with these scintillator arrangements were sufficiently encouraging in their efficiency, although the energy resolution is poor, at these higher energies, to attempt to observe the neutrons in a more complex spectrum and in the presence of γ-rays.

An unsuccessful attempt, to use the apparatus with the scintillators in the geometrical situation shown in FIG.III.25C on these 14 MeV neutrons and employing a time of flight discrimination method with pulse height analysis in the primary scatterer, was made due to difficulties encountered in obtaining a linear response from the primary photomultiplier.

(ii) $B^{11}(d,n)C^{12}$ reaction

The intensities and energies of the neutron groups from the $B^{11}(d,n)C^{12}$ reaction have been studied by Johnson (22) and Gibson (23). In Table III.2 are shown the Q values and energies of the corresponding excited levels in C^{12}, derived from the measurements made by Johnson. A level at 7.67 MeV of low intensity was tentatively suggested by Gibson but did not appear in the neutron groups observed by Johnson. Further, measurements of the γ-rays from this reaction by Rutherglen (24) showed that only one γ-ray of energy 4.4 MeV could be attributed to the $B^{11}(d,n,\gamma)C^{12}$. The observations on the neutron groups were performed using photographic plates.

Observations of neutrons in the energy range from 1 to 20 MeV were carried out by the author using the time-of-flight spectrometer in order to test its

operation in resolving a complex neutron spectrum.

With the spectrometer assembly shown in FIG.III.25B the neutrons from the above reaction, using a deuteron beam of energy 550 KeV and a separated B^{11} target, were recorded in a similar manner to the 14 MeV neutrons from the $T(d,n)He^4$ reaction. The spectrum obtainedis shown in FIG.III.31,on observing at an angle of 45° to the incident deuteron beam.

The spectrum shows clearly groups of energy 13.6, 9.3,3.2 & 1.9 MeV with a poorly resolved group at 4.7 MeV. In accordance with the measurements of Johnson they also demonstrate the existence of energy levels in C^{12} at 4.4,9.6 and 12.4 MeV. The group at 3.2 MeV is associated with the presence of deuterium as a contaminant on the target giving rise to the reaction $D(d,n)He^3$.

Comparison of the relative intensities of the neutron groups of FIG.III.31, with the results of Gibson, at the same bombarding energy does, however, suggest that the efficiency of the arrangement decreases with decreasing neutron energy. This effect is due to the sensitivity of the present coincidence unit, to the energy dissipated in the counters, when it is operated at short resolving times. Improvement of the electronic equipment, whereby the rise-time of the output pulses from the anode of the limiting valve is increased, for example, by the introduction of fast amplifier as suggested previously, would enable the coincidence unit to be operated at these low resolving times without a large sensitivity to the energy of the incident neutron. An alternative method of operation of the spectrometer using a longer resolving time and a longer flight path will reduce the variation in efficiency with neutron energy without decreasing the energy resolution of the instrument.

The energy resolution improves as the neutron energy decreases; in the present experimental arrangement it is 50% for the highest energy group decreasing to 25% for the neutrons from the $D(d,n)He^3$ reaction. These figures

are determined by the electronic assembly which was operated at a resolving time of 5 $m\mu$ secs. Similar improvements in the coincidence unit would enable it to be operated at shorter resolving times and thus lead to much improved energy.resolution.

III.5(5) CONCLUSIONS

The success of the present technique in resolving the neutron groups from the $B^{11}(d,n)C^{12}$ reaction demonstrates the power of the method in neutron spectroscopy. The present electronic assembly, although incapable of providing relative intensity measurements of the neutron groups, is adequate to make practicable, angular distribution measurements on a neutron group in reactions of the type given above. The fast response and high efficiency of the instrument suggests its application in angular correlation experiments, for which a spectrometer of this type is so desired.

In the arrangement employed in the above experiments the energy resolution is inferior at high energies but comparable at low energies to that of the pulse height methods previously described. By using a longer flight path, however, the resolution of the time of flight method can be reduced to a value smaller than is possible with these pulse height spectrometers for which the energy resolution is limited by the response of the photomultiplier. It has further been demonstrated by the experiments on the $T(d,n)He^4$ neutrons that it is possible by using large spherical shells to preserve the efficiency over long flight paths. The poor light collection from the spherical cap employed in this experiment, however, mitigate against the quality of the results recorded. It is clear that by improving the light collection by viewing the large scintillators with a number of photomultipliers the high efficiency can be maintained when much longer flight paths are employed to improve the energy resolution.

Its use of the desirable properties of liquid scintillators, namely their fast response, high efficiency and ability of construction in large volumes of any shape, and at the same time its independence of the major difficulties associated with their non-linear response to protons and high efficiency to γ-rays, commends this method to the fast neutron spectroscopist. Of the methods previously described in this Part, this time-of-flight technique is the most complete and with the further improvements suggested in the above discussion promises to be the best fast neutron spectrometer as yet available for studies in the energy range from 1 MeV to 20 MeV.

REFERENCES TO PART III.

1. POST, R.F. :- Phys.Rev.79 p.735 (1950)
2. GILES, R. :- Rev.Sci.Inst.24 p.986 (1953)
3. MUEHLHAUSE C.O. & THOMAS, G.E. :- Nuc.Vol.II No.1 p.44 (1953)
4. HARRISON, F.B. :- Nuc.Vol.12.No.3 p.44 (1954)
5. HOFSTADTER, R. :- Phys.Rev.78 p.619 (1950)
6. DRAPER, J.E. :- Rev.Sci.Inst.25 p.558 (1954)
7. CHAGNON, P.R. et alia :- Rev.Sci.Inst.24 p.656 (1953)
8. BEGHIAN, L.E. et alia :- Phys.Rev. 86, p.1044 (1952)
9. HUTCHINSON,G.W. & SCARROTT,G.G. :- Phil.Mag. 42 p.792 (1951)
10. BIRKS, J.B. :- Phys.Rev.84 p.364 (1951)
11. HARRISON, F.B. :- Nuc. Vol.10 No.6 p.40 (1952)
12. REYNOLDS, G.T. :- Nuc.Vol.10 No.7 p.46 (1952)
13. TAYLOR, C.J. et alia :- Phys.Rev.84 p.1034 (1951)
14. NEILER, R. et alia :- U.S.Office of Naval Res.Report Univ. of Pittsburg (1951)
15. CLELAND, M.R. :- Phys.Rev.89 p.896 (1953)
16. KIRKBRIDE, J. :- Nature 171 p.564 (1953)
17. PRINGLE, J.R. et alia :- Phys.Rev.92 p.1582 (1953)
18. REINES, F. et alia :- Rev.Sci.Inst.25 p.1061 (1954)
19. POST, R.F. & SCHIFF, L.I. :- Phys.Rev.80 p.1113 (1950)
20. POST, R.F. :- Nuc.Vol.10 No.6 p.56 (1952)
21. BELL, R.E. et alia :- Can.Jour.of Phys.Vol.30 p.35 (1952)
22. JOHNSON, V.R. :- Phys.Rev.86 p.302 (1952)
23. GIBSON, W.H. :- Proc.Phys.Soc.A62 p.586 (1949)
24. RUTHERGLEN, J.R. :- Proc.Harwell Nuc.Phys. Conference (1950)

PART IV GENERAL DISCUSSION OF FAST NEUTRON SPECTROMETRY

The work described in this thesis has been devoted to the development of a spectrometer, suitable for the measurement of the intensity and energy of groups of fast neutrons in the energy range from 1 to 20 MeV, using organic scintillators and in particular liquid scintillators. During the course of this work the results of independent investigations have been published; reference has been made to some of these in Part III. It is the purpose of this part of the thesis to discuss more generally these publications in the light of the work performed by the author and to consider the application of these new spectrometers to the problems in nuclear physics of the type described in Part I.

The success of inorganic phosphors, particularly sodium iodide, in γ-ray spectrometry had led to the investigation of certain inorganic crystals containing lithium or boron for the detection of fast neutrons. Various difficulties have arisen however in this work, notably in the preparation of a large uniformly sensitive volume, the low conversion coefficient compared to sodium iodide ($\sim 4\%$ of sodium iodide) and the relatively high sensitivity to γ-rays. A review of the properties of these crystals has been written by Schenck (1). The main object in developing this type of neutron detector must be to obtain a linear response to the products of the lithium disintegration and thus enable one of the serious difficulties associated with organic crystals to be overcome. Sensitivity to γ-rays will, however, always be a serious disadvantage. Although the present results are not encouraging the abundance of possibilities in the search for a good inorganic phosphor suggests that further development may yield a crystal similar in response to sodium iodide. An interesting and useful scintillator has been employed by Frey(2) in the detection of fast neutrons, employing small crystals of zinc sulphide

in polystrene. This phosphor, although it is unable to discriminate between neutrons of different energies, produces large pulses from neutrons compared to its γ-ray response.

The most important developments in fast neutron spectrometry during the past three years have, however, been made using organic scintillation counters. Although the direct application of this type of counter as a fast neutron spectrometer has been shown by the author, in Part II, to present many difficulties, the simplicity of the experimental arrangement commends it to the neutron spectroscopist. Great care has to be taken, however, in the choice of dimensions of the scintillator (due to the effects of the various distorting factors) and in the interpretation of the results; only in certain types of experiment, notably, the inelastic scattering of fast neutrons from heavy nuclei, has some success been achieved. The work of Eliot et alia (3) illustrates the difficulties and range of applicability of the single counter technique. These investigators employed a small stilbene crystal to consider the inelastic scattering of 2.5 MeV neutrons from heavy nuclei. The dimensions of the crystal were chosen so that predominantly single scattering events occurred in it. To overcome the difficulties associated with the measurement of the energiesof the neutrons, directly from the pulse height distribution, a method involving a plot of the ratio of counts with and without the scatterer was used. By this means, the energies of the neutron groups were estimated to the same precision as γ-ray measurements using sodium iodide crystals. These ratio plots did not, however, distinguish between neutrons and γ-rays and a complementary experiment was necessary using a sodium iodide crystal to measure the energies and intensities of the accompanying γ-rays. Also from the ratio plots the authors were able to measure the intensities of the neutron groups with sufficient accuracy to give the cross-section for

excitation of each energy level involved to between 0.1 and 0.3 barn. A similar type of experiment was performed by Poole (4) but using an alternative but less accurate method of determining the energies and intensities of the neutron groups, and a less satisfactory way of overcoming the effects of γ-ray background. (In this experiment the neutron spectrum was derived by differentiation of the proton recoil spectrum which was calculated from the pulse height distribution. The pulses from γ-ray background were eliminated using a difference method involving the subtraction of the distributions observed with polythene and lead absorbers placed between the scattering medium and the counter). Although the results from this type of experiment, especially those of Eliot et alia (3), are satisfactory in giving the intensities and energies of the neutron groups, the measurement of these quantities in a more complex spectrum are much more difficult using a similar technique. Illustrative of the application of a small scintillator to measurements on complex spectra is the work of Ward and Grant (5) on the products of the reaction $B^{11}(d,n)C^{12}$. The pulse height distribution from this reaction observed with a thin plastic scintillator, the dimensions of which were chosen to cause an attenuation of the pulses due to recoil electrons from the 4.4 MeV γ-rays emitted in the reaction, showed clearly steps corresponding to the two highest energy neutron groups but with no such indication of the lower energy groups. In this experiment the interpretation of pulse height distribution for the highest energy groups was considerably facilitated by observations on the 14 MeV neutrons from the D-T reaction using the same scintillator; these 14 MeV neutrons have approximately the same energy as the highest energy group in the $B^{11}(d,n)C^{12}$ reaction. From these results the authors were able to derive the angular distributions of the two high energy groups; but for the use of the tritium neutrons the

accuracy of these results would have been considerably poorer. These results show the limitations of the single counter technique and indicate that in order to obtain a more satisfactory spectrometer more refined single counter or double counter methods, which incorporate some method of discriminating against γ-rays, should be employed.

Two refined single counter methods have been described by the author in Part III, namely the collimating tube spectrometer and the large scintillator loaded with boron. These methods have both presented serious difficulties; in the former case the problem of light collection from a large number of collimating tubes and in the latter the adverse effects on the pulse height distribution of the non-linear response of the liquid scintillator to protons. As fast neutron detectors, however, both of these arrangements have been shown to have characteristics better than existing techniques already described in Part I. Details of a similar detecting technique employing a large scintillator incorporating a cadmium compound have been described by Harrison (6). It is clear, therefore, that only in a double scattering method will the problem of a completely satisfactory fast neutron spectrometer be solved.

The use of two scintillation counters to record the successive scatterings of a fast neutron allows the energies of the neutrons to be calculated either, by analysis of the pulse height distributions in the counters or, by observation of the time of flight of the neutrons between the counters. From the results of the author given in Part III a general comparison of these two types can be drawn. In pulse height methods the resolution is limited by the statistical fluctuations in the scintillator and photomultiplier and by the effects of multiple scattering of the incident neutrons in the primary counter, combined with the non-linear response of the scintillator to protons. At low neutron energies this resolution

is rather poor. For time-of-flight methods the resolution depends on the resolving time of the coincidence unit and the separation of the scatterers, thus theoretically the resolution for time-of-flight methods can always be made better than in pulse height methods. Consideration of the efficiencies of the two methods, however, shows that in the simple time-of-flight methods the practical difficulties in preserving the efficiency over large distances set a limit to the resolution that can be obtained even with the best coincidence unit. At low energies the resolution of the time-of-flight method is at its best, and provides better resolution than in the pulse height methods. The great advantage of the time-of-flight method is its independence of the pulse height response of the organic scintillators to protons.

In Part III both the pulse height methods investigated by the author and those tested by other investigators and published during the course of the author's research notably by Chagnon et alia (7), Draper (8) and Beghian et alia (9), have been described in detail. From these results it is clear, that the pulse height method, incorporating time-of-flight discrimination against γ-rays, used by Chagnon et alia and Draper, together with the scintillator arrangement, namely the conical shell geometry suggested by the author, gives a spectrometer with good resolution and efficiency and capable of operation in a high energy γ-ray background. The method due to Beghian et alia, which is similar in principle to the above method, suffers from the grave disadvantage of having a very low efficiency; the extension of this method using the boron loaded scintillator as the slow neutron detector may, however, be sufficient to improve its efficiency, and, at the same time, retain the improvement in the resolution of the spectrometer over the former method. In the former case, the instrument has properties which satisfy most of the conditions for an ideal

neutron spectrometer, with the exception of the inherent disadvantage of organic scintillators, used in energy measurements, for protons, namely, the non-linear response; this factor tends to distort the pulse height spectrum, when multiple scattering occurs in the primary scatterer, and complicates the conversion of the pulse height distribution into an energy spectrum.

In the field of time-of-flight measurements of neutron energies, the work of James and Treacey (10) and Ward (11) is worthy of note. These investigators have measured the time of flight of neutrons by using two counters in delayed coincidence, one of which detected the neutrons at a given distance from the source, the other, a secondary particle such as a γ-ray or α-particle which was emitted simultaneously with the neutrons. This method has been found by these authors, who employed coincidence units of resolving times $\sim 10^{-8}$ secs, to have a very poor efficiency, in experimental conditions which provided adequate resolution. In the time of flight method described by the author in Part III.5 the geometrical situation of the scintillators together with the faster coincidence unit of resolving time $\sim 10^{-9}$ secs, ensured a resolution and efficiency adequate for most applications of the type mentioned in Part I. Further, the geometry of the spectrometer is such that the resolution could be improved without reducing the overall efficiency, provided the practical difficulties in making a large volume secondary scatterer were overcome. The properties and power of this spectrometer in measurements of neutrons in the energy range from 1 MeV to 20 MeV are illustrated in the distribution observed in the experiment on the reaction $B^{11}(d,n)C^{12}$. Further extension of the method in the manner suggested in Part III.5 would enable this spectrometer to provide results on fast neutrons comparable with those for high energy γ-rays, using sodium iodide crystals.

At the present time the state of knowledge of nuclear structure is largely

based on semi-empirical ideas dependent on the accumulation of experimental data. The development of a new technique, or advance in technique, in the spectrometry of nuclear radiations should, therefore, lead to rapid strides in the solution of the problems of nuclear physics. The great advances in recent years in the investigation of the energy levels of nuclei has been due to the discovery of the scintillation counter and, in particular, the sodium iodide crystal as applied to γ-ray spectrometry. Although similar rapid progress has not taken place in the application of organic scintillators to fast neutron measurements the properties of the spectrometers discussed in the foregoing pages indicate, that, in the next few years, many of the existing problems outlined in Part I will be adequately considered.

The measurements of importance, and common to all the fields of study described in Part I are the energy, intensity, angular distribution and correlation of fast neutrons. The techniques discussed in Part I have provided, and will continue to provide, much valuable information on the energies, intensities and angular distributions of fast neutrons, but it is clear that they are inadequate in providing information when fast response and high efficiency are desirable in a technique, for example, in angular correlation measurements and the determination of the properties of neutron groups of low intensity. The development of the fast neutron spectrometers utilising organic scintillation counters and the experiments which have up to the present been performed using them (and described earlier) have shown that the problems of angular correlations can be adequately tackled using these methods.

The experimental data on the properties of nuclei, although very considerable in quantity, is very far from complete, but it is to be hoped

that when further data, especially in the field of fast neutron physics, is accumulated, it will lead to the development of more fruitful approaches to the theories of nuclear structure and to a much more complete understanding of nuclear forces.

References in Part IV.

(1)	SCHENCK, J.	:	Nuc.Vol.12 No.8 p.54	(1952)
(2)	FREY, H.B.	:	Rev.Sci.Inst.Vol.21 p.886	(1950)
(3)	ELIOT, E.A. et alia	:	Phys.Rev.94 p.144	(1954)
(4)	POOLE, M.J.	:	Phil.Mag.43. 1060	(1952)
(5)	WARD, A, & GRANT, P.J.	:	Paper submitted for publication in Proc.Phys.Soc.	(1955)
(6)	HARRISON, F.B.	:	Nuc. Vol.12 No.3 p.44	(1954)
(7)	CHAGNON, P.P., et alia	:	Rev.Sci.Inst.24. p.656	(1953)
(8)	DRAPER, J.E.	:	Rev.Sci.Inst.25 p.538	(1954)
(9)	BEGHIAN, L.E., et alia	:	Phys.Rev. 86 p.1044	(1952)
(10)	JAMES & TREACY	:	Proc.Phys.Soc.A.64 847	(1951)
(11)	WARD, A.	:	Nat.173 April 24. p.771	(1954)

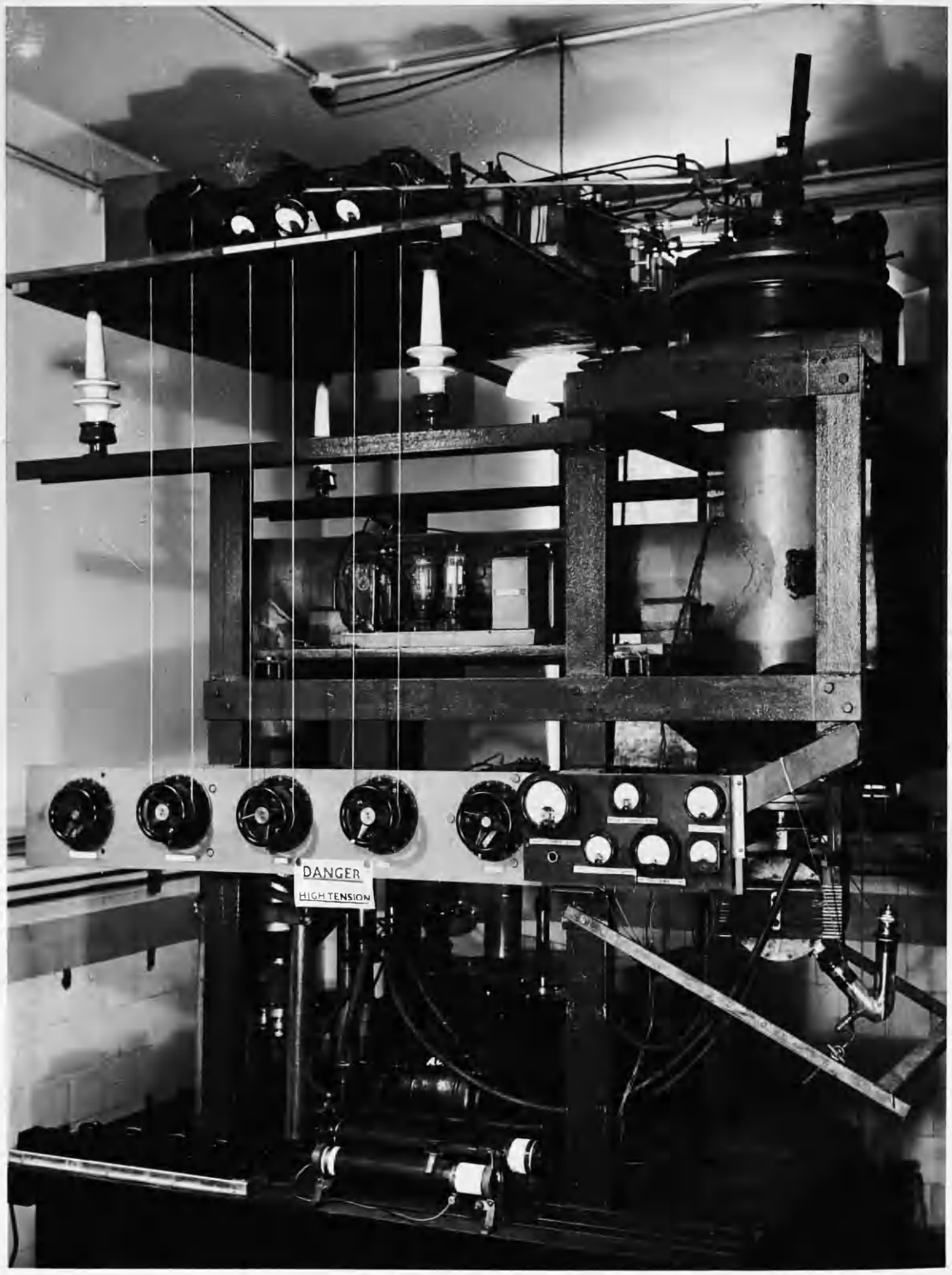

FIG. A1. THE 50 KV GENERATOR

APPENDIX I

THE NEUTRON SOURCES

In the investigations on the development of the neutron spectrometers described in this thesis, it has been necessary to have sources of monoenergetic neutrons which were free from γ-ray background. Two such sources are the 2.6 MeV neutrons from the $d(d,n)He^3$ reaction and the 14 MeV neutrons from the $H^3(d,n)He^4$ reaction. These reactions give a high yield of neutrons at very low bombarding energies of deuterons. A 50 KV accelerating machine in the laboratory shown in FIG.A.1., was maintained and further developed by the author in collaboration with Mr. D.J. Silverleaf, to provide a suitable source of low energy deuterons for the neutron reactions. This work has given the author considerable experience in vacuum physics.

(a) Mode of Operation of the Accelerator

The general principles behind the operation of the accelerator are the following :-

Deuterium gas is fed into a 6" long pyrex cylinder, where ionisation of the gas is produced and maintained by means of a radio-frequency field. The flow of gas into the cylinder is controlled by varying the temperature of the palladium, through which the gas is allowed to leak. The deuterium ions produced in this ion source are then extracted from the main body of the discharge, by the application of an electrostatic field, and pass through a small aperture into the main vacuum system which is continuously pumped. After extraction, the ions are focussed into a fine beam by means of an electrostatic lens system. In this fine beam the ions are then accelerated to an energy of 50 KeV and after passing through a small resolving magnet the beam of monenergetic deuterons impinges on the appropriate target.

(b) The 50 KV Generator

The generator consisted of a conventional type two stage Cockcroft-Walton voltage doubling circuit, constructed mainly from ex-Admiralty equipment. The output of the generator was varied by means of a variac on the input to the primary of the input 12.5 KV transformer. The output voltage was measured by drawing a small current through a large known resistance and a milliammeter. After considerable difficulty had been encountered in "sparking" from the generator, it was eliminated by completely rewiring the circuit.

(c) The Ion Source

The ion source for the generator was of the type developed by Rutherglen (1) for use in the 800 KV high tension set installed in the laboratory.

Deuterium gas was fed into a 6" long by $1\frac{1}{2}$" diameter pyrex cylinder which was sealed at one end and had a small channel at the other through which the ions were extracted. The discharge took place in this cylinder, and was maintained by a 200 mega-cycle radio frequency field. The system had also a magnetic field of 300 gauss, applied along the axis of the cylinder, in order to increase the ionisation in the source. The application of this field caused electrons in the discharge to spiral along the lines of force, and thus increased their effective path in the gas, and, therefore, the amount of ionisation they produced.

This ion source was connected through the extraction aperture to the main vacuum system. By this means the pressure in the ion source depended on the external pressure in the main vacuum system and vice versa. Investigation of the yield of monatomic deuterons from the ion source as a

function of pressure in the ion source showed that there was a critical pressure where operation was most satisfactory. This pressure was controlled by adjusting the flow of deuterium through the palladium leak.

(d) The Vacuum System

The vacuum system of capacity ~600 litres was continuously pumped by a Metro-Vick 8" diffusion pump backed by a 2" diffusion pump and a large rotary pump. Considerable difficulty was encountered at first in obtaining a good vacuum. For this reason the system was redesigned together with the addition of a liquid air trap between the large diffusion pump and the main system. At this stage a high vacuum valve was added to the target chamber to allow rapid changing of the targets.

The absolute pressures in the system were measured using an ionisation gauge in the high vacuum side and a thermocouple gauge in the backing line. The ultimate pressure, which could be obtained, in this system was 10^{-5} m.m. rising to 5×10^{-5} m.m when the ion source was running.

(e) The Targets

(1) Deuterium Target.

The target was made in the form of a layer of heavy ice. It was formed in the main vacuum system by causing a controlled amount of heavy water to evaporate into it near a copper plate (cooled with liquid nitrogen) on which a layer of heavy ice was deposited. This layer lasted for the order of 15 minutes before renewal was required after evaporation due to the continual deuteron bombardment.

The reaction which takes place on bombardment of this target with deuterons is

$$D + D \longrightarrow He^3 + n + 3.2 \text{ MeV}$$

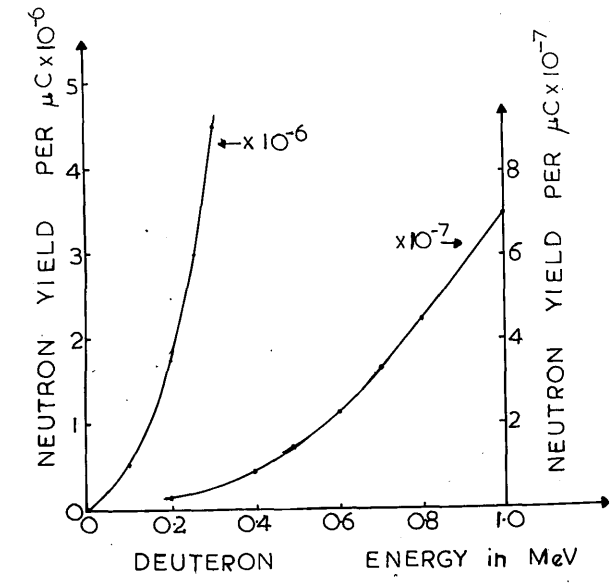

FIG. A2. YIELD OF NEUTRONS FROM A THICK DEUTERIUM TARGET IN D(d n)He^3 REACTION

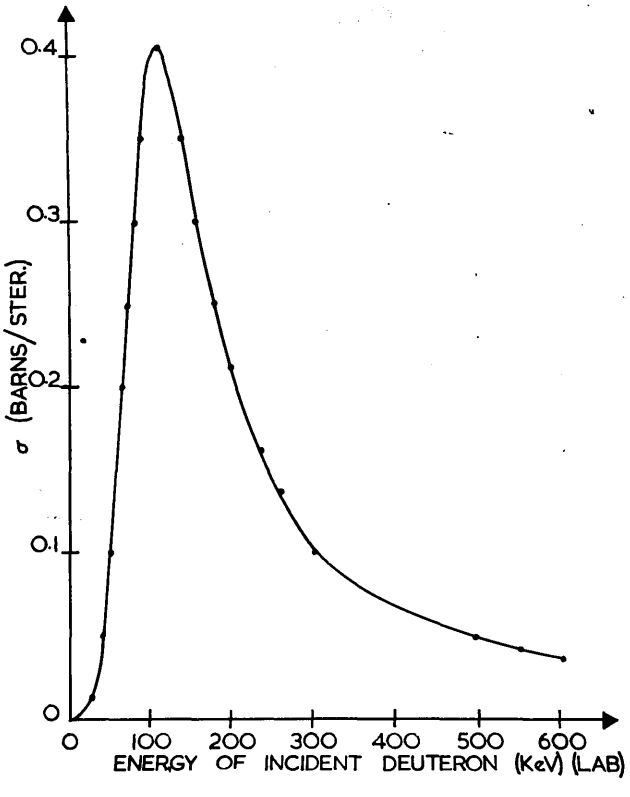

FIG. A3. CROSS SECTION FOR T(d,n)He^4 REACTION

The neutrons have energies from 2.46 MeV at $\theta = 0^{\circ}$ to 2.67 MeV at $\theta = 90^{\circ}$, for θ the angle of emergence of the neutron with respect to the bombarding deuterons of energy 50 KeV.

The thick target yield for this reaction for different bombarding energies is shown in FIG.A.2. At 50 KeV the number of neutrons per μ-coulombs of incident deuterons, is 0.25×10^{6}. The 50 KV accelerator produced on the average of the order of 30 μamps of resolved deuterons on the target, giving a yield of neutrons of approximately 10^{7} neutrons per sec.

(2) Tritium Target

The tritium target was obtained in the form of a disc of zirconium (on a molybdenum backing) into which of the order of 0.09 c.c. of tritium gas had been absorbed. This target appears as a thick one when bombarded with the 50 KeV deuterons from the accelerator.

A serious difficulty was encountered in the continuous use of this target in the production of neutrons. This was the formation of a layer of carbon (due to oil vapour in the system) on the surface of the target which resulted in a decrease in the neutron flux due to the stopping of the low energy deuterons by the carbon. This difficulty was overcome by maintaining the target at a temperature of 30°C and by surrounding the deuteron beam in the neighbourhood of the target with a liquid air cooling jacket.

The reaction is :-

$$H^{3} + d \rightarrow He^{4} + n + 17.6 \text{ MeV}$$

At incident deuteron energies of 50 KeV the neutrons have energies of approximately 14 MeV when a thick target is used. The cross-section for the reaction is shown in FIG.A.3. A simple calculation showed that for 1 μcoulomb of incident 50 KeV deuterons, the yield from this target was 10^{7} neutrons, i.e. for 30 μamps of resolved beam the neutron flux was 3×10^{8} neutrons/sec.

A discussion of these reactions has been given by Hanson and Taschek(2).

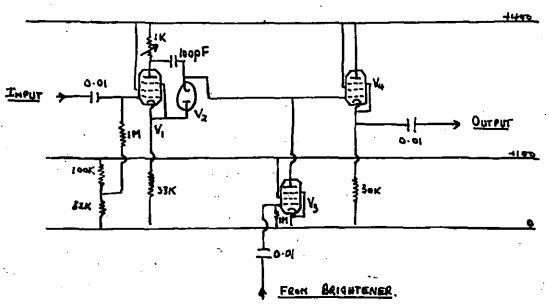

FIG. A4. THE PULSE LENGTHENING UNIT

APPENDIX II

THE ELECTRONIC EQUIPMENT

This appendix describes the electronic equipment which was used by the author in the work on neutron spectrometry.

The application of the lengthening, brightening and coincidence units to the photographic technique has been a standard practice in the Glasgow Physics Department for a few years. These units were tested and calibrated by the author.

The aingle channel kicksorter, which is a simple extension of the photographic method, was built and fully tested by the author. The incorporation of an electronic channel width control is a novel feature in this design, due to Mr. R. Giles.

These methods of pulse height analysis were largely replaced by the 100 channel analyser built in the laboratory to the design of Hutchinson and Scarrott (3).

The apparatus for the (E_p, E_n) method was designed by the author and built by the departmental electronics staff.

The electronic equipment for the simple (t) method was built and tested by Mr. D.J. Silverleaf and is included here for the sake of completeness. The extension to the many channel method of time of flight analysis was performed in collaboration.

(1) The Pulse Lengthening Unit

The circuit diagram is shown in FIG.A.4. The unit consists essentially of a cathode follower input valve V_1 and a cathode follower output valve V_4., whose grid is tied to the -ve H.T. line through the pentode V_3 which is normally just running. If now a nagative pulse is applied to the grid of V_3 immediately

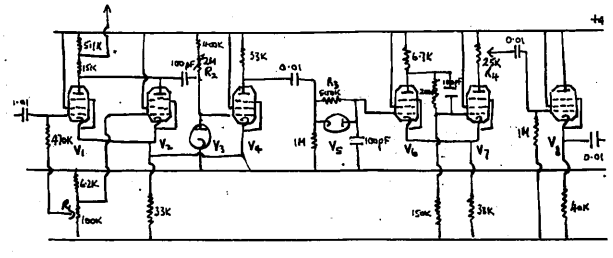

FIG. A.5 THE PULSE BRIGHTENING UNIT

a pulse arrives on the grid of V_4, then V_3 is cut-off and because of the diode V_2 the grid of V_4 is completely isolated. The grid of V_4 remains at the maximum potential of the signal pulse just as long as the negative pulse is applied to the grid of V_3. The output pulses are therefore lengthened at their maximum value and the duration of the pulse is controlled by the length of the signal applied to the grid of V_3.

(2) The Pulse Brightening Unit

In this unit, shown in FIG.A.5., a pulse of fixed height is produced in valves V_1 to V_4. The duration of this pulse is determined by the time constant R_2C_2. The pulse length control is provided by the 5 Meg-ohm potentiometer making up R_2. From the anode of V_1 and V_2 is taken the negative signal which is applied to the valve V_3 in the lengthening unit.

The output from the anode of V_4 is fed through the cathode coupled valves V_6 and V_7 and then through the cathode follower V_8 to the grid of the oscilloscope. A square pulse is produced with a variable delay on the front edge determined by R_3, and a variable amplitude determined by R_4. The delay is encorporated to ensure that the signal pulse has reached its maximum before the brightening pulse is applied. As is obvious, the control R_2 varies the length of both signal and brightening pulses. The circuit is designed so that the brightening pulse is cut off at a fixed time before the back edge of the signal pulse.

(3) The Coincidence Unit

FIG.A.6 shows one half of the coincidence unit comprising valves V_1 to V_5.

Valves V_1 and V_2 are used to produce from the input signal a square output pulse whose length is governed by the input pulse and whose amplitude is fixed. This pulse is then differentiated, the amount of differentiation being controlled by the resistance R_2, i.e. the slope on the back edge of the pulse applied to the grid of V_4 is governed by R_2.

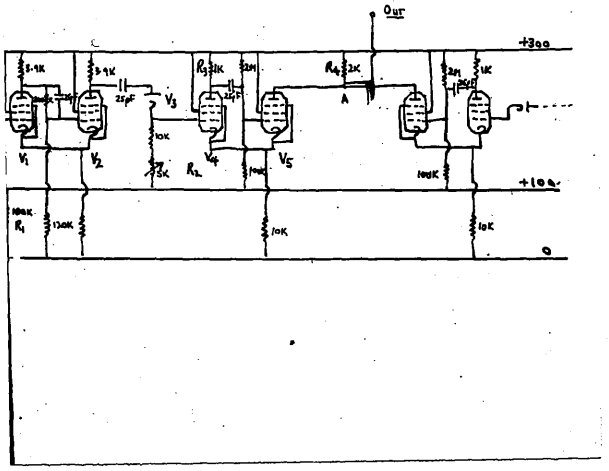

FIG. A.6 THE COINCIDENCE UNIT

Valves V_4 and V_5 constitute an A.C. coupled flip-flop, which produces an output pulse of fixed amplitude and whose length is varied by the amount of differentiation on the pulse applied to the grid of V_4 i.e. by the resistor R_2.

A similar argument applies to the other half of the coincidence unit. The result of a coincidence is the presence of a double sized pulse at the point A. The resolving time of the unit is determined by the lengths of the output pulses from the two sides of the coincidence unit, i.e. by the values of resistors R_2 on both sides of the unit. By this method resolving times from $\frac{1}{2}$ μsec upwards have been obtained.

4. THE PHOTOGRAPHIC METHOD OF PULSE HEIGHT ANALYSIS

Pulses from a photo-multiplier are amplified and after suitable shaping using the pulse lengthener and brightener they are applied to an oscilloscope made suitable for photography. In this method, the tops of the pulses appear as spots on the face of the oscilloscope, the height of the spot above the base-line being a measure of the pulse height. Thus a film of spots obtaining during an experiment provides a means of determining a pulse height distribution. By projecting the film on a large calibrated screen it is easy to count the spots and deduce the pulse height distribution.

In a case where only coincidence pulses are to be analysed, e.g. in the (E_ρ, θ) experiments, the method is to cause the brightening unit to he triggered by pulses from the coincidence unit so that only coincident pulses in the primary counter are recorded as spots. Although this method has proved extremely satisfactory it suffers from the grave disadvantage of being very tedi ous.

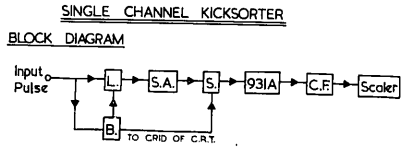

L. Lengthening Unit.
B. Brightening Unit.
S. Oscilloscope.
C.F. Cathode Follower.
S.A. Scope Amplifier with Channel Height and Channel Width Control.

FIG. A.7 BLOCK DIAGRAM OF KICKSORTER

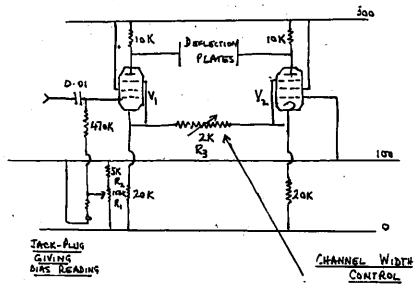

FIG. A.8 THE 'SCOPE AMPLIFIER

5. THE SINGLE CHANNEL KICKSORTER

The block diagram of the apparatus is shown in FIG.A.7. It is a simple extension of the method of analysis described above. In this case the lengthened pulses are fed to the grid of the push-pull amplifier, shown in FIG.A.8, whose anodes are connected to the plates of the oscilloscope. In a similar manner only the tops of the pulses appear on the oscilloscope screen. The method used to analyse the spot distribution is simply to blacken out of the face of the 'scope except for a small slit of the order of 0.3 cm wide and observe this slit using a photomultiplier, so that, only when a pulse appears on this slit does a pulse register on the output of the multiplier. The pulses from the photomultiplier are fed into a scaler thus allowing the number of pulses appearing in the slit to be recorded.

CHANNEL BIAS

The scope amplifier (FIG.A.8) controls the settings of the bottom of the analyser channel by means of the resistors R_1 and R_2 since these resistors determine the bias on the input grid and thus the size of the output pulse. The size of the pulse determines its position on the screen of the ocilloscope.

CHANNEL WIDTH

The channel width is primarily controlled by the gain control of the push-pull amplifier. This control is the resistor R_3. It effectively controls the amount of feedback in the cathodes of the pair of valves and thus the gain of the arrangement. By varying this resistor, channel widths from 1v to 10v are obtained. The kicksorter was generally operated with a channel width of 2v. Other controls which can vary the channel width are the amplitude of the brightening pulse and the scope brilliance, are generally preset.

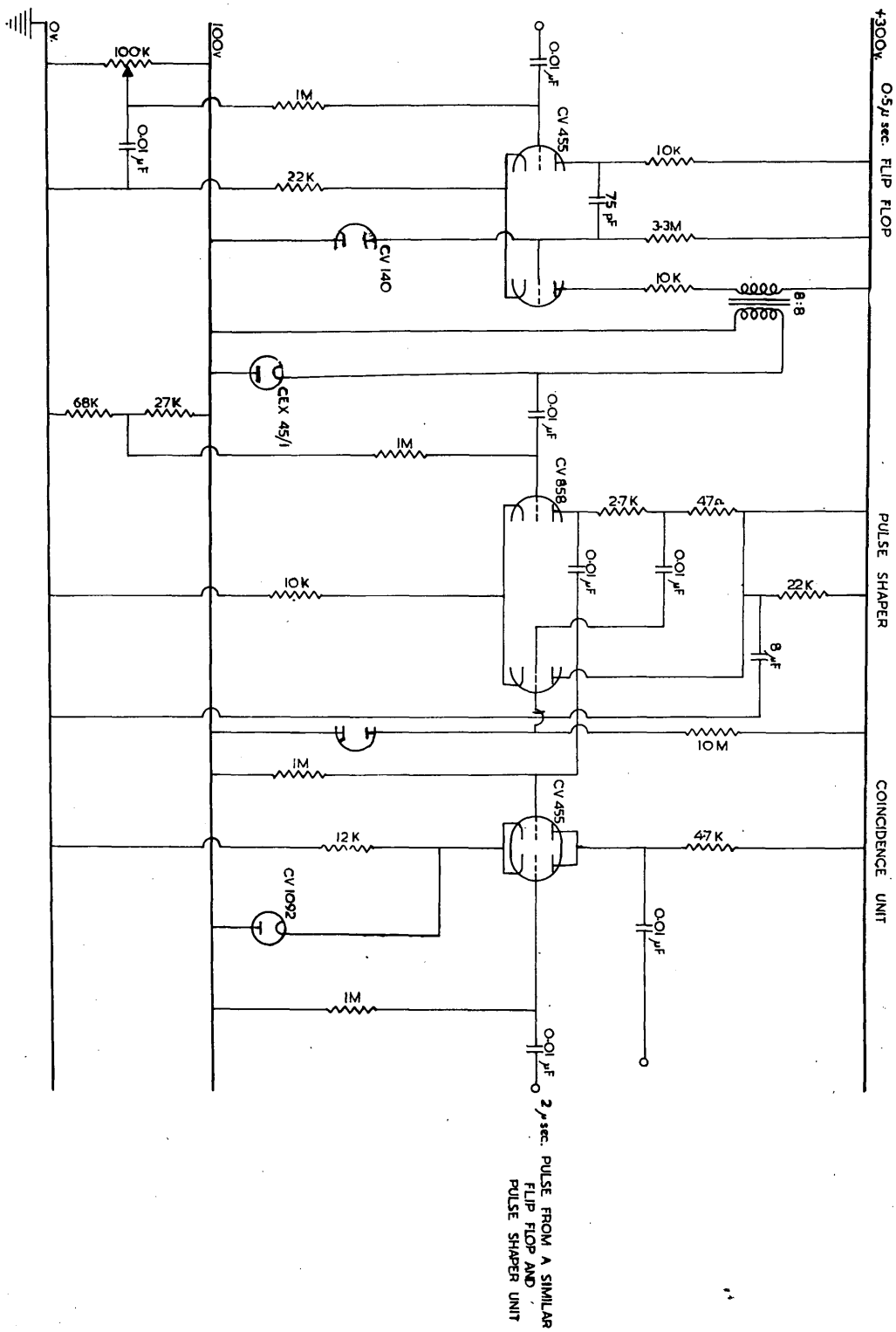

FIG. A.9 THE COINCIDENCE UNIT

6. THE ELECTRONICS OF THE (E_ρ, E_n) METHOD

The principles of the electronic arrangement in the (E_ρ,E_n) method has been given in Part III.4 and the block diagram of the circuit in FIG.III.2. It is proposed in this section to present in more detail the important parts of the circuitry.

THE COINCIDENCE UNIT

One channel of the triple coincidence unit is shown in FIG.A.9. The other channels are identical. In this channel pulses from L_2 of FIG.III.2 of width 10 μsec and height 30 to 40v. are fed into the input grid of the initial flip-flop which produces a pulse of duration approximately $\frac{1}{2}$ μsec. This pulse is then made square and of width exactly $\frac{1}{2}$ μsec by the two valve pulse shaper. The $\frac{1}{2}$ μsec pulse is then fed to one of the coincidence unit grids. The pulses from limiter L_1 and the low-level discriminator D, are similarly treated and appear as pulses of 2 μsec and 10 μsec respectively on the grids of the two remaining coincidence triodes. The coincidence valves are connected in such a way as to ensure that, only when all three pulses arrive simultaneously, does an appreciable voltage pulse appear on their common anode.

THE LOW LEVEL DISCRIMINATOR

The circuit of the discriminator is shown in FIG.A.10. It comprises a secondary emission pentode, an EFP60, and two crystal diodes D_1 and D_2. A positive pulse on the input causes a positive pulse to appear on the secondary emission electrode which is connected by a feed-back loop to the input grid. The feedback to the input grid is, however, limited by the diode D_2 since the pulse only appears on the grid if it is large enough to overcome the bias on D_2 which is adjusted by the potentiometers P_1 and P_2. The use of this diode enables low level discrimination to be made, since the input pulse is

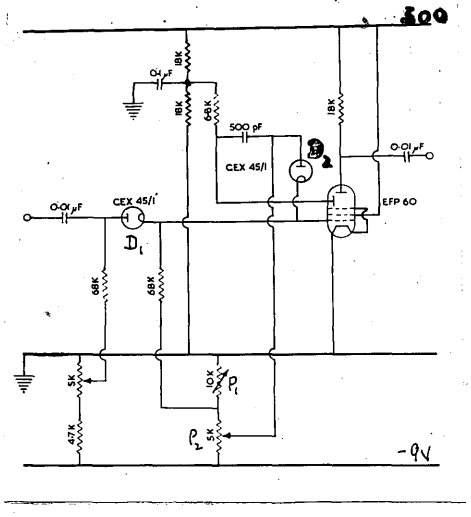

FIG. A.10 LOW LEVEL DISCRIMINATOR

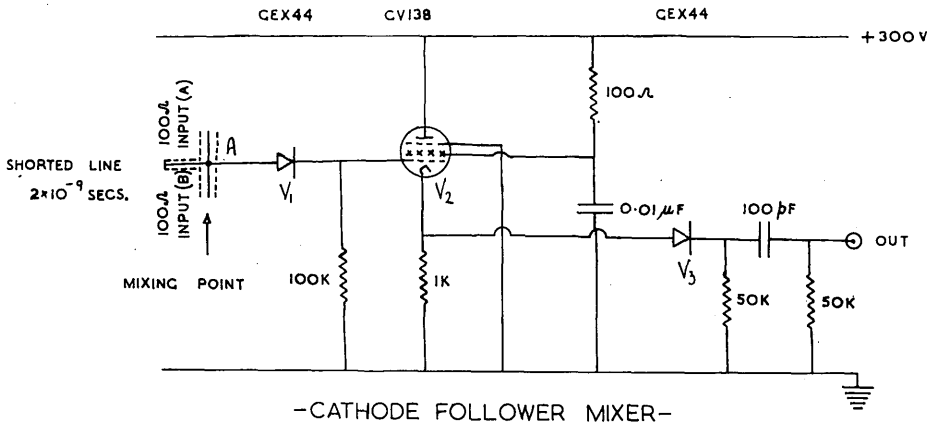

FIG. A.11 CATHODE FOLLOWER MIXER

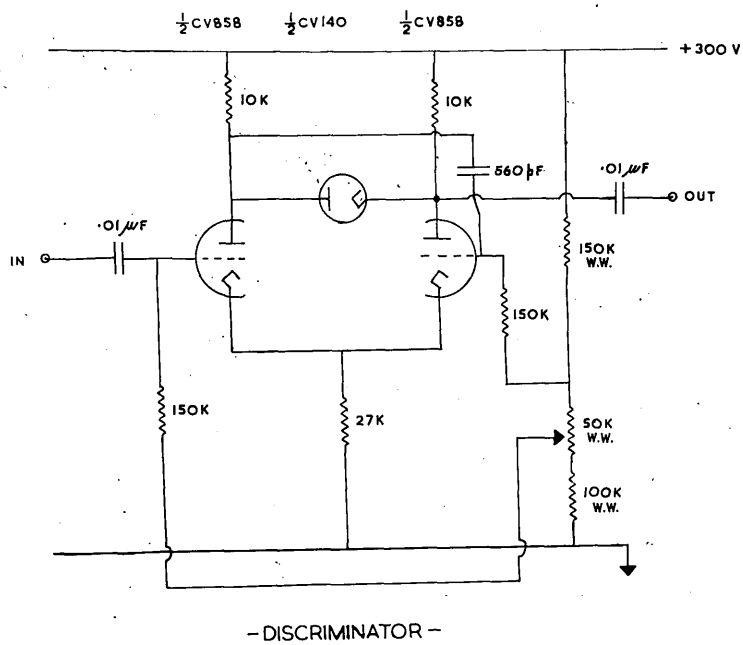

FIG. A.12 DISCRIMINATOR

effectively amplified before discrimination. This circuit gives 40v pulses of widths ~ 10 μsecs, with a discrimination level as low as 0.2 volts.

In using the limiter L_2, without the low-level discriminator it was found that, if the input bias setting on L_2 was high, many prompt coincidences were registered as delayed coincidences. This was traced to the relatively long rise time of pulses from the limiter which were too small to be completely saturated. The long rise time resulted in a delayed firing of the coincidence unit. Reduction of the input bias did not solve the problem since in this case a large number of amplifier and photomultiplier noise pulses appeared on the output of the limiter, leading to a high chance coincidence rate. The introduction of the fast low level discriminator, however, allowed discrimination against these noise pulses and still enabled the small prompt coincident pulses to be completely limited.

7. THE FAST COINCIDENCE UNIT

The block diagram of this unit has been given in FIG. III[26] and its operation described in Part III.5. In this section only those parts of the unit will be considered in detail, which are different in design from the basic circuitry originally designed by Bell et alia (4).

THE CATHODE FOLLOWER MIXER

Pulses are fed from two multipliers and associated valve limiters along delay lines to the mixing point shown in FIG.A.II. The pulses from each delay line are shaped in the 50 Ω shorted line and mixed at the point A.

The use of the diode V_1 (specially selected), a non-linear element, enables the difference in pulse height between single pulses and coincident pulses to be accentuated before application to the grid of V_2. The cathode follower valve V_2, together with the diode V_3, and associated components ensure that the

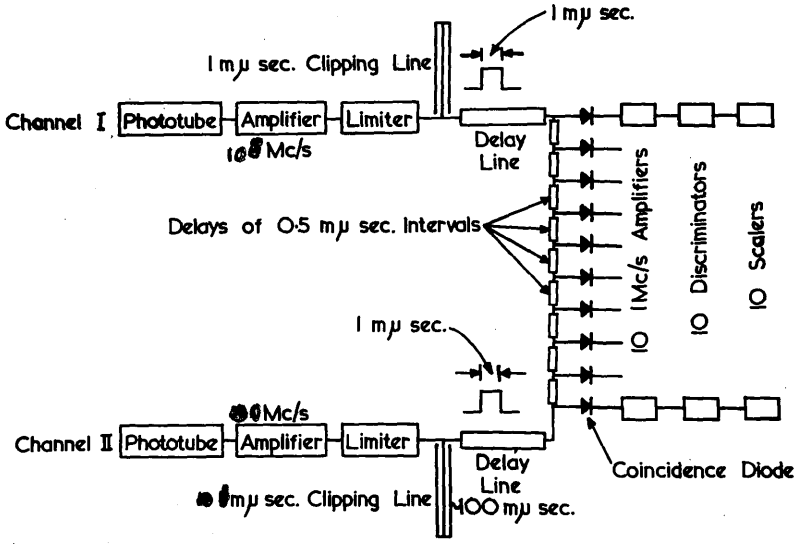

FIG. A.13 MULTIPLE CHANNEL ANALYSER

pulses from the mixing diode V_1 are lengthened before application to the 1 Mc/s amplifier. Coincident pulses are selected using the simple discriminator shown in FIG.A.12. by a suitable choice of discriminator level. The efficiency and resolving time of the coincident unit are controlled by the discriminator setting. The lowest possible setting, just sufficient to reject single counts, gives the highest efficiency, of the order of 50 per cent.

A complete account of theproblems in this type of coincidence circuitry has been given by Bell et alia (4) and summarised by Curran (5).

MULTIPLE CHANNEL TIME ANALYSER

FIG.A.13 gives the block diagram of the multichannel analyser, designed by Mr. D.J. Silverleaf in collaboration with the author, mentioned in Part III.5. This design was successfully tested over three channels.

The analyser comprises ten coincidence mixers as described above. In this case the pulses from the limiting valves are shaped separately in shorted lines and appear as 1 milli-microsecond pulses in the positions shown in the diagram. By the observation of coincident pulses in each of the ten coincidence channels the time spectrum of pulses at intervals of 10^{-9} seconds is obtained by the insertion of 0.5 milli-microsecond delays between the coincidence channels. To ensure that reflection of pulses from one channel in the shorted line of the other does not interfere with the original pulses, long delay lines of the order of 100 milli-microseconds are inserted in both channels as shown in FIG.A.13. This analyser reduces considerably the time required to analyse a delayed coincidence spectrum of the type observed in the time-of-flight neutron spectrometer.

REFERENCES IN APPENDICES

1. RUTHERGLEN, J.R. : Ph.D.Thesis Glas.Univ. May 1951
2. HANSON,A.O. AND TASCHEK, R.F. : Prel.Rep.No.4 Nuc.Sci.Series
3. HUTCHINSON, G.W. AND SCARROTT,G.G. : Phil.Mag. 42 p.792 (1951)
4. BELL, R.F. ET ALIA : Can.Jour.of Phys.30 p.35 (1952)
5. CURRAN, S.C. : Luminescence and the scintillation Counter - Butterworth Sci.Pub.(1953)